

CIBERINFEC COMMUNICATIONS

16.ª Jornada de Formación CIBERES-CIBERINFEC del Centro de Investigación Biomédica en Red (CIBERES)

Madrid, 15 y 16 de junio de 2023

3. NON-AIDS DEFINING CANCER MORTALITY IN PEOPLE LIVING WITH HIV

Marta Rava^{1,2}, Félix Gutierrez^{2,3}, José A Pérez-Molina^{2,4}, Inés Suarez-García^{2,5}, Francisco Jesús Vera Méndez⁶, Fernando Baigorria Feltrin⁷, Mar Masía^{2,8}, Juan Macías^{2,9}, Gemma Navarro¹⁰, Santiago Moreno^{2,11}, Inma Jarrín^{1,2}, Cohorte Coris¹²

¹Instituto de Salud Carlos III, Madrid, Spain. ²Centro de Investigación Biomédica en Red de Enfermedades Infecciosas (CIBERINFEC), Madrid, Spain. ³Hospital General Universitario de Elche & Universidad Miguel Hernández, Alicante, Spain. ⁴Hospital Universitario Ramón y Cajal, IRYCIS, Madrid, Spain. ⁵Hospital Universitario Infanta Sofía, Madrid, Spain. ⁶Hospital General Universitario Santa Lucía, Cartagena, Spain. ⁷Complejo Hospitalario de Navarra, Pamplona, Spain. ⁸Hospital General Universitario de Elche, Alicante, Spain. ⁹Hospital Universitario Virgen de Valme, Sevilla, Spain. ¹⁰Parc Taulí Hospital Universitari, Barcelona, Spain. ¹¹Hospital Ramón y Cajal, Madrid, Spain. ¹²CIBER, Instituto de Salud Carlos III, Madrid, Spain.

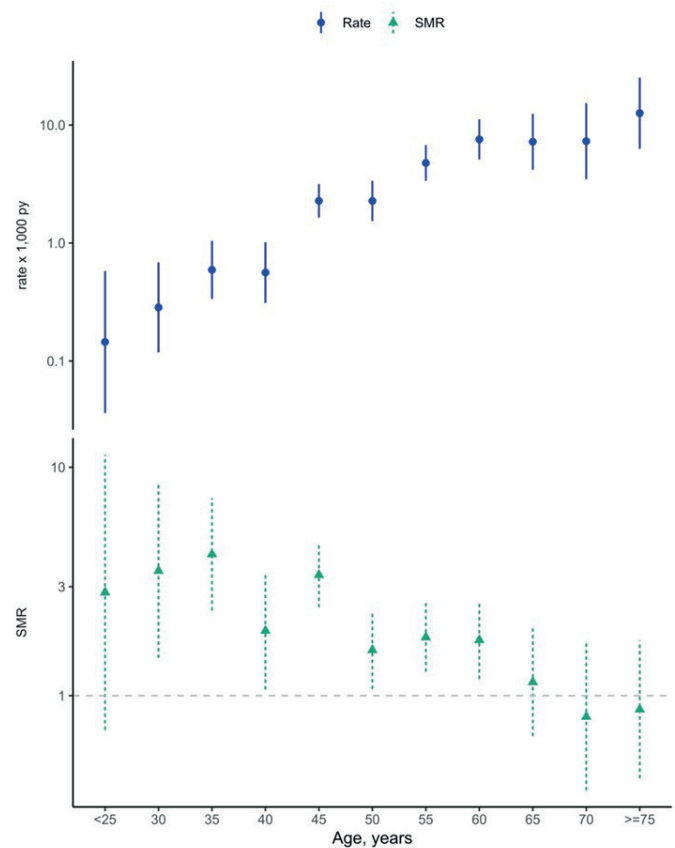
Introduction: Non-AIDS-defining cancers (NADC) represent one of the leading causes of death in people living with HIV (PLWH), with higher rates than in the general population. Both traditional and HIV-related risk factors play a role in NADC mortality and characterizing them may suggest areas of intervention.

Objectives: Our aim was to evaluate rate and prognostic factors of NADC mortality among PLWH from the Coris cohort.

Methods: We included antiretroviral-naïve individuals aged ≥ 20 years at enrolment recruited during 2004–2021. NADC deaths were all deaths due to cancer, except those due to AIDS defining malignancies such as Kaposi sarcoma, certain types of non-Hodgkin lymphomas and cervical cancer. We estimated mortality rates and standardised mortality ratios (SMRs) using NADC mortality rates from the Spanish general population. We applied cause-specific Cox proportional hazard models, accounting for competing risk, with age as time-scale to identify prognostic factors for NADC mortality.

Results: Of the 17,978 study participants, 85% were men and median age was 35 years. NADC mortality rate was 1.58 (95% confidence interval: 1.36, 1.83) per 1,000 person-years (PY), 79% higher as that in the general population (SMR: 1.79, 95%CI 1.54, 2.07). The highest mortality rates were found for lung (0.57 per 1,000 PY; 95%CI 0.45, 0.73) and liver cancer (0.20 per 1,000 PY, 95%CI 0.13, 0.30). NADC mortality

rates increased with age, while SMR decreased with age: NADC mortality in PLWH was three times higher than that of the general population in age groups under 50 years and gradually decreased to a similar rate than that of the general population in age groups over



	<25	30	35	40	45	50	55	60	65	70	≥ 75
Rate	0.15	0.28	0.59	0.56	2.28	2.27	4.77	7.57	7.23	7.31	12.63
SMR	2.83	3.52	4.16	1.92	3.38	1.58	1.8	1.75	1.15	0.81	0.87

Mortality rates and SMRs according to age.

70 years (Figure). NADC mortality risk was higher in participants that acquired infection through heterosexual contact (Hazard Ratio: 1.50; 95%CI 1.08, 2.10) and injection drug use (HR: 1.89 (1.03, 3.47), compared to men having sex with other men. NADM mortality risk was associated with active smoking (HR: 2.23; 95%CI 1.05, 4.70), hepatitis C (HR: 1.59, 95%CI 0.98, 2.57) and hepatitis B virus (HR: 2.03, 95%CI 1.22, 3.38) and low CD4 count (HR: 9.76; 95%CI 5.35, 17.80 for CD4 < 200 cells/ μ L, HR: 4.17; 95%CI 2.31, 7.54 for CD4 200-349 cells/ μ L; HR: 2.61; 95%CI 1.62, 4.22 for CD4 350-499 cells/ μ L compared to CD4 \geq 500 cells/ μ L).

Conclusions: Mortality due to NADC in PLWH was higher than in the general population, mainly at younger ages. It was associated mainly to immune suppression, smoking, and coinfection with hepatitis B and C, which are all preventable risk factors.

Funding: Gilead Scholarship Program for Biomedical Research (GLD19_00106), ISCIII- Miguel Servet CP19CIII - 00002 contract.

4. CHAMIGRENES ISOLATED FROM THE LAURENCIA DENDROIDEA AGAINST NAEGLERIA FOWLERI

Javier Chao Pellicer^{1,2,3}, Iñigo Arberas Jiménez^{1,2}, Ines Sifaoui^{1,2}, María Reyes Batlle^{1,2,3}, Rubén Leocadio Rodríguez Expósito^{1,2}, Patricia Pérez Pérez¹, Atteneri López Arencibia^{1,2,3}, Carlos Javier Bethencourt Estrella^{1,2}, Desirée San Nicolás Hernández^{1,2}, Ana Raquel Díaz Marrero^{4,5}, José Javier Fernández Castro^{6,7}, José Enrique Piñero Barroso^{1,2,3}, Jacob Lorenzo Morales^{1,2,3}

¹Instituto Universitario de Enfermedades Tropicales y Salud Pública de Canarias, Universidad de La Laguna, La Laguna, Spain. ²Departamento de Obstetricia y Ginecología, Pediatría, Medicina Preventiva y Salud Pública, Toxicología, Medicina Legal y Forense y Parasitología, Universidad de La Laguna, La Laguna, Spain. ³Centro de Investigación Biomédica en Red de Enfermedades Infecciosas (CIBERINFEC), Madrid, Spain. ⁴Instituto de Productos Naturales y Agrobiología, Consejo Superior de Investigaciones Científicas, La Laguna, Spain. ⁵Instituto Universitario de Bio-Orgánica Antonio González (IUBO AG), Universidad de La Laguna, La Laguna, Spain. ⁶Instituto Universitario de Bio-Orgánica Antonio González, La Laguna, Spain. ⁷Departamento de Química Orgánica, Universidad de La Laguna, La Laguna, Spain.

Introduction: Primary amoebic meningoencephalitis (PAM) is a central nervous system affecting disease caused by the opportunistic protozoa *Naegleria fowleri*. It is a fulminant disease with a rapid progression and affects mostly children and young adults who reported previous exposure to warm water bodies, such as lakes, hot springs or untreated swimming pools. The trophozoite stage of this amoeba penetrates the nasal cavity and migrates through the olfactory nerves to the brain causing infection and subsequent death a few weeks after the onset of the first symptoms. Although the disease has a case fatality rate of over 97%, currently available therapies are not at all effective and it is associated with a wide range of serious side effects. Therefore, the search for novel molecules with anti-*Naegleria* activity and low toxicity remains an urgent issue in the fight against the PAM. Some red algae of the *Laurencia* genus have been proved to be an important source of bioactive molecules. In fact, some compounds obtained from different red algae namely *Laurencia viridis* or *Laurencia johnstonii* have shown great activity against diverse protozoa, including some parasites that belong to the free-living amoeba group.

Objectives: In the present study, the activity and cytotoxicity of different molecules obtained from the *Laurencia dendroidea* algae was evaluated. In addition, the presence of different metabolic events that are characteristic of the programmed cell death were evaluated in *Naegleria fowleri* trophozoites.

Methods: To evaluate the selectivity against *Naegleria fowleri*, activity assays were performed on two strains of the pathogen (ATCC®

30808™ and ATCC® 30215™) and, in turn, cytotoxicity assays against a murine macrophage cell line. Afterwards, those with a better selectivity index against *Naegleria* were used to study the induction of programmed cell death (PCD) process. These metabolic events studied were DNA condensation, plasma membrane damage, reduction of mitochondrial membrane potential and ATP levels or generation of ROS.

Results: As a result, the chamigrenes (+) - elatol, (+) - obtusol and (-) - elatol were the most active molecules against *Naegleria fowleri* trophozoites. Moreover, the type of cell death process that produces the (+) - elatol, the most active compound, was also determined, showing a programmed cell death induction in treated cells.

Conclusions: Hence, (+) - elatol could be considered as a good candidate for the development of new treatments against the primary amoebic meningoencephalitis.

Funding: CIBERINFEC (CB21/13/00100), FEDER, RTI2018-101818-B-I00, Fundación La Caixa-Caja Canarias (2022CLISA26), ACIISI (I.A.J./C.J.B.E./D.S.N.H./R.L.R.E./P.P.P.), Cabildo Insular de Tenerife 2023-2028 y MSCBS.

10. SYNERGISTIC EFFECT BETWEEN ANTIBIOTICS AND TWO BACTERIOPHAGES CAPABLE OF INFECTING MULTIRESTANT CLINICAL STRAINS OF KLEBSIELLA PNEUMONIAE

Abbrar Senhaji, Jaime Esteban, Meritxell García Quintanilla

Fundación Jiménez Díaz, Madrid, Spain.

Introduction: *Klebsiella pneumoniae* is a gram-negative, facultative anaerobic bacteria belonging to the *Enterobacteriaceae* family. With a total of 8.56% of the isolates, it's the fourth most frequent bacteria in Spain. The incidence of infections caused by carbapenemase-producing *Enterobacteriaceae* family is increasing every year.

Objectives: The objective is to study the combination effect of antibiotics in combination with two new bacteriophages against clinical MDR *K. pneumoniae*, evaluating the in vivo synergistic capacity of the bacteriophage and the study of combinations with antibiotics that can combat these infections.

Methods: Bacteriophages were isolated from sewage and hand-washing samples from the Hospital Universitario Fundación Jiménez Díaz (HUFJD). The synergistic antibacterial activity of the F4KP and F5KP bacteriophages was assigned by the modified broth microdilution method in multiwell 96 flat-bottom microplates (Thermo-Fischer) also known as Checkerboard. Experimental conditions were designed for the antibiotic-phage mixture and colistin, polymyxin B, fosfomicin, amikacin, doripenem and ciprofloxacin were tested along with the bacterial control at a final volume of 200 μ L. Briefly, the culture was allowed to grow at an OD600 of 0.44 until 4×10^7 CFU was reached. Next, 50 μ L of antibiotic at different concentrations was added to each well containing 50 μ L of Mueller Hinton II 90922 broth (Millipore, Sigma Aldrich, Merck) supplemented with 10 mM CaCl2

Summary of synergistic effect between F4KP, F5KP and antibiotics against KP5 *K. pneumoniae* strain

Antibiotic	Phage	Effect	FIC
Polymyxin B	F13	Synergism	0.162
Colistin	F13	Additive	0.501
Doripenem	F13	Additive	0.510
Polymyxin B	F14	Additive	0.5001
Colistin	F14	Additive	0.600
Doripenem	F14	Additive	0.501
Fosfomicin	F13/F14	No effect	-
Ciprofloxacin	F13/F14	No effect	-
Amikacin	F13/F14	No effect	-

and 10 mM MgSO₄. In addition, 50 µl of each phage dilution (109 to 105 PFU) was added to the suspension and 100 µl of bacterial suspension was added to the mixing wells. Plates were incubated at 37 °C overnight and FIC (fractional inhibitory concentration) was calculated according to bacterial growth measured at OD₅₉₅. This experiment was performed in duplicate.

Results: Bacteriophage F4KP was found to have a synergistic effect in combination with polymyxin B (FIC = 0.162) and additive effect with colistin and doripenem (0.501 and 0.510, respectively). F5KP showed additive effect in combination with polymyxin B, colistin and doripenem obtaining a FIC of 0.5001, 0.600 and 0.501 respectively. The checkerboards performed proved that F4KP and F5KP showed no effect in combination with fosfomicin, ciprofloxacin and amikacin.

Conclusions: The F4KP and F5KP bacteriophages have shown synergistic and additive effects in combination with certain antibiotics and to combat infections caused by clinical strains of multiresistant *K. pneumoniae*. We tested which phage-antibiotic combinations could have a clinical use and which antibiotics don't produce any effect in combination with these bacteriophages. It could be a promising alternative for infections caused by MDR bacteria that cannot be treated by conventional antibiotics alone.

Funding: CIBER-Enfermedades infecciosas.

13. ACTIVITY OF CEFTAZIDIME-AVIBACTAM AND MEROPENEM, ALONE AND IN COMBINATION, AGAINST *KLEBSIELLA PNEUMONIAE* HIGH-RISK CLONES PRODUCING NOVEL KPC VARIANTS WITH COLLATERAL SENSITIVITY TO CARBAPENEMS

Marta Hernández García, Marta Nieto-Torres, Marina Domínguez, Patricia Ruiz-Garbajosa, Rafael Cantón

Hospital Universitario Ramón y Cajal, Madrid, Spain.

Introduction: Ceftazidime-avibactam (CAZ-AVI) has been introduced in clinical practice to combat difficult-to-treat infections caused by carbapenem-resistant Enterobacterales, including KPC-producing *Klebsiella pneumoniae* (KPC-Kp). Nevertheless, emergence of CAZ-AVI resistance due to novel KPC enzymes in Kp high-risk clones, such as ST307-Kp, is increasing. Additionally, clinical isolates expressing mutated KPC enzymes frequently exhibit a restored susceptibility to carbapenems, phenomenon known as "collateral sensitivity" (CS).

Objectives: To explore two potential strategies to treat CAZ-AVI resistant KPC-ST307-Kp infections based on the CS effect to carbapenems: combined therapy of ceftazidime-avibactam and carbapenems (CAZ-AVI+CBs) and to recuperate the monotherapy use of carbapenems.

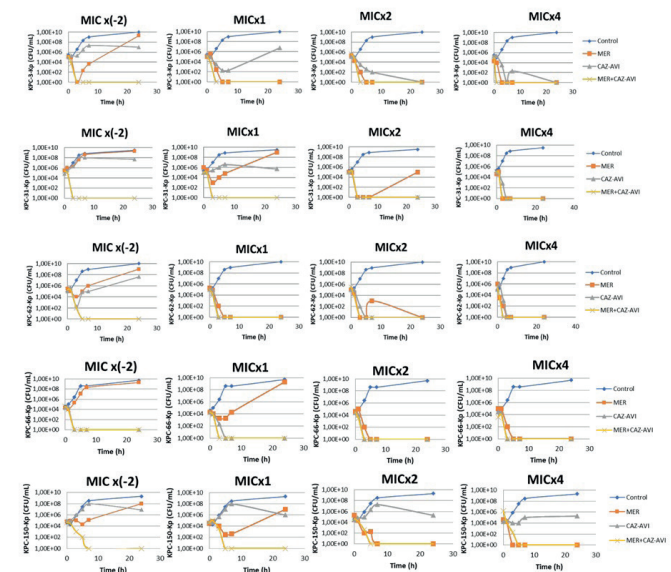
Methods: Between 2018-2023, we detected in our hospital a total of 7 mutated KPC variants (KPC-31, KPC-46, KPC-61, KPC-62, KPC-66, KPC-92 and KPC-150) in clinical ST307-Kp isolates. MICs were determined using standard broth microdilution (EUCAST-2023 breakpoints). Synergy assessments were performed by crossing the gradient strips at a 90° angle at the respective MICs of each antibiotic (Etest synergy test). Results were expressed using the fractional inhibitory concentration index [FICI = (MIC-A in combination/MIC-A alone) + (MIC-B in combination/MIC-B alone)]. FICI ≤ 0.5 was considered as synergistic, 0.5 < FICI ≤ 4 as indifferent and FICI > 4 as antagonistic. The *in vitro* effect of CAZ-AVI, meropenem (MER) and CAZ-AVI+MER combination was evaluated performing killing kinetics (KC) studies in a selection of KPC-ST307-Kp mutants (KPC-31-Kp, KPC-62-Kp, KPC-66-Kp and KPC-150-Kp) and in a KPC-3-ST307-Kp strain. Tested antibiotic concentrations were: (-2)xMIC, 1xMIC, 2xMIC and 4xMIC; and activity was assessed at 0h, 1h, 3h, 5h, 7h and 24h. Synergy was defined as ≥ 2log₁₀ CFU/ml decrease.

Results: All KPC-ST307-Kp mutants showed resistance to CAZ-AVI (MIC range: 32-128 mg/L) and CS to meropenem (MIC range: ≤ 0.06-8 mg/L) (Table). The Etest synergy test revealed that the CAZ-AVI+MER

combination was synergistic in all clinical KPC-ST307-Kp mutants (FICI < 0.5) (Table). The KC study demonstrated a synergistic effect of the CAZ-AVI+MER combination in all concentrations even below the MIC of both antibiotics. Moreover, meropenem was also active at the MIC concentration in the KPC-62-ST307-Kp and at higher concentrations (≥ 2xMIC) in KPC-31-ST307-Kp, KPC-66-ST307-Kp and KPC-150-Kp mutants (Figure).

Ceftazidime-avibactam and meropenem MIC values of KPC-Kp mutants by microdilution and gradient strips. Results (FICI) of the Etest synergy test

KPC mutant	Microdilution		Etest		FICI (interpretation)
	MIC-MER (mg/L)	MIC-CAZ-AVI (mg/L)	MIC-MER (mg/L)	MIC-CAZ-AVI (mg/L)	
KPC-3	8	2	0.19	0.016	0.032 (synergy)
KPC-31 (D179Y)	0.125	128	0.032	12	0.35 (synergy)
KPC-46 (L168P)	≤ 0.06	64	0.004	0.75	0.08 (synergy)
KPC-61 (S170P)	0.25	64	0.032	6	0.22 (synergy)
KPC-62 (L168Q)	8	32	0.38	2	0.11 (synergy)
KPC-66 (E167_L168del)	≤ 0.06	64	0.012	2	0.23 (synergy)
KPC-92 (E167_L169delinsD)	0.125	64	0.016	6	0.22 (synergy)
KPC-150 (L166_L169delinsH)	8	64	1.5	2	0.22 (synergy)



Killing kinetics results of using CAZ-AVI, meropenem (MER) and CAZ-AVI+MER combination in KPC-3-Kp and in KPC-31-Kp, KPC-62-Kp, KPC-66-Kp, KPC-150-Kp mutants.

Conclusions: Our study demonstrated that the combination of CAZ-AVI and meropenem is synergistic and that meropenem is active against KPC-Kp mutants. Therapies based on combination or collateral sensitivity could be a potential therapeutic option to treat infections caused by Kp-KPC mutants and could help prevent the evolution of CAZ-AVI resistance.

Funding: FIBio-Intramural-research grant (2021/0442), ISCIII-research grant (PI22/01283), and CIBER de Enfermedades Infecciosas (CIBERINFEC) (CB21/13/00084).

17. TELOMERE LENGTH IN AVIREMIC PWH: HOW DIFFERENT IS IT FROM PERSONS WITHOUT HIV?

Javier Rodríguez-Centeno^{1,2}, Julen Cadiñanos^{1,2}, Rocío Montejano^{1,2}, Andres Esteban-Cantos^{1,2}, Beatriz Mena-Garay¹, María Jimenez-Gonzalez¹, Gabriel Saiz-Medrano¹, Rosa de Miguel^{1,2}, Fernando Rodriguez-Artalejo¹, Jose Ignacio Bernardino^{1,2},

Cristina Marcelo-Calvo^{1,2}, Lucia Gutierrez-García¹,
Patricia Martínez-Martin^{1,2}, Berta Rodes^{1,2}, Jose Ramon Arribas^{1,2}

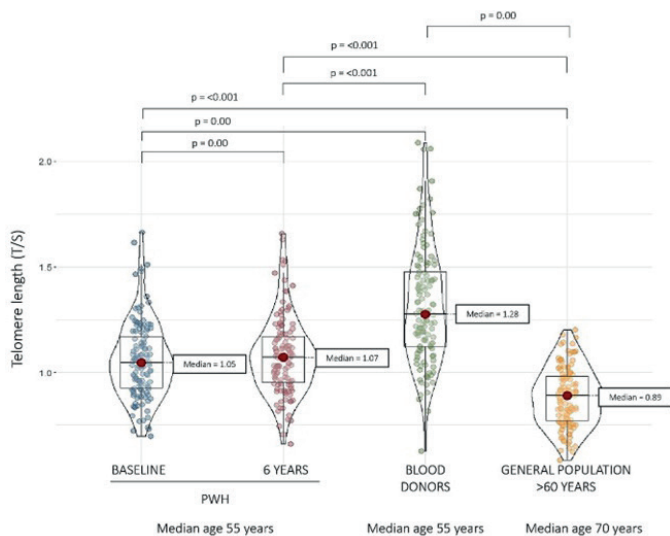
¹Hospital La Paz Institute for Health Research, Madrid, Spain. ²Centro de Investigación Biomédica en Red de Enfermedades Infecciosas (CIBERINFEC), Madrid, Spain

Introduction: Blood telomere length (BTL) attrition is a surrogate biomarker of immunosenescence and aging associated with HIV infection. BTL recovers in long-term virologically suppressed PWH, but it is unknown if recovery is complete compared with persons without HIV.

Objectives: In a prospective cohort of aviremic HIV infected adults to evaluate after six years of follow-up: 1. Sequential changes in BTL. 2. Differences in BTL versus HIV negative persons matched by age and sex and versus adults aged 60-80 years matched by sex.

Methods: Prospective 6-year observational study assessing the evolution of BTL in virologically suppressed PWH and a cross-sectional analysis comparing BTL with age and sex-matched blood donors, and sex matched persons older than 60 from a general population cohort. Relative BTL was determined by monochrome quantitative multiplex PCR assay and expressed as the ratio of telomere to single-copy gene (T/S).

Results: We included 128 PWH, 128 blood donors, and 128 persons over 60. Median age at 6 years of follow-up was 55 (IQR: 51.0-58.3), 55.2 (IQR: 67.5-73) and 55.2 (IQR: 51.3-59) years, respectively. 27.3 % were women in each group. In the PWH group 78.1% were active/former smokers, 93.0% had hazardous alcohol consumption, 32.0% had ever been injected drugs users, 92.2% were Caucasian, 34.4% resolved hepatitis C virus infection, 90.6% positive CMV IgG and 41.5% with ≥ 1 comorbidity. At 6 years of follow-up, the median time with known HIV-1 infection and virological suppression were 23.6 (IQR: 18.5-27.9) and 13.2 (IQR: 12.1-13.7) years, respectively. Nadir/current median CD4 count were 181.5 (IQR: 80.5-255) and 773.5 (IQR: 540-1,020) cells/ μ L, and the median CD4/CD8 ratio was 1.11 (IQR: 0.80-1.44). In the elderly population 9.6%, 45.2% and 45.2% were active, former and never smokers, respectively. BTL of PWH increased after 6 years of virological suppression (median BTL at baseline 1.04 [IQR: 0.93-1.16] vs. 1.07 [IQR:0.95-1.17] after 6 years [$p < 0.001$]), without reaching the median BTL of blood donors of the same age and sex (1.28 [IQR: 1.11-1.45]; $p < 0.001$), but significantly above the median BTL of the older than 60 general population group (0.89 [IQR: 0.77-0.97]; $p < 0.001$) (Figure).



Conclusions: During the 6 years of follow-up the median BTL of aviremic PWH increased but still was shorter than the BTL of age/sex matched blood donors. However, compared to the elderly population

our data do not support that aviremic PWH have a very pronounced BTL shortening.

Funding: This work was supported by the Fondo de Investigaciones Sanitarias, Instituto de Salud Carlos III (PI19/00294, PI18/01327, PI18/00569).

18. DETECTION/IDENTIFICATION OF THE MPOX VIRUS AND/OR OTHER ORTHOPOXVIRUSES BY MOLECULAR METHODS: CIBERINFEC QUALITY CONTROL

Ruben Cebrián^{1,2,3}, Miguel J. Martínez^{4,5}, Jessica Navero-Castillejos⁴, Anabel Negredo^{3,6}, Adolfo de Salazar^{1,2,3}, Juan Carlos Galán^{7,8}, Estrella Rojo Molinero^{3,9}, Eduardo Lagarejos¹⁰, Carmen Muñoz-Almagro^{8,11,12}, Águeda Hernández Rodríguez¹³, José Antonio Lepe^{3,14,15}, Andrés Antón Pagarolas¹⁶, Sonia Pérez Castro^{17,18}, María Isabel Zamora Cintas¹⁹, Marta Domínguez-Gil González^{8,20}, Jordi Niubo Bosch^{21,22}, Almudena Gutiérrez Arroyo²³, Ana Vázquez^{6,8}, Federico García^{1,2,3}, María Paz Sánchez-Seco Fariñas^{3,6}

¹Hospital Universitario Clínico San Cecilio, Granada, Spain. ²Instituto de Investigación Biosanitaria Ibs.Granada, Granada, Spain. ³Centro de Investigación Biomédica en Red de Enfermedades Infecciosas (CIBERINFEC), Madrid, Spain. ⁴Hospital Clinic de Barcelona, Barcelona, Spain. ⁵ISGlobal, Barcelona Centre for International Health Research (CRESIB), Hospital Clinic, Barcelona, Spain. ⁶Centro Nacional de Microbiología, Instituto de Salud Carlos III, Majadahonda, Spain. ⁷Servicio de Microbiología, Hospital Universitario Ramón y Cajal, Instituto Ramón y Cajal de Investigación Sanitaria (IRYCIS), Madrid, Spain. ⁸Centro de Investigación Biomédica en Red de Epidemiología y Salud Pública (CIBERESP), Madrid, Spain. ⁹Hospital Universitario Son Espases, Instituto de Investigación Sanitaria Islas Baleares (IdISBa), Palma de Mallorca, Spain. ¹⁰Hospital Universitario de Gran Canaria Dr. Negrín, Las Palmas de Gran Canaria, Spain. ¹¹Hospital Sant Joan de Deu, Barcelona, Spain. ¹²Departamento de Medicina, School of Medicine, Universitat Internacional de Catalunya, Barcelona, Spain. ¹³Servei de Microbiologia, Laboratori Clínic de la Metropolitana Nord, Hospital Universitari Germans Trias i Pujol, Barcelona, Spain. ¹⁴Hospital Universitario Virgen del Rocío, Sevilla, Spain. ¹⁵Instituto de Biomedicina de Sevilla (IBiS), Sevilla, Spain. ¹⁶Hospital Universitari Vall d'Hebron, PROSICS Barcelona, Universitat Autònoma de Barcelona, Barcelona, Spain. ¹⁷Complejo Hospitalario Universitario de Vigo, Vigo, Spain. ¹⁸Instituto de Investigación Sanitaria Galicia Sur (IIS Galicia Sur). SERGAS-UVIGO, Vigo, Spain. ¹⁹Hospital Central de la Defensa, Madrid, Spain. ²⁰Hospital Universitario Río Hortega, Valladolid, Spain. ²¹Laboratori Clínic Territorial Metropolitana Sud, Hospital Universitari de Bellvitge, Institut Català de la Salut (ICS), Hospitalet de Llobregat, Spain. ²²Bellvitge Biomedical Research Institute (IDIBELL), Hospitalet de Llobregat, Spain. ²³Hospital Universitario La Paz, Madrid, Spain.

Introduction: The Mpox virus (MPXV) is a double-stranded DNA virus belonging to the Orthopoxvirus (OPX) genus. In 2022, an outbreak of MPXV spread worldwide, reaching over 80,000 detected cases in more than 100 countries. Due to the lack of uniformity in the molecular diagnosis of this virus, quality control is necessary to evaluate diagnostic capacity in different centers.

Objectives: The aim of this study was to evaluate the molecular assays for OPX and MPXV diagnosis available in different Microbiology services in Spain through a Quality Control to determine analytical sensitivity, percentage agreements and compare them with those used in Reference Laboratories.

Methods: A total of 14 centers from across Spain participated in the study. From the Reference Laboratory, 8 serum samples (200 microliters) and 8 nucleic acid extractions (20 microliters) were sent to each of the participating centers. Some of the samples were contaminated with MPXV or another Orthopoxvirus (Vaccinia virus). Centers were asked to provide data on extraction method, diagnostic kit and results.

Results: Of the 14 participating centers, 2 performed determinations only for OPXV and 4 only for MPXV, while the rest of the centers performed determinations for both viruses. Among the 14 centers, 7 different commercial assays were used, with the most commonly used kit being LightMix Modular Orthopox/Monkeypox Virus (Roche®). Of the 12 centers that performed determinations for MPXV, a concordance of between 62.5% (1 center) and 100% (11 centers) was observed for eluate samples and between 75.0% (1 center) and 100% (10 centers) for serum samples. Of the 10 centers performing determinations for OPXV, a concordance of 100% was observed for eluate samples and between 87.5% (6 centers) and 100% (4 centers) for serum samples in the diagnosis of OPXV. A false negative was repeatedly observed in 6 different centers in a serum sample for the diagnosis of OPXV, in a sample with Ct values at the limit (39). On the other hand, one center reported false positives in the diagnosis of MPXV in samples positive for OPXV due to cross-reactivity with the TaqMan™ Monkeypox Virus Microbe Detection Assay (Thermo Fisher) technique.

Conclusions: The quality control results show a high correlation with those of the reference center. Specific cases of false positives/negatives were resolved thanks to this quality control. This study highlights the need for external quality controls when implementing new determinations in the microbiological diagnosis of infectious diseases.

Funding: This study was funded by the AES of CIBERINFEC MONKPOX-ESP22 World Package 5 (INFEC22PI01WP5).

26. EUCAST-OBTAINED OLOROFIM MICs AGAINST NON-FUMIGATUS ASPERGILLUS CLINICAL ISOLATES: HIGH AGREEMENTS BETWEEN VISUAL INSPECTIONS AND SPECTROPHOTOMETRIC READINGS

Julia Serrano Lobo, Ana Gómez, Elena Reigadas, Patricia Muñoz, Pilar Escribano, Jesús Guinea

Hospital General Universitario Gregorio Marañón, Madrid, Spain.

Introduction: We previously showed a high agreement between olorofim MIC values obtained by visual inspection and spectrophotometric readings against *Aspergillus fumigatus* sensu lato following EUCAST methodology (DOI: 10.1128/aac.00849-22).

Objectives: The objective of this work is to expand those comparisons against non-fumigatus *Aspergillus* spp. clinical isolates.

Methods: A total of 87 participating hospitals, covering all Spanish regions, stored, and identified *Aspergillus* spp clinical isolates – regardless their clinical significance – collected from the 1st of February to the 31st of March 2022. We here report a preliminary analysis of isolates (n = 439) collected at 55 hospitals and belonging to sections

Flavi (n = 89), *Nidulantes* (n = 55), *Nigri* (n = 192), and *Terrei* (n = 103). Antifungal susceptibility to olorofim was performed according to EUCAST 9.4 methodology. Visually-set MICs were compared with spectrophotometrically-obtained MICs (combinations of either ≥ 95% or ≥ 90% fungal growth inhibition endpoints compared to drug-free control endpoints and read at 540 nm). Essential (± 1 twofold dilution) agreement values were calculated and wild-type upper limits (wt-ULs) were set according to the eye-ball method (calculated as two two-fold dilutions higher than modal MIC).

Results: MIC distributions are shown in the Table. With only a few exceptions, olorofim MIC values were up to 0.03 mg/L against *Flavi* and *Terrei*, 0.06 mg/L against *Nidulantes*, and 0.125 mg/L against *Nigri*. Essential agreement between visually-obtained MIC values and spectrophotometric-obtained MIC values were higher when the ≥ 95% fungal growth inhibition endpoint was used (*Flavi* and *Terrei* [98.1%]; *Nidulantes* [96.4%]), except for section *Nigri* (Table). The fungal growth inhibition endpoints that led to modal MIC and wt-UL values identical to the ones obtained by visual inspections were: *Flavi* section (≥ 95%), *Nidulantes* section (≥ 95% or ≥ 90%), *Nigri* section (≥ 90%). In section *Terrei*, both endpoints led to lower modal MICs and wt-UL values (Table).

Conclusions: MICs of olorofim against non-fumigatus *Aspergillus* were low, showing the activity of the drug against the isolates tested. MIC values obtained by spectrophotometer and by visually inspection showed high agreement values, specially using the 95% fungal growth inhibition endpoint, against all section except *Nigri*.

Funding: This work was supported by grants PI21/00450 from Fondo de Investigación Sanitaria (FIS. Instituto de Salud Carlos III. Plan Estatal de Investigación Científica, Técnica y de Innovación 2021 –2023 (PEICTI)). The study was co-funded by the European Regional Development Fund (FEDER) 'A way of making Europe'. This study was partially funded by F2G.

27. EUCAST-OBTAINED MIC OF AZOLES AND AMPHOTERICIN B AGAINST ASPERGILLUS FUMIGATUS SENSU STRICTO: SPECTROPHOTOMETRIC READINGS VISUAL INSPECTIONS SHOWED HIGH AGREEMENT

Julia Serrano Lobo, Ana Gómez, Elena Reigadas, Patricia Muñoz, Pilar Escribano, Jesús Guinea

Hospital General Universitario Gregorio Marañón, Madrid, Spain.

Introduction: Previous studies show high essential and categorical agreements between MICs of azoles and amphotericin B obtained by spectrophotometric readings and visual inspection against *Aspergillus fumigatus*, according to EUCAST methodology. Visual MIC readings

Sections	Endpoints used to obtain the MIC	MIC distributions (no. of isolates at each MIC, mg/L)										EA (%)	wt-UL*	% non-wild isolates
		0.001	0.002	0.004	0.008	0.016	0.03	0.06	0.125	0.25	≥ 0.5			
Flavi (n = 89)	Visual	0	0	0	10	64	14	0	0	0	1	-	0.06	1.1
	95%	0	1	1	35	44	7	0	0	0	1	98.9	0.06	1.1
	90%	0	3	13	46	25	1	0	0	0	1	80.9	0.03	1.1
Nidulantes (n = 55)	Visual	0	0	3	7	30	12	2	0	1	0	-	0.06	1.8
	95%	0	3	1	4	34	11	0	0	1	1	96.4	0.06	3.6
	90%	0	3	2	10	34	4	0	0	1	1	90.9	0.06	3.6
Nigri (n = 192)	Visual	0	0	1	4	121	52	12	2	0	0	-	0.06	1.0
	95%	0	0	1	1	61	92	31	4	2	0	91.1	0.125	3.1
	90%	0	0	1	9	119	51	11	0	1	0	98.4	0.06	0.5
Terrei (n = 103)	Visual	0	0	27	65	9	1	0	0	0	1	-	0.03	1
	95%	0	3	49	46	3	1	0	0	0	1	98.1	0.016	1
	90%	0	14	67	19	2	0	0	0	0	1	91.3	0.016	1

Drug	Endpoints used to obtain the MIC	MIC distributions (no. of isolates at each MIC, mg/L)											EA (%)	CA (%)	VME (%)	ME (%)	wt-UL*	wt-UL**	EUCAST ECOFF
		0.016	0.03	0.06	0.125	0.25	0.5	1	2	4	8	16							
Amphotericin B	Visual	0	0	2	12	262	315	33	0	0	0	0	-	-	-	-	2	1	1
	95%	0	0	5	13	283	297	25	0	0	0	1	99.8	99.8	0	0.2	2	1	
	90%	0	0	7	13	312	275	16	0	0	0	1	99.8	99.8	0	0.2	1	1	
Itraconazole	Visual	1	4	1	36	366	197	4	0	0	0	15	-	-	-	-	1	1	1
	95%	1	4	2	68	365	162	7	0	0	0	15	98.7	99.4	0.3	0.3	1	1	
	90%	4	3	8	129	350	110	6	0	0	14	0	96.8	99.5	0.3	0.2	1	1	
Voriconazole	Visual	0	0	0	3	94	391	123	1	9	3	0	-	-	-	-	2	2	1
	95%	0	0	0	3	185	360	57	8	9	1	1	97.9	99	0	1	2	2	
	90%	0	0	7	11	312	255	24	9	6	0	0	92.3	99.7	0	0.3	1	2	
Posaconazole	Visual	6	146	371	82	5	13	1	0	0	0	0	-	-	-	-	0.25	0.25	0.25
	95%	8	233	301	56	10	12	1	3	0	0	0	98.4	99	0	0.8	0.25	0.5	
	90%	21	322	229	33	7	9	0	3	0	0	0	97.3	99	0.3	0.6	0.25	0.25	
Isavuconazole	Visual	0	0	0	1	10	388	204	6	2	11	2	-	-	-	-	2	4	2
	95%	0	0	1	3	22	417	157	8	4	9	3	99.2	99.5	0.2	0.3	2	4	
	90%	0	0	2	7	81	459	56	7	7	4	1	96.3	99.8	0.2	0.0	2	4	

EA, essential agreement; CA, categorical agreement; VME, very major error; ME, major error. Numbers in bold indicate modal MIC. *Two two-fold dilutions higher than the modal MIC. **99% of the isolates inhibited.

requires experiences and may lead to some degree of subjectivity. In contrast, spectrophotometric reading is more objective and automated and thus requires less skilled readers.

Objectives: The objective of this work is to assess such comparisons, paying special attention to the MIC distributions (modal MIC and wild type upper limits [wt-UL]) obtained by using each endpoint.

Methods: A total of 87 participating hospitals, covering all Spanish regions, stored, and identified *Aspergillus* spp clinical isolates – regardless their clinical significance – collected from the 1st of February to the 31st of March 2022. We here report a preliminary analysis of *A. fumigatus* sensu stricto isolates (n = 624) collected at 55 hospitals, including 15 azole-resistant isolates with the following cyp51A gene mutations: TR34-L98H (n = 12), and other substitutions (n = 3). Antifungal susceptibility to amphotericin B, itraconazole, voriconazole, posaconazole, and isavuconazole was performed according to EUCAST 9.4 methodology. Visually-set MICs were compared with spectrophotometrically-obtained MICs (fungal growth reduction $\geq 95\%$ and $\geq 90\%$ compared to control and read at 540 nm); essential (± 1 twofold dilution) and categorical agreement were calculated. Errors were classified as very major (isolate classified as resistant by visual MIC and as susceptible by spectrophotometric reading) and major (isolate classified as susceptible by visual MIC and as resistant by spectrophotometric reading). wt-ULs were set according to the eye-ball method.

Results: Essential and categorical agreement values were 98.8% and 99.4% ($\geq 95\%$ fungal inhibition endpoint), and 96.5% and 99.6% ($\geq 90\%$ fungal inhibition endpoint), respectively. No very major errors were found with amphotericin B or voriconazole. Very few very major errors were detected in itraconazole (n = 2), isavuconazole (n = 1), or posaconazole (n = 2, one involving an isolate harbouring the TR34-L98H substitutions). Values of wt-UL were not affected by the fungal inhibition endpoints studied; however the modal MIC in the distributions may be one two-fold dilution lower when the $\geq 90\%$ fungal inhibition endpoint was used.

Conclusions: MICs of azoles and amphotericin B against *A. fumigatus* sensu stricto obtained either by spectrophotometer or visually showed very high agreement. Essential agreement was slightly higher when spectrophotometric endpoint was $\geq 95\%$. Categorical agreement was almost identical.

Funding: This work was supported by grants PI21/00450 from Fondo de Investigación Sanitaria (FIS. Instituto de Salud Carlos III. Plan Estatal de Investigación Científica, Técnica y de Innovación 2021–2023 (PEICTI)). The study was co-funded by an investigational grant by Gil-ead Ltd.

31. INFLUENCE OF THE GEOGRAPHICAL ORIGIN OF THE PARASITE ON THE SIZE OF *S. HAEMATOBIIUM* SUB-SAHARAN EGGS

María Cecilia Fantozzi^{1,2}, Marta Reguera-Gómez¹, María Adela Valero^{1,2}, Patricio Artigas^{1,2}, Alejandra de Elías-Escribano^{1,2}, María Pilar Luzón-García³, Joaquín Salas-Coronas³, Jerome Boissier⁴, Santiago Mas-Coma^{1,2}, María Dolores Bargues^{1,2}

¹Departamento de Parasitología, Facultad de Farmacia, Universidad de Valencia, Valencia, Spain. ²Centro de Investigación Biomédica en Red de Enfermedades Infecciosas (CIBERINFEC), Instituto de Salud Carlos III, Madrid, Spain. ³Unidad de Medicina Tropical, Hospital Universitario Poniente, Almería, Spain. ⁴Host Pathogen Environments Interactions (IHEP) Laboratory, University of Montpellier, CNRS, IFREMER, University of Perpignan, Perpignan, France.

Introduction: Schistosomiasis is a Neglected Tropical Disease caused by trematode species of the genus *Schistosoma*. Both, autochthonous and imported cases of urogenital schistosomiasis have been described in Europe. Schistosome eggs play an important role in schistosomiasis diagnosis. Previous studies characterizing *S. haematobium* eggs showed great variability in their phenotype measurements, demonstrating the necessity of new studies focused on the influence of distinct factors that may potentially be involved, such as the geographical origin of the parasites.

Objectives: In the present work, the intraspecific variability of *Schistosoma haematobium* eggs, found in sub-Saharan migrants present in Spain, associated with the country of origin of the parasite, is characterized, as well as, the phenotypes present in each country, using the previously proposed methodology.

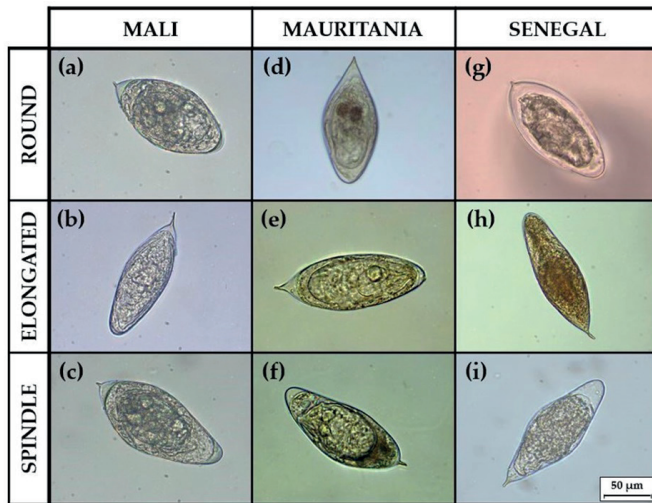
Methods: Only eggs considered “pure” *S. haematobium* by genetic characterization (rDNA ITS-2 and mtDNA cox1) have been used. A total of 162 eggs obtained from 20 migrants from Mali (n = 11), Mauritania (n = 4) and Senegal (n = 5) living in Spain and diagnosed with urogenital schistosomiasis, were included in the study. For the morphometric phenotyping seventeen standardised measurements were applied to each individualized egg. Image Pro Plus software was used. CVA and Mahalanobis distances were performed using the CLIC package and the available online XYOM software.

Results: Three morphotype classes were described based on the results of the Egg Shape Ratio (ESR) (Figure): (a) morphotype round (ESR < 2.00) (N = 55, 34.0%); (b) morphotype elongated (2.01 < ESR < 2.29) (N = 62, 38.3%); and (c) morphotype spindle (ESR > 2.30) (N = 45, 27.7%). Overall, *S. haematobium* eggs from Senegal showed the

greatest length, area, perimeter and radius. Eggs from Mali have greater roundness and spine medium width (SMW), while Mauritanian eggs are characterized by the smallest radius and width. Mahalanobis distances, when all egg measurements were analyzed, showed differences between: (i) Mali-Mauritania, Mali-Senegal and Mauritania-Senegal in the round morphotype; (ii) Mali-Mauritania and Mauritania-Senegal in the elongated morphotype; and (iii) Mauritania-Senegal in the spindle morphotype. Mahalanobis distances, when spine variables were analyzed, showed differences between Mali-Senegal in the round morphotype (Table).

Mahalanobis distances between the three *S. haematobium* populations (Mali, Mauritania and Senegal) for the two discriminant analyses performed: (a) all measurements (17) and (b) spine measurements. * Statistically different over 1,000 permutations using the Bonferroni correction ($p < 0.05$)

(a)	Mali	Mauritania	Senegal
Mali	0.00		
Mauritania	1.68*	0.00	
Senegal	1.23*	1.71*	0.00
(b)	Mali	Mauritania	Senegal
Mali	0.00		
Mauritania	0.59*	0.00	
Senegal	0.64*	0.62	0.00



Representative *S. haematobium* egg samples of the different morphotypes from each country: (a) round, (b) elongated and (c) spindle eggs from Mali; (d) round, (e) elongated, and (f) spindle eggs from Mauritania; (g) round, (h) elongated, and (i) spindle eggs from Senegal.

Conclusions: This is the first phenotypic study performed on individually genotyped “pure” *S. haematobium* eggs, allowing the assessment of the intraspecific morphological variations associated with the geographical origin of the schistosome eggs. The results suggest that *S. haematobium* eggs show great shape variability within the three populations, and, unexpectedly, round or elongated shapes are not always the most common phenotypes of genetically “pure” *S. haematobium* eggs, as previously believed.

Funding: Red de Investigación de Centros de Enfermedades Tropicales—RICET (RD16/0027/0013 and RD16/0027/0023), ISCIII-Subdirección General de Redes y Centros de Investigación Cooperativa RETICS, Ministry of Health and Consumption and European FEDER funds, Madrid; Centro de Investigación Biomédica en Red de Enfermedades Infecciosas (CIBERINFEC) (CB21/13/00056 and IM22/INF/6), ISCIII, Ministry of Science and Innovation and European Union—NextGenerationEU; PROMETEO Program, Programa de Ayudas para Grupos de Investigación de Excelencia (2021/004), Generalitat Valenciana, Valencia. M.C.F. is currently a recipient of a fellowship (CIA-POS/2021/166).

32. ZONOTIC ROCAHEPEVIRUS RATTI IN RODENTS IN SPAIN

Javier Caballero Gómez^{1,2,3}, Tomás Fajardo Alonso^{1,2,3}, Ignacio García Bocanegra^{1,3}, Adrián Beato Benítez¹, Rosario Panadero⁴, Remigio Martínez^{1,5}, Moisés González^{1,6}, Rafael Guerra⁷, Débora Jiménez Martín¹, Eva Martínez Nevado⁸, David Cano Terriza^{1,3}, Pilar Soriano⁹, Miguel Ángel Quevedo¹⁰, Andrea González¹¹, Santiago Borragán¹², Raúl Cuadrado Matías¹³, Dietmar Crailsheim¹⁴, Andrea Carretero Alonso¹⁵, Antonio Rivero^{2,3}, Antonio Rivero Juárez^{2,3}

¹Departamento de Sanidad Animal, Grupo de Investigación GISAZ, UIC Zoonosis y Enfermedades Emergentes ENZOEM, Universidad de Córdoba, Córdoba, Spain. ²Grupo de Virología Clínica y Zoonosis, Unidad de Enfermedades Infecciosas, Instituto Maimónides de Investigación Biomédica de Córdoba (IMIBIC), Hospital Universitario Reina Sofía, Universidad de Córdoba, Córdoba, Spain. ³Centro de Investigación Biomédica en Red de Enfermedades Infecciosas (CIBERINFEC), Madrid, Spain. ⁴Investigación en Sanidad Animal: Galicia (Grupo INVESAGA), Facultad de Veterinaria, Universidad de Santiago de Compostela, Lugo, Spain. ⁵Departamento de Sanidad Animal, Facultad de Veterinaria, Universidad de Extremadura, Cáceres, Spain. ⁶Departamento de Sanidad Animal, Facultad de Veterinaria, Campus de Excelencia Internacional Regional “Campus Mare Nostrum”, Murcia, Spain. ⁷Centro de Conservación Zoo Córdoba, Córdoba, Spain. ⁸Zoo Aquarium de Madrid, Madrid, Spain. ⁹Rio Safari Elche, Alicante, Spain. ¹⁰Zoobotánico Jerez, Jerez de La Frontera, Spain. ¹¹Fundación Zoo Santillana, Santillana Del Mar, Spain. ¹²Parque de la Naturaleza de Cabárceno, Obregón, Spain. ¹³Grupo Sanidad y Biotecnología (SaBio), Instituto de Investigación en Recursos Cinegéticos, Ciudad Real, Spain. ¹⁴Centro de Recuperación de Primates Fundación Mona, Girona, Spain. ¹⁵Centro de Rescate de Primates Fundación Rainfer, Madrid, Spain.

Introduction: An increasing number of cases of acute and chronic hepatitis associated with the recently considered zoonotic *Rocahepevirus ratti* (RHEV) has been reported during the last few years in Hong Kong, Canada, China, and more recently in Spain. Although rodents are the main reservoirs of this emerging virus, large-scale studies to assess the circulation of this pathogen in these species have not been conducted to date in Spain.

Objectives: The main aims of this study were to determine the prevalence of RHEV infection in urban and periurban rodents from Spain and to assess the risk of transmission from these to other sympatric species, including humans.

Methods: During the period 2020-2022, liver samples from 342 rodents, including 212 Norway rats (*Rattus norvegicus*), 60 water voles (*Arvicola scherman*), 51 mouse (*Mus musculus*), 14 European moles (*Talpa europaea*) and 5 black rats (*Rattus rattus*), were collected throughout Spain. The presence of active RHEV infection was assessed by two real time RT-PCRs assays and phylogenetic analyses were carried out using two nested RT-PCRs.

Results: A total of 73 (21.3%; 95%CI: 17.1-25.8) of the 342 analyzed rodents were positive to RHEV RNA. By species, the prevalence of infection was 29.7% in Norway rats, 19.6% in mouse and 0% in water voles, European mole and black rats. Infected rodents were detected in seven (58.3%) of the 12 provinces sampled, with frequency of positivity ranging from 6.3% to 70.5%. Phylogenetic analyses showed a nucleotide identity of 89.0-99.5% with other RHEV previously detected in rodents and humans from different European countries, including Spain.

Conclusions: The prevalence of RHEV detected in Norway rats and mouse populations of this country is of public health concern. The high homology with other hepevirus sequences obtained in these species and in humans point the risk of zoonotic transmission of RHEV from urban and periurban rodents.

Funding: This work was supported by the Ministerio de Sanidad (RD12/0017/0012) integrated in the Plan Nacional de I+D+I and cofinanced by the ISCIII-Subdirección General de Evaluación and the Fon-

do Europeo de Desarrollo Regional (FEDER), Fundación para la Investigación en Salud (FIS) del Instituto Carlos III (PI19/00864 and PI21/00793). This research was supported by CIBER –Consortio Centro de Investigación Biomédica en Red– (CB 2021), Instituto de Salud Carlos III, Ministerio de Ciencia e Innovación and Unión Europea-Next-GenerationEU.

35. ALTERED MICRORNA EXPRESSION IN SERUM AND SALIVA SAMPLES FROM ASYMPTOMATIC AND MILD COVID-19 CASES

Angélica Domínguez de Barros¹, Malena Gajate Arenas¹, Omar García Pérez¹, Candela Sirvent Blanco¹, Javier Chao Pellicer^{1,2}, Roberto Dorta Guerra^{1,3}, José E Piñero^{1,2,4}, Jacob Lorenzo Morales^{1,2,4}, Elizabeth Córdoba Lanús^{1,2}

¹Instituto Universitario de Enfermedades Tropicales y Salud Pública de Canarias (IUETSPC). Universidad de La Laguna, La Laguna, Santa Cruz de Tenerife, Spain. ²Centro de Investigación Biomédica en Red de Enfermedades Infecciosas (CIBERINFEC), Madrid, Spain. ³Departamento de Matemáticas, Estadística e Investigación Operativa, Facultad de Ciencias, Universidad de La Laguna, La Laguna, Santa Cruz de Tenerife, Spain. ⁴Departamento de Obstetricia y Ginecología, Pediatría, Medicina Preventiva y Salud Pública, Toxicología, Medicina Legal y Forense y Parasitología, La Laguna, Santa Cruz de Tenerife, Spain.

Introduction: Host-encoded microRNA (miRNA) response to SARS-CoV-2 infection has been reported to be altered mostly in relation to severe COVID-19 cases. However, there is scarce information in relation to host miRNAs profiles in asymptomatic or mild symptomatic COVID-19 cases, that might also provide important insights into both viral pathogenesis and patient management.

Objectives: The aim of the present study was to determine a potential miRNAs profile to be altered in asymptomatic/mild COVID-19 cases in different biological samples such as serum or oropharyngeal/saliva samples.

Methods: Circulating miRNAs from serum and oropharyngeal/saliva belonging to eight asymptomatic or mild symptomatic COVID-19 patients and eight age and gender matched healthy controls were determined by NGS. RNA was isolated and converted into miRNA NGS libraries to subsequent sequence on a NextSeq (Illumina Inc.) instrument. In silico analysis was performed for target prediction.

Results: We observed 18 miRNAs significantly dysregulated in serum from asymptomatic/mild symptomatic COVID-19 cases when compared to healthy controls, being miR-485-3p and miR-143 the most up-regulated (Log₂FC = 3.77 and 3.23, FDR = 2.2e-7 and 0.0018, respectively) while miR-12136 and miR-1275 were the most down-regulated ones (Log₂FC = -4.70 and -3.05, FDR = 5.2⁻⁸ and 0.000073, respectively). The oropharyngeal/saliva samples from the same individuals presented the miR-3195 as the strongly up-regulated miRNA (Log₂FC = 5.24, FDR = 0.00027). The principal component analysis (PCA) revealed that the miRNA profile based on 500 dysreg-

ulated miRNAs could independently classified serum from nasopharyngeal samples of COVID-19 cases.

Conclusions: This study demonstrates that SARS-CoV-2 infection induces a robust host miRNA response also in asymptomatic or mild COVID-19 cases. miR-485-3p is a promising useful inflammatory biomarker while miR-143-5p may efficiently combat SARS-CoV-2 by reducing host cell apoptosis via mTOR. Validation of the present findings in a large patient cohort are warranted.

Funding: CB21/13/00100 (CIBERINFEC), Instituto de Salud Carlos III, Spain.

36. MALARIA DIAGNOSIS USING A COMBINED SYSTEM OF A SIMPLE AND FAST EXTRACTION METHOD WITH A LYOPHILISED DUAL-LAMP ASSAY IN A NON-ENDEMIC SETTING

Alexandra Martín Ramírez^{1,2}, Lourdes Barón Argos³, Marta Lanza Suárez³, Ana Pérez-Ayala⁴, José M. Rubio Muñoz⁵

¹Centro de Investigación Biomédica en Red de Enfermedades Infecciosas (CIBERINFEC), Instituto de Salud Carlos III, Madrid, Spain. ²Laboratorio de Malaria y Parásitos Emergentes, Instituto de Salud Carlos III, Madrid, Spain. ³Laboratorio de Malaria y Parásitos Emergentes, Instituto de Salud Carlos III, Madrid, Spain. ⁴Servicio de Microbiología, Hospital Universitario Doce de Octubre, Madrid, Spain. ⁵Laboratorio de Malaria y Parásitos Emergentes, Instituto de Salud Carlos III, Madrid, Spain.

Introduction: Malaria is the most important parasitic disease in humans, with 247 million malaria cases in 2021 worldwide. Malaria LAMP methods are more sensitive and specific than conventional methods, however they have some limitations.

Objectives: This study aims to solve some limitations of LAMP assays with the optimization and validation of a Dual-LAMP assay using a simple purification method, two ways of result readings, the incorporation of a reaction control and lyophilisation of reagents.

Methods: A total number of 523 samples were used in this study. Six Dual-LAMP assays (Dual-LAMP-Plasmodium spp., Dual-LAMP-P. falciparum, Dual-LAMP-P. vivax, Dual-LAMP-P. ovale, Dual-LAMP-P. malariae and Dual-LAMP-P. knowlesi), were validated retrospectively with column purification method; meanwhile 95 samples were used prospectively with Dual-LAMP-Pspp and Dual-LAMP-Reaction Control assays, using a new saline extraction and the column purification methods. Result readings were based on colorimetry and fluorescence (Figure). Nested Multiplex-PCR was the reference method. Dual-LAMP-RC and Dual-LAMP-Pspp assays were lyophilised in set of three tubes and assessed with 64 samples extracted by both purification methods.

Results: Limit of Detection for the Dual-LAMP-Pspp assay was 1.22 parasites/μl and 5.82 parasites/μl when column or saline DNA extraction methods were used, respectively, without differences in result readings. No cross-reactivity with any of the samples tested was found with Dual-LAMP-Pspp assay. Quantitative result obtained with the fluorescence reading showed a linear relationship with parasite concentration (R² = 0.618 with saline and R² = 0.779 with column extracted samples). Retrospective assessment of the six Dual-LAMP assays provided 100% sensitivity for the Dual-LAMP-Pf and Dual-LAMP-Pv assays and 100% specificity for Dual-LAMP-Pf, Dual-LAMP-Pm, Dual-LAMP-Po and Dual-LAMP-Pk assays (Table). Agreement between the Dual-LAMP-Pspp assay with column and saline purified samples was 88.04% for colorimetric and 90.22% for fluorescence reading. Dual-LAMP-RC assay showed color change and fluorescence amplification with both purification methods in Plasmodium spp. positive and negative samples, meanwhile no-DNA controls were negative. Lyophilised sets of three tubes yield 100% agreement between Dual-LAMP-Pspp assay and NM-PCR with both extraction and result readings methods.

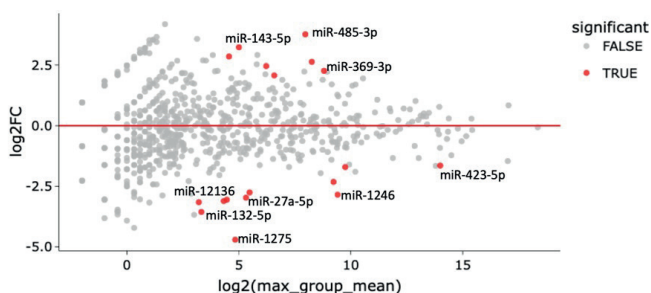
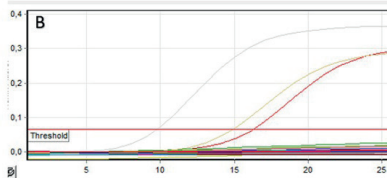
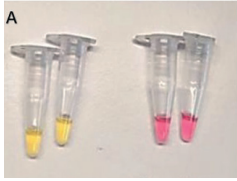


Figure 1. Each gene's fold change (FC) is plotted against its mean expression among all serum samples. All significantly differentially expressed genes are marked in red. Significant changes are defined as p-value < 0.001, FDR < 0.01, and Log₂FC > 2.

	Value (95%CI)	Sensitivity	Specificity	PPV	NPV	Kappa coefficient
Dual-LAMP-Plasmodium spp. assay	Colorimetric reading	95.4% (90.4%-100%)	96.3% (91.5%-100%)	96.5% (92.1%-100%)	95.1% (89.7%-100%)	0.92 (0.86-0.98)
	Fluorescence reading	96.5% (92.1%-100%)	97.5% (93.5%-100%)	97.7% (93.9%-100%)	96.3% (91.6%-100%)	0.94 (0.88-0.99)
Dual-LAMP-P. falciparum assay	Colorimetric reading	100% (98.5%-100%)	100% (98.9%-100%)	100% (98.5%-100%)	100% (98.7%-100%)	1 (1.00-1.00)
	Fluorescence reading	100% (98.5%-100%)	100% (98.9%-100%)	100% (98.5%-100%)	100% (98.7%-100%)	1 (1.00-1.00)
Dual-LAMP-P. vivax assay	Colorimetric reading	100% (98.5%-100%)	96.6% (88.2%-100%)	97.1% (90.2%-100%)	100% (98.2%-100%)	0.97 (0.91-1.0)
	Fluorescence reading	100% (98.5%-100%)	96.6% (88.2%-100%)	97.1% (90.2%-100%)	100% (98.2%-100%)	0.97 (0.91-1.0)
Dual-LAMP-P. ovale assay	Colorimetric reading	90.9% (69.4%-100%)	100.0% (92.9%-100.0%)	100.0% (95.0%-100.0%)	87.5% (58.3%-100%)	0.89 (0.67-1.10%)
	Fluorescence reading	90.9% (69.4%-100%)	100.0% (92.9%-100.0%)	100.0% (95.0%-100.0%)	87.5% (58.3%-100%)	0.89 (0.67-1.10%)
Dual-LAMP-P. malariae assay	Colorimetric reading	75.0% (20.1%-95.4%)	100.0% (90.0%-100.0%)	100.0% (83.3%-100.0%)	83.3% (45.2%-97.0%)	0.77 (0.35-1.0%)
	Fluorescence reading	75.0% (20.1%-95.4%)	100.0% (90.0%-100.0%)	100.0% (83.3%-100.0%)	83.3% (45.2%-97.0%)	0.77 (0.35-1.0%)
Dual-LAMP-P. knowlesi assay	Colorimetric reading	83.3% (45.2%-100%)	100.0% (83.3%-100.0%)	100.0% (90.0%-100.0%)	75.0% (20.1%-100%)	0.77 (0.35-1.0%)
	Fluorescence reading	83.3% (45.2%-100%)	100.0% (83.3%-100.0%)	100.0% (90.0%-100.0%)	75.0% (20.1%-100%)	0.77 (0.35-1.0%)



A) Colorimetric result reading: yellow tubes indicate positive results; meanwhile pink tubes are negative results. B) Fluorescence result reading: fluorescence above the threshold are considered positive results, with the T_a as the minutes until fluorescence overtake the threshold.

Conclusions: This study outlines the ability of six Dual-LAMP assays for malaria diagnosis. Dual-LAMP-Pspp assay with the addition of Dual-LAMP-RC assay and the possibility of a simple and fast purification provided low limit of detection and no cross-reactivity. Reagents lyophilisation plus the chance to read the results in two ways allow their application in many settings.

Funding: This work was supported by the Spanish Strategic Health Action [Grant number PI17CIII/00035, PI22CIII/00033]. Alexandra Martín Ramírez was supported by a grant from ISCIII-Río Hortega [Grant number CM17CIII/00012].

37. EPIGENETIC AGEING ACCELERATES BEFORE ANTIRETROVIRAL THERAPY AND DECELERATES AFTER VIRAL SUPPRESSION IN PEOPLE WITH HIV IN SWITZERLAND: A LONGITUDINAL STUDY OVER 17 YEARS

Isabella Schoepf¹, Andrés Esteban-Cantos², Christian W. Thorball³, Berta Rodés⁴, Peter Reiss⁵, Javier Rodríguez-Centeno⁴, Carlotta Ribensahm⁶, Dominique L Braun⁷, Catia Marzolini⁸, Marco Seneghini⁹, Enos Bernasconi¹⁰, Matthias Cavassini¹¹, H el ene Buvelot¹², Maria Christine Thurnheer⁶, Roger D. Kouyou¹³, Jacques Fellay³, Huldrych F G unthard¹³, Jos e Ram on Arribas⁴, Bruno Ledergerber¹³, Philip E.E. Tarr¹

¹University of Basel, Basel, Switzerland. ²CIBERINFEC-IdiPAZ, Madrid, Spain. ³Centre hospitalier universitaire vaudois, Lausanne, Switzerland. ⁴IdiPAZ-CIBERINFEC, Madrid, Spain. ⁵University of Amsterdam, Amsterdam, The Netherlands. ⁶Bern University Hospital, Bern, Switzerland. ⁷University Hospital Zurich, Zurich, Switzerland. ⁸University of Zurich, Zurich, Switzerland. ⁹Division of Infectious Diseases, Kantonsspital St Gallen, St Gallen, Switzerland. ¹⁰Division of Infectious Diseases, Ente Ospedaliero Cantonale, University of Geneva, Geneva, Switzerland. ¹¹Infectious Diseases Service, Lausanne University Hospital, Lausanne, Switzerland. ¹²Division of Infectious Disease, Geneva University Hospital, Geneva, Switzerland, Geneva, Switzerland. ¹³Department of Infectious Diseases and Hospital Epidemiology, University Hospital Zurich, Zurich, Switzerland

Introduction: Epigenetic age is an accurate predictor of biological age based on changes in DNA methylation. Accelerated epigenetic ageing

can occur in untreated HIV infection and is partially reversible with effective antiretroviral therapy (ART).

Objectives: To assess a long-term comparison of epigenetic ageing dynamics in people with HIV during untreated HIV infection and during suppressive ART.

Methods: In this longitudinal study conducted over 17 years, we applied 5 established epigenetic age estimators (Horvath's clock, Hannum's clock, SkinBlood clock, PhenoAge and GrimAge) in peripheral blood mononuclear cells in Swiss HIV Cohort Study participants before or during suppressive ART. All participants had a longitudinal set of samples available at four timepoints. We assessed epigenetic age acceleration (EAA) and a novel rate of epigenetic ageing.

Results: We analysed 80 people with HIV from the Swiss HIV Cohort Study. 52 (65%) of patients were men, 76 (95%) were white, and the median patient age was 43 (IQR 37.5-47) years. Per year of untreated HIV infection (median observation 8.08 years, IQR 4.83-11.09), mean EAA was 0.47 years (95%CI 0.37-0.57) for Horvath-EAA, 0.43 years (0.3-0.57) for Hannum-EAA, 0.36 years (0.27-0.44) for SkinBlood-EAA, and 0.69 years (0.51-0.86) for PhenoAge-EAA. Per year of suppressive ART (median observation 9.8 years, IQR 7.2-11), mean EAA was -0.35 years (95%CI -0.44 to -0.27) for Horvath-EAA, -0.39 years (-0.50 to -0.27) for Hannum-EAA, -0.26 years (-0.33 to -0.18) for SkinBlood-EAA, and -0.49 years (-0.64 to -0.35) for PhenoAge-EAA. These findings indicate that people with HIV epigenetically aged by 1.47 years for Horvath, 1.43 years for Hannum, 1.36 years for SkinBlood, and 1.69 years for PhenoAge, per year of untreated HIV infection; and 0.65 years for Horvath, 0.61 years for Hannum, 0.74 years for SkinBlood, and 0.51 years for PhenoAge, per year of suppressive ART. GrimAge showed little change in the mean EAA during untreated HIV infection (0.1 years, 0.02 to 0.19) and suppressive ART (-0.05 years, -0.12 to 0.02). We obtained very similar results using the rate of epigenetic ageing. Contribution of multiple HIV-related, antiretroviral, and immunological variables to epigenetic ageing was not significant.

Conclusions: In a longitudinal study over 17 years, epigenetic ageing accelerated during untreated HIV infection and decelerated during suppressive ART, highlighting the importance of limiting the duration of untreated HIV infection including early ART start.

Funding: Swiss HIV Cohort Study, Swiss National Science Foundation, Gilead Sciences.

39. MULTIPARAMETRIC CHARACTERIZATION OF TELOMERE LENGTH IN T CELLS FROM PLWH BY FULL SPECTRUM FLOW-FISH

Macedonia Trigueros¹, Maria Nevt¹, Francisco Mu oz-L pez¹, Ana Mart nez², Sandra Gonzalez², Jordi Puig², Cora Loste², Patricia Echevarria², Diana Hern andez², Marco A. Fern andez³, Juli a Blanco¹, Eugenia Negrodo², Marta Massanella¹

¹IrsiCaixa-AIDS Research Institute and Germans Trias i Pujol Health Research Institute, Badalona, Spain. ²Fundaci  Lluita contra les Infecci ns, Germans Trias Pujol Health Research Institute, Badalona,

Spain. ³Flow Cytometry Facility, Germans Trias i Pujol Health Science Research Institute, Badalona, Spain.

Introduction: People living with HIV (PLWH) on antiretroviral therapy (ART) present higher prevalence of ageing-associated morbidities than uninfected individuals.

Objectives: We assessed markers of immunosenescence in CD4 and CD8 T cells from well clinically characterized older PLWH and HIV-negative individuals.

Methods: We included 27 PLWH on ART and 24 HIV-negative controls (HNC) from the OVER50 cohort. We performed a multiparametric flow-FISH technique on frozen PBMCs to simultaneously assess the relative telomere length (RTL) of T cells with a telomere-specific peptide nucleic acid probe by spectral flow cytometry, using 1301 cells as reference. We studied the frequency and RTL of CD4 and CD8 T cell subsets (CD45RA, CCR7, CD27, CD28 CD25, CD127), and activated (HLA-DR+CD38+), senescent (CD57+, KRLG1+) and exhausted (PD-1+) cells.

Results: PLWH were 85% males with a median age of 72 IQR [70-75] years and on suppressive ART for a median of 16 IQR [8-20] years. HNC were matched by age and gender (79% males, median age 73 IQR [69-75] years). Clinically, there were no significant differences in the number of comorbidities between PLWH and HNC (median 3.6 IQR [2-5] and 3.25 IQR [2-5], respectively). Only dyslipidemia was significantly higher in PLWH (70%) compared with uninfected group (17%, $p < 0.01$). The frequency of total CD4 T cells was lower in PLWH compared to HNC group ($p < 0.01$), while no major differences in the CD4 T-cell maturation subsets or T-regulatory cells were found. No differences were observed in the RTL in total or CD4 T cell subsets, except for transitional memory (TM, $p = 0.09$) and effector memory ($p = 0.06$) cells from PLWH, which tended to have shorter RTL than HNC. PLWH show higher frequencies of total CD8 T cells than HNC ($p < 0.01$), but CD8 T-cell distribution was similar between groups. We did not observe differences in RTL in total CD8 T cell between groups, whereas naïve ($p = 0.06$), central memory (CM, $p = 0.03$) and TM ($p = 0.05$) CD8 T cell subsets showed shorter RTL in PLWH compared to HNC. The frequencies of senescent, exhausted and activated CD4 and CD8 T cells were similar between groups, and no differences in the RTL in these subsets were observed.

Conclusions: Flow-FISH technique using full spectrum flow cytometry allowed a deep immune-characterization of the RTL in total and CD4 and CD8 T cell subsets from older PLWH and uninfected controls. Limited differences in RTL were observed between groups, suggesting similar immunoageing status in older individuals independently of HIV serostatus.

Funding: Proyecto PID2020-114929RA-I00 financiado por MCIN/AEI/10.13039/501100011033. Ayuda RYC2020-028934-I financiada por MCIN/AEI/10.13039/501100011033 y por el FSE invierte en tu futuro. PERIS:SLT017/20/000095.

40. FORECASTING THE GEOGRAPHICAL DISTRIBUTION OF RISKY AREAS WEST NILE VIRUS IN SPAIN

Patricio Artigas^{1,2}, Pablo Cuervo^{1,2,3}, Santiago Mas-Coma^{1,2}, María Cecilia Fantozzi^{1,2}, María Dolores Bargues^{1,2}

¹Universitat de València, Valencia, Spain. ²L Centro de Investigación Biomédica en Red de Enfermedades Infecciosas (CIBERINFEC), Instituto de Salud Carlos III, Madrid, Spain. ³Laboratorio de Ecología de Enfermedades, Instituto de Ciencias Veterinarias del Litoral (ICIVET-Litoral), Universidad Nacional del Litoral (UNL)/Consejo Nacional de Investigaciones Científicas y Técnicas (CONICET), Esperanza, Argentina.

Introduction: West Nile virus (WNV), a well-known emerging vector-borne arbovirus with a zoonotic life cycle, represents a threat to

both public and animal health. Transmitted by ornithophilic mosquitoes, its transmission is difficult to predict and even more difficult to prevent. The massive and unprecedented number of human cases and equid outbreaks in Spain during 2020 interpellates for new approaches.

Objectives: Provide an insight to the situation of West Nile Disease (WND) in Spain, from the perspective of the ecological niches defining the circulation of WNV and the presence of its main vectors.

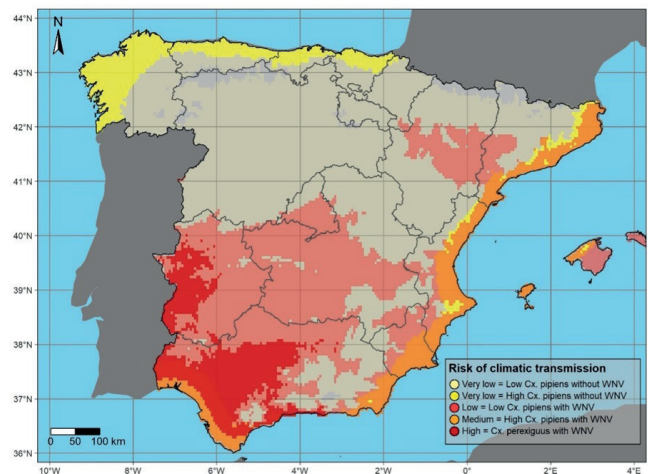
Methods: Applying niche model techniques, we modelled the climatic conditions suitable for the circulation and occurrence of outbreaks of WND in Spain, as well as for the presence of its main vectors *Culex pipiens* and *Culex perexiguus* with molecular identification. A total of 19,710 models were calibrated. Each model was evaluated for statistical significance (partial ROC tests), performance (omission rate) and the Akaike Information Criterion corrected for small sample sizes (AICc). A map of climatic risk of transmission was constructed considering the overlapping areas of the 10th-percentile thresholded binary maps with low uncertainty, which delimited suitable areas for circulation of WNV and for the presence of its vectors.

Results: After spatial filtering and removal of duplicates, global occurrences were reduced to: 62 records of *C. pipiens*, 16 records of *C. perexiguus* and 105 outbreak records of WND in equids. Maps of the climatic suitability for the presence of the two vectors species and for the circulation of WNV are provided (Table). The main outcome of our study is a map delineating the areas under certain climatic risk of transmission. Our analyses indicate that the climatic risk of transmission of WND is medium in areas nearby the south Atlantic coastal area of the Cadiz Gulf and the Mediterranean coast, and high in south-western Spain (Figure).

Table 1 Schematic representation of the criteria adopted to determine the climatic risk of transmission

Risk	Presence of suitable conditions		
	West Nile	<i>Culex pipiens</i>	<i>Culex perexiguus</i>
Very low	▼	▼/▲	▼/▲
Low	▲	▲	▼
Medium	▲	▲▲	▼
High	▲	▼/▲	▲

Note: ▼ absence; ▲ presence; ▲▲ presence with high; Suitability.



Map of climatic risk of transmission, constructed considering the binary maps after applying a 10th-percentile threshold and with low uncertainty.

Conclusions: The higher risk of transmission in the basins of the rivers Guadiana and Guadalquivir can- not be attributed exclusively to the local abundance of *C. pipiens*, but could be ascribed to the pres-

ence and abundance of *C. perexiguus*. Furthermore, this integrated analysis suggests that the WNV presents an ecological niche of its own, not fully overlapping the ones of its hosts or vector, and thus requiring particular environmental conditions to succeed in its infection cycle.

Funding: CIBER de Enfermedades Infecciosas, Grant/Award Number: CB21/13/00056 and IM22/INF/6; ISCIII, Ministry of Science and Innovation and European Union NextGenerationEU; Red de Investigación de Centros de Enfermedades Tropicales, Grant/Award Number: RD16/0027/0023; ISCIII-Subdirección General de Redes y Centros de Investigación Cooperativa RETICS, Ministry of Science and Innovation; PROMETEO Program, Programa de Ayudas para Grupos de Investigación de Excelencia, Generalitat Valenciana, Grant/Award Numbers: 2016/099, 2021/004.

45. IMMUNE RESPONSE IN SARS-COV-2 INFECTION

Elena Morte Romea^{1,2,3}, Iratxe Uranga^{2,4}, Sandra Hidalgo², Ariel Ramírez-Labrada^{2,5}, Diego de Miguel², Eva Gálvez^{6,4}, Luis Martínez Lostao^{2,7,8}, Galadriel Pellejero Sagastizábal^{1,2}, Santiago Letona Jiménez², Julián Pardo^{2,7,4}, José Ramón Paño Pardo^{1,2,4}

¹Servicio de Enfermedades Infecciosas, Hospital Clínico Universitario Lozano Blesa, Zaragoza, Spain. ²Fundación Instituto de Investigación Sanitaria Aragón (IIS Aragón), Zaragoza, Spain. ³Centro de Investigación Biomédica en Red de Enfermedades Infecciosas (CIBERINFEC), Madrid, Spain. ⁴Centro de Investigación Biomédica en Red (CIBER) en Enfermedades Infecciosas, Madrid, Spain. ⁵Unidad de nanotoxicología e inmunología experimental (UNATI). Centro de Investigación Biomédica de Aragón, Zaragoza, Spain. ⁶Instituto de Carboquímica ICB-CSIC, Zaragoza, Spain. ⁷Departamento de Inmunología, Pediatría, Radiología y Salud Pública, Universidad de Zaragoza, Zaragoza, Spain. ⁸Departamento de Inmunología, Hospital Clínico Universitario Lozano Blesa, Zaragoza, Spain.

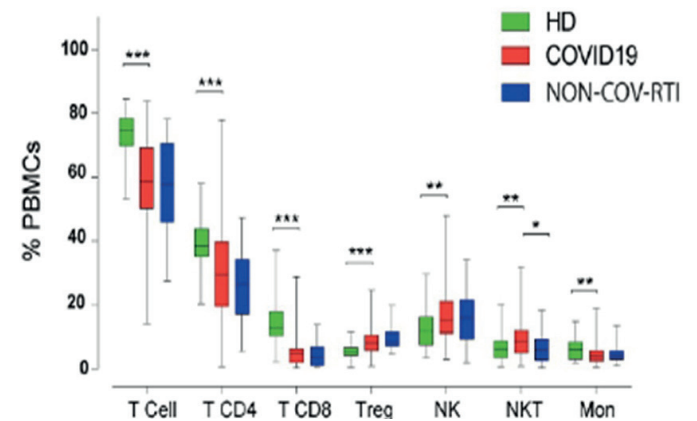
Introduction: We analyzed several parameters of the immune response of COVID-19 patients who required hospital admission, comparing them to healthy donors (HDs) and other patients admitted for respiratory infections not caused by SARS-CoV-2 (non-COV-RTI). We focused on the main cells involved in innate immunity and soluble inflammatory factors that regulate their activity.

Objectives: The main objective was to characterize the immune profile of COVID-19 patients compared to HDs and non-COV-RTI patients. We aimed to identify useful patterns that differentiate COVID-19 from other infections and predict the severity and risk of death.

Methods: We screened patients admitted to Lozano Blesa Hospital for SARS-CoV-2 infection from April to May 2020. Patients with respiratory tract infection and negative tests for SARS-CoV-2 (PCR and serological test) were classified as non-COV-RTI. We classified COVID-19 patients into mild and moderate/severe groups according to the WHO score. Peripheral blood was collected from all participants within the first 24 hours after hospital admission before any treatment was prescribed and clinical data were compiled from the electronic medical record. We performed flow cytometry, multiplex plasma protein analyses and enzyme activity assays.

Results: We included 86 COVID-19 patients and 27 non-COV-RTI patients. Sex, age, number of days from symptoms onset to blood sampling and median length of hospital stay were not significantly different between the cohorts. COVID-19 patients, especially those in the moderate/severe group, had lower lymphocyte counts (794 cell/ μ L) and significantly longer hospital stays (mean of 17 and 6 days). Figure A represented the differences in cell populations. We observed a significant increase in the expression of both activation (CD38+HLA-DR+GzmBHigh) and exhaustion (TIM3+, LAG3+, PD1+) markers in CD8+T cell population in COVID-19 patients compared to HDs. Similarly, we found a significant increase in activated (GzmBHighPD1,

GzmBHighLAG3+, GzmBHighTIM3+) and exhausted (GzmBLowPD1+, GzmBLowLAG3+, GzmBLowTIM3) NKCD56Dim cells in COVID-19 compared to HD and non-COV-RTI. Regarding inflammatory cytokine and chemokine levels, we observed a general increase during COVID-19 in compared to HD (IL1B, IL31, IL33). Specifically, we consistently found elevated levels of IL18 and CXCL10 in COVID-19 patients, which were also related to the more severe group, as well as NKG2D soluble ligands and granzymes.



Conclusions: We detected a high activation of CD8+ and NK cells, with an early expression of inhibitory checkpoints and NKG2D soluble ligands, but with the maintenance of the excretion of granzymes and an aggressive production of mainly interleukins. This pattern is specific to Covid-19 patients when compared to HDs and non-COV-RTI. Funding: Instituto de Salud Carlos III (COV20/00308).

48. ANTIMICROBIAL PEPTIDES FOR PSEUDOMONAS AERUGINOSA COLONIZATION IN CYSTIC FIBROSIS: A MICROBIOLOGICAL APPROACH WITH MUREPAVADIN

José Avendaño-Ortiz^{1,2}, Raquel Barbero-Herranz¹, Marta Hernández-García^{1,2}, Natalia Bastón-Paz¹, María Díez-Aguilar^{2,3}, Luna Ballester¹, Blanca Pérez-Viso¹, Eduardo López-Collazo^{4,5}, Miquel B. Ekkelenkamp⁶, Ad Fluit⁶, Rosa del Campo^{1,2}, Rafael Cantón^{1,2}

¹Servicio de Microbiología, Hospital Universitario Ramón y Cajal, Madrid, Spain. ²Centro de Investigación Biomédica en Red de Enfermedades Infecciosas (CIBERINFEC), Madrid, Spain. ³Servicio de Microbiología y Parasitología, Hospital Universitario La Princesa, Madrid, Spain. ⁴Centro de Investigación Biomédica en Red de Enfermedades Respiratorias (CIBERES), Madrid, Spain. ⁵Innate immune response group, Madrid, Spain. ⁶Department of Medical Microbiology, University Medical Center Utrecht, Utrecht, The Netherlands.

Introduction: Colistin is a cationic antimicrobial peptide active against *Pseudomonas aeruginosa* (PA) colonization in people with cystic fibrosis (pwCF). Its resistance acquisition involves genetic alterations leading to lipid A modifications like 4-aminoarabinose (L-Ara4N) addition. PA adaptation to pwCF airway also involves immune evasion and reduced susceptibility to host-derived antimicrobial peptides. Recently, murepavadin has been proposed as a topical inhaled antimicrobial peptide in pwCF by targeting PA-LPS transport protein D (LptD).

Objectives: We aim to explore genomic and lipid modifications in PA isolates according to their colistin and murepavadin susceptibility and their relationship with immune response and host-derived antimicrobial peptides.

Methods: Antibiotic susceptibility was determined by broth microdilution in 497 CF PA isolates that were classified in: 1) colistin-resistant

(COLR, n = 15), 2) murepavadin-resistant (MURR, n = 116), 3) double-resistant (COLRMURR, n = 17), and 4) double-susceptible (COLSMURS, n = 349) according to EUCAST-2022 and ECOFFs (COL > 4 mg/L and MUR > 0.25 mg/L). Whole genome sequencing (Illumina Miseq), assembling (SPAdes), annotation (Prokka) and Genome-Wide Association Studies (GWAS) were performed. To study the immunogenic properties of lipid A, six strains were employed: one COLR, two COLS, and their three isogenic MURR mutants counterparts obtained in mutant prevention concentration assays. Lipid A was analyzed by negative-ionization mass-spectrometry. LPS was isolated, quantified, and used to study cytokine production and apoptosis by flow cytometry. Phagocytosis was evaluated by internalized bacteria count after monocytes infection at MOI (bacteria/monocyte ratio) of 10. Effects in bacterial growth of immune-derived peptides cathelicidin, indolicidin and β -defensin at 100 μ g/mL were determined by 20-h OD600 monitoring.

Results: In the GWAS analysis, hisJ and rstA variations were significantly associated with MURR. Regarding Lipid A, only COLR strains exhibited m/z 1577 and 1750 ions corresponding to L-Ara4N addition to penta-acylated and hexa-acylated lipid A. These modifications were not detected in COLS strains. MURR strains in contrast exhibited decreased relative abundance of the hexa-acylated m/z 1616 lipid A compared with their MURS counterparts. Regarding inflammatory response, we found overall low inflammatory cytokine production triggered by MURR LPS compared with MURS. Significant changes between murepavadin-susceptible and resistant strains were not found in apoptosis, neither phagocytosis. Cathelicidin and β -defensin resulted in slightly longer lag-phase in MURR.

Conclusions: GWAS revealed genetic variations associated to MURR. Decreased abundance in hexa-acylated Lipid A, but not L-Ara4N addition, were found in MURR strain possibly explaining their lower ability of inflammatory induction. Murepavadin-resistance did not translate to reduced host-antimicrobial peptide susceptibility, in contrast, it slightly increased.

Funding: ISCIII CB21/13/00084, CD21/00059, P19/01043, PI20/00164, ICI21/00012.

49. HEALTH-RELATED QUALITY OF LIFE IN PEOPLE LIVING WITH HIV IN SPAIN. A STUDY IN THE MULTICENTER CORIS COHORT (CORIS-QOL)

Rebeca Izquierdo^{1,2}, Inés Suárez-García^{3,2}, Cristina Moreno^{1,2}, Marta Ruiz-Alguero^{1,2}, Melchor Riera^{4,2}, Joaquín Peraire^{5,2}, Julián Olalla⁶, Luis Ramos⁷, Clara Martínez⁸, María Remedios Alemán⁹, Pepa Galindo¹⁰, Sofía Ibarra¹¹, José Antonio Iribarren^{12,13}, Asunción Díaz^{1,2}, Inmaculada Jarrín^{1,2}, Cohorte Coris²

¹Centro Nacional de Epidemiología, Instituto de Salud Carlos III, Madrid, Spain. ²Centro de Investigación Biomédica en Red de Enfermedades Infecciosas (CIBERINFEC), Madrid, Spain. ³Hospital Universitario Infanta Sofía, San Sebastián de Los Reyes, Spain. ⁴Hospital Universitario Son Espases, Palma de Mallorca, Spain. ⁵Hospital Universitari de Tarragona Joan XXIII, Tarragona, Spain. ⁶Hospital Costa del Sol, Marbella, Spain. ⁷Hospital Universitario La Paz, Madrid, Spain. ⁸Hospital Universitario Clínico San Cecilio, Granada, Spain. ⁹Hospital Universitario de Canarias, San Cristóbal de La Laguna, Spain. ¹⁰Hospital Clínico Universitario de Valencia, Valencia, Spain. ¹¹Hospital Universitario Basurto, Bilbao, Spain. ¹²Hospital Universitario Donostia, Donostia-San Sebastián, Spain. ¹³Instituto de Investigación BioDonostia, Donostia-San Sebastián, Spain.

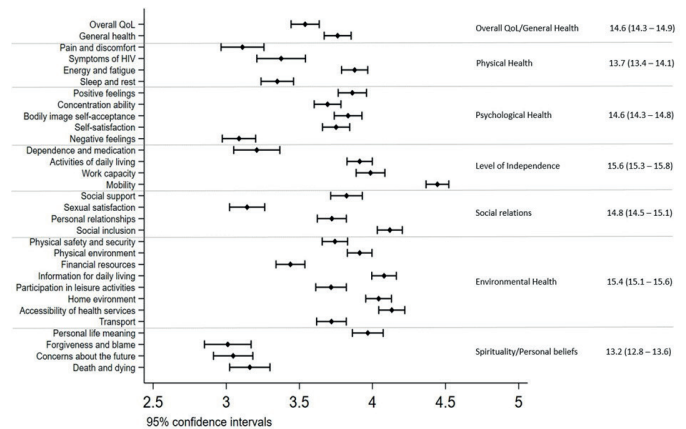
Introduction: As HIV becomes a chronic disease, viral suppression is not the only goal of treatment, and that HIV care must also ensure healthy lives and promote well-being.

Objectives: The aim of this study was to describe health-related quality of life (HRQoL), its most affected dimensions, and its clinical and

sociodemographic determinants in people with HIV (PWH) from the Spanish multicenter CoRIS cohort.

Methods: We designed and implemented a mobile app to routinely collect, every 3 months, data on HRQoL among individuals in active follow-up in CoRIS from July 1, 2021; recruitment is still on-going. HRQoL was measured through the self-reported WHOQOL-HIV-Bref questionnaire, comprising 31 items: one on global HRQoL, one on general health and 29 covering six domains: physical health, psychological health, level of independence, social relationships, environmental health, and spirituality, religion and personal beliefs (SRPB). We calculated means and 95% confidence intervals (95%CI) for each item (rated 1-5) and domain (rated 4-20); higher scores denote higher quality of life. We used multivariable logistic regression models to calculate Odds Ratios (OR) for the association between sociodemographic (sex, age, transmission route and country of origin) and clinical characteristics (time from HIV diagnosis, AIDS diagnosis, CD4 count and suppressed viral load) with good/very good global HRQoL.

Results: By November 15, 2022, 378 individuals from 21 centers answered the baseline questionnaire: 91.5% men, median age 45 (IQR: 38-52) years and 77.2% had acquired HIV through sex between men. Median time from HIV diagnosis was 8 (IQR: 5-13) years, 11.4% had had a previous AIDS-defining condition, 98.4% were on ART (most of them receiving BIC/FTC/TAF (29.0%), DTG/3TC (23.9%) and DTG/3TC/ABC (8.9%)), and 94.6% were virally suppressed. The Figure shows mean scores (95%CI) of each item and domain. The items showing the lowest scores were sexual satisfaction, and sleep and rest, while mobility and symptoms of HIV showed the highest scores. Across domains, level of independence and physical and environmental health showed the highest scores while the SRPB domain showed the lowest score. 55.3% of individuals reported good/very good HRQoL. Having had an AIDS diagnosis (adjusted OR: 0.47; 95%CI: 0.24-0.93) was associated with a lower chance of good/very HRQoL.



Mean scores (95%CI) for each item and domain of the WHOQOL-HIV-Bref.

Conclusions: Only 55.3% of PWH, mostly on ART and virally suppressed, reported good/very good HRQoL, and this percentage was even lower among those with an AIDS diagnosis. The most affected items were sexual satisfaction and sleep and rest.

Funding: ISCIII-AESI2020.

52. DEVELOPMENT OF REAL TIME PCR TECHNIQUES TO IMPROVE THE DIAGNOSIS AND IDENTIFICATION OF THE EMERGING YEAST CANDIDA AURIS, CAUSING INTRA-HOSPITAL OUTBREAKS

Leticia Bernal Martínez¹, Ana Cecilia Mesa Arango², Laura de Francisco Abad³, Carolina Zapata Zapata², Javier Pemán⁴, María José Buitrago¹

¹Laboratorio de Referencia e Investigación en Micología-CNM, Instituto de Salud Carlos III-CIBERINFEC, Majadahonda, Spain. ²Instituto de Ciencias Médicas, Universidad de Antioquia, Medellín, Colombia. ³Laboratorio de Referencia e Investigación en Micología-CNM, Instituto de Salud Carlos III, Majadahonda, Spain. ⁴Servicio de Microbiología, Hospital Universitario y Politécnico La Fe, Valencia, Spain; Instituto de Investigación Sanitaria La Fe, Valencia, Spain.

Introduction: *Candida auris* is associated with nosocomial outbreaks and high mortality rates, both due to its extremely rapid propagation capacity, and due to the difficult to treat as it is a multi-resistant pathogen. For all these reasons, the WHO has recently included it as a critical fungal pathogen. Rapid detection and identification are essential, however, this specie is often misidentified by common laboratory identification methods.

Objectives: To improve the diagnosis and identification of *C. auris* by the development of two rapid methods based on real time PCR: Monoplex-qPCR and Multiplex-qPCR, which allows the detection of the four most frequent *Candida* spp. in clinical setting and species resistant to antifungals. In addition, a method based on High Resolution Melting (HRM), for the rapid identification of a total of 6 *Candida* spp., including *C. auris*.

Methods: New primers and a probe targeting the ITS1 region were designed for the specific detection of *C. auris* by using Beacon Design 9.1 program (Premier Biosoft, USA). The reaction conditions were optimized. All the techniques were performed on the LC480II equipment (Roche, Madrid, Spain). DNA concentrations between 1 ng and 1 fg/μl were used. Sensitivity, specificity and reproducibility of the technique were determined with a total of 44 clinical strains (31 *C. auris*). For the HRM technique, ITS 3-4 primers were used, and DNA adjusted a 5 ng/μl. The clinical validation was carried out with exudate samples, from 18 patients admitted to the Hospital Universitario de la Fe, Valencia.

Results: The techniques developed presented high sensitivity, and reproducibility, the detection limit was established between 100-1 fg/μl of sample and the coefficient of variation was 2.2%-3% respectively. Furthermore, no cross-reaction with other related species was detected. In the clinical validation, *C. auris* was detected in 17/18 samples, 100% sensitivity.

Conclusions: The techniques developed for the detection of *C. auris* turned out to be sensitive, specific, and reproducible for the diagnosis. The HRM technique can be considered a simple and fast method, it could be a simple tool to identify this emerging species. Results obtained are quite promising and it seem to indicate that these techniques could be implemented applied in the clinical setting. Further validation with a larger number of patient samples will be required.

Funding: This work was supported by the Instituto de Salud Carlos III: PI20CIII/00012, PI21CIII/00007, and CIBERINFEC CB21/13/00105.

53. MOLECULAR DETECTION OF RICKETTSIA SPP. IN WILD UNGULATES AND THEIR TICKS IN MEDITERRANEAN AREAS OF SOUTHWESTERN SPAIN

David Cano-Terriza^{1,2}, Susana Remesar³, Patrocinio Morrondo³, Saúl Jiménez-Ruiz¹, Ceferino M. López³, Débora Jiménez-Martín¹, Pablo Díaz³, Jorge Paniagua¹, Javier Caballero-Gómez^{1,2,4}, Antonio Rivero-Juárez^{2,4}, Ignacio García-Bocanegra^{1,2}

¹Departamento de Sanidad Animal, Grupo de Investigación GISAZ, UIC Zoonosis y Enfermedades Emergentes ENZOEM, Universidad de Córdoba, Córdoba, Spain. ²Centro de Investigación Biomédica en Red de Enfermedades Infecciosas (CIBERINFEC), Madrid, Spain. ³Investigación en Sanidad Animal: Galicia (Grupo INVESAGA), Facultad de Veterinaria, Universidad de Santiago de Compostela, Lugo, Spain. ⁴Grupo de Virología

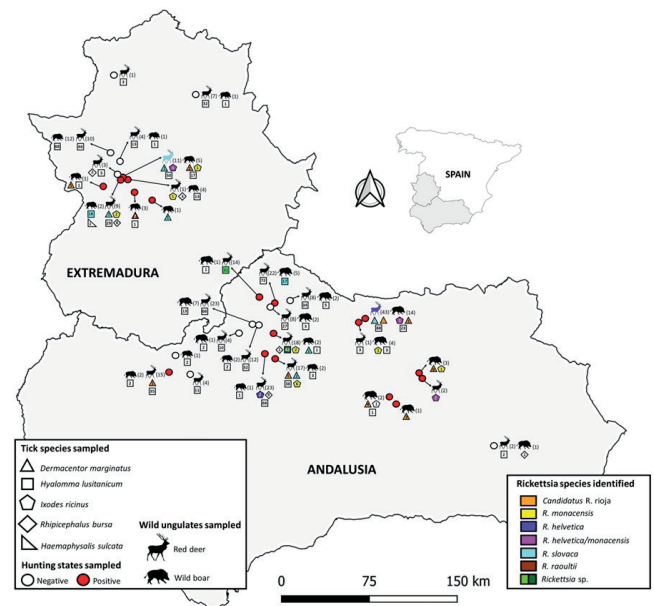
Clinica y Zoonosis, Unidad de Enfermedades Infecciosas, Instituto Maimónides de Investigación Biomédica de Córdoba (IMIBIC), Hospital Universitario Reina Sofía, Universidad de Córdoba, Córdoba, Spain.

Introduction: Wildlife is an important reservoir of zoonotic pathogens.

Objectives: The objective of the present study was to assess the importance of wild ungulates in the epidemiology of *Rickettsia* spp.

Methods: Ticks and spleen samples were collected from 262 red deer (*Cervus elaphus*) and 83 wild boar (*Sus scrofa*) hunted in southwestern Spain during the period 2016-2021. DNA was extracted from tick pools (n = 191) and spleens (n = 345) and *Rickettsia* DNA was detected using two nested PCR targeting the rOmpA and rOmpB genes.

Results: Five tick species were identified (*Hyalomma lusitanicum*, *Dermacentor marginatus*, *Ixodes ricinus*, *Rhipicephalus bursa* and *Haemaphysalis sulcata*). *Rickettsia* DNA was detected in 31 (16.2%) tick pools and two red deer spleen samples (0.8%). Four validated *Rickettsia* species (*R. slovaca*, *R. monacensis*, *R. helvetica* and *R. raoultii*), one uncultivated species (*Candidatus R. rioja*) and two uncharacterized *Rickettsia* spp. were detected in ticks. *Rickettsia helvetica* and *R. slovaca* were also detected in spleen samples from red deer.



Conclusions: The overall prevalence in ungulate spleen samples was lower than in tick pools suggesting that these ungulates do not play a major role in the transmission of *Rickettsia* spp. However, their importance as spreaders of positive ticks cannot be ruled out. The results present a challenge for the veterinary and public health communities since most of the *Rickettsia* spp. detected are pathogenic. Furthermore, the new *Rickettsia* species could be potential pathogens. For these reasons, identifying *Rickettsia* species present in ticks and wildlife is of particular interest to clarify their sylvatic cycle and establish appropriate control measures.

Funding: This study is part of the TED2021-132599B-C22 project, funded by MCIN/AEI/10.13039/501100011033 and by the European Union "NextGenerationEU"/PRTR. Recovery, Transformation and Resilience Plan - Funded by the European Union - NextGenerationEU. It was also partially funded by the research project LifeWATCH INDALO - Scientific Infrastructures for Global Change Monitoring and Adaptation in Andalusia (LIFEWATCH-2019-04-AMA-01), financed with FEDER funds (POPE 2014-2020) and by CIBER -Consorcio Centro de Investigación Biomédica en Red- (CB 2021), Instituto de Salud Carlos III, Ministerio de Ciencia e Innovación and Unión Europea-NextGenerationEU.

57. ZONOSIS SCREENING IN SPANISH IMMUNOCOMPROMISED CHILDREN AND THEIR PETS

Paula García¹, David Romero Trancón¹, Belén Pérez¹, **Jara Hurtado Gallego**^{2,3}, Rocío Sánchez⁴, Jorge Atucha⁴, Iker Falces^{5,6}, David Carmena⁷, Antonio Rivero Juárez^{8,9,10}, Antonio Rivero Román^{11,10,9}, Paula Navarro Carrera¹², Guillermo Ruiz Carrascoso⁶, Laura Moya¹³, Sonia Alcolea^{14,5}, Cristina Calvo^{14,5,15}, Talía Sainz^{14,15,3}, Ana Méndez Echeverría^{14,16,17}

¹Hospital Infantil La Paz, Madrid, Spain. ²Instituto de investigación IdiPaz, Madrid, Spain. ³Centro de Investigación Biomédica en Red de Enfermedades Infecciosas (CIBERINFEC, CB21/13/00025), Madrid, Spain. ⁴Instituto de investigación IdiPaz, Madrid, Spain. ⁵CIBERINFEC CB21/13/00025, Madrid, Spain. ⁶Servicio de Microbiología, Hospital La Paz, Madrid, Spain. ⁷CIBERINFEC CB21/13/00029; Laboratorio de Referencia e Investigación en Parasitología, Centro Nacional de Microbiología, Madrid, Spain. ⁸CIBERINFEC CB21/13/00083. Unit of Infectious Diseases, Córdoba, Spain. ⁹Instituto Maimonides de Investigación Biomédica de Córdoba (IMIBIC), Córdoba, Spain. ¹⁰Universidad de Córdoba (UCO), Córdoba, Spain. ¹¹Unit of Infectious Diseases, Hospital Universitario Reina Sofía, Córdoba, Spain. ¹²Hospital Universitario La Paz, Madrid, Spain. ¹³Iddex, Madrid, Spain. ¹⁴Instituto de Investigación IdiPAZ, Madrid, Spain. ¹⁵Servicio de Pediatría, Enfermedades Infecciosas y Tropicales, Hospital La Paz, Madrid, Spain. ¹⁶CIBERINFEC CB21/13/00025, Madrid, Spain. ¹⁷Servicio de Pediatría, Enfermedades Infecciosas y Tropicales, Hospital La Paz, Madrid, Spain.

Introduction: Pets provide health benefits for children, but the risk of zoonotic infections must be considered, especially among immunocompromised patients. A One Health perspective is essential for effective prevention and to provide evidence-based medical and veterinary recommendations.

Objectives: To determine the prevalence of colonization/infection by zoonotic microorganisms in immunocompromised children and their pets.

Methods: A prospective study in immunocompromised children from La Paz Hospital who have cats and/or dogs (2022-2023). Serologies were performed in patients and pets (according to host-related pathogens): *Bartonella*, *Toxocara canis*, *Strongyloides*, *Toxoplasma gondii*, *Leishmania*, *Leptospira*, *Ehrlichia canis*, *Borrelia burgdorferi*, *Hepatitis E virus*, *Rickettsia*, *Babesia canis* and *Anaplasma*. PCR for 16 protozoa and bacteria in faeces as well as for *Rocahepevirus ratti* and *Paslahepevirus balayani* were performed. Nasopharyngeal and rectal swabs were obtained in patients and pets to study bacterial colonisation (*Staphylococcus aureus*, *Staphylococcus pseudintermedius* and resistant *enterobacteriaceae* colonisation). Sanger sequencing was used for species/genotypes identification when possible.

Results: We present preliminary results from an ongoing research study including 57 children and 68 pets. Up to 17% of faecal samples from pets were positive by PCR for one or more faecal microorganisms including *Enterocytozoon bieneusi* (4.5%; 3/67), *Campylobacter jejuni* (4.4%; 3/68), *Giardia* spp. (3%; 2/68), *Paslahepevirus balayani* genotype 3 (HEV-3) (2.6%; 1/38), *Cryptosporidium* spp. (1.4%; 1/68) and *Blastocystis* sp. (1.4%; 1/68). Among children, gastrointestinal pathogens were found in 31% of the patients: HEV-3 (9%; 2/21), *Giardia intestinalis* (6.6%; 3/45), *Cryptosporidium* spp. (3.3%; 2/46), *Blastocystis* sp. (2%; 1/46), *C. jejuni* (2.2%; 1/46) and *Yersinia enterocolitica* (2.2%; 1/46). We found positive serologies among children for *Bartonella* spp. (17%; 3/17), *Strongyloides* spp. (8.1%; 4/49), *Toxocara* spp. (4%; 2/49) and HEV (3.5%; 2/57). Colonization by *S. pseudintermedius* was common among pets (10.6%; 7/66), but not among children (0%). Two patients were colonised by *K. pneumoniae* OXA-48 and ESBLs *K. pneumoniae* (3.4%). No other colonisations were detected. Until the date, we have not identified shared colonisations/infections between pets and owners, although samples are still being collected and analysed. Results from pet's serology and faeces studies such as coproantigen diagnostic im-

munoassay, microscopy following centrifugal flotation and PCR for hookworms, whipworms and ascarids are currently undergoing.

Conclusions: Although preliminary, our results indicate that a non-negligible percentage of dogs/cats living with immunocompromised children are colonized/infected by potentially zoonotic agents. Although no events of zoonotic transmission could be identified, the role of infected animals as potential reservoirs of human infections cannot be overlooked, as suggested by the finding.

Funding: Spanish Pediatrics Association (AEP) 2021 Research Grant and MAPFRE Foundation Research grants "by Ignacio H. de Larramendi 2021".

63. BACTERAEMIA AS AN INDICATOR OF QUALITY OF CARE IN ELDERLY PATIENTS

Martha Kestler, Patricia Muñoz, Carlos Sanchez, Luis Alcalá, Rodrigo Valdovinos, Jose Antonio Serra, Emilio Bouza

Gregorio Marañón University Hospital, Madrid, Spain.

Introduction: The incidence and origin of blood stream infections (BSI) in patients over 80 years of age is not well known. Of particular interest is the knowledge of episodes of hospital onset bacteraemia (HOB), as this figure is currently proposed as an indicator of quality of care.

Objectives: To know the real incidence of BSI in the elderly population, with particular interest in the place of origin, aetiology and clinical outcome.

Methods: Observational study, from January to June 2021, in a large tertiary Spanish centre; in which all BSI in patients over 80 years of age were prospectively recorded.

Results: During study period, a total of 624 patients suffered one or more episodes of significant bacteraemia. Of these, 147 patients were

General characteristics of 147 BSI in patients over 80 years old, according to acquisition

	Community	Health Care Related	Nosocomial
	85 (23.8%)	17 (11.6%)	45 (30.6%)
Sex			
Male	47 (55.3%)	10 (58.8%)	25 (55.6%)
Origen			
Catheter Related	0 (0%)	1 (5.9%)	21 (46.7%)
Urinary Tract	31 (36.5%)	9 (52.9%)	12 (26.7%)
Abdominal	33 (38.8%)	1 (5.9%)	5 (11.1%)
Respiratory	1 (12%)	3 (17.6%)	2 (4.4%)
Skin and Soft tissue	7 (8.2%)	1 (5.9%)	1 (2.2%)
Unknown	6 (7%)	1 (5.9%)	4 (8.9%)
Aetiology			
Gram Positives			
S. aureus	7 (8.3%)	3(17.6%)	7 (15.6%)
SAMS	5 (5.9%)	0	4 (8.9%)
SAMR	2 (2.4%)	3 (17.6%)	3 (6.7%)
Enterococci	3 (3.6%)	0 (0%)	8 (17.8%)
E. faecalis	2 (2.4%)	-	5 (11.1%)
E. faecium	1 (1.2%)	-	3 (6.7%)
Gram Negatives			
E. coli	39 (44.7%)	4 (23.5%)	4 (8.9%)
P. aeruginosa	3 (3.5%)	1 (5.9%)	5 (11.5%)
Klebsiella spp	5 (5.9%)	5 (29.4%)	3 (6.7%)
BLEE	1(1.2%)	5 (29.4%)	1 (2.2%)
Fungi			
Candida spp	1 (1.2%)	0 (0%)	4 (8.9%)
Clinical Outcome			
Mortality during admission	16 (18.8%)	5 (29.4%)	14 (31.1%)

over 80 years of age and 477 under 80 years of age. The incidence of bacteraemia per 1,000 admissions in the population under and over 80 years of age was 26.57 and 37.81/1,000 admissions, respectively. Of the 147 BSI patients over 80 years old, episodes were community-acquired in 85 cases (57.8%), health-care-related in 17 (11.6%) and 45 (30.6%) suffered bacteraemia of Hospital Onset (HOB). Of the HOB episodes, 21 (46.7%) originated from vascular catheters (CR-BSI) and 12 (26.7%) from the urinary system in catheterised patients (CAUTI), 5 (11.1%) were of intra-abdominal origin, 2 (4.4%) of respiratory origin, 1 (2.2%) originated in a skin and soft tissue infection and 4 (8.9%) were of unknown origin. The aetiology of the HOB episodes had a predominance of Gram-positives (*Enterococcus* spp 9, *S. aureus* 7, other *Staphylococci* 9). Among the Gram negatives, the most frequent isolates were *Pseudomonas aeruginosa* 5, and *E. coli* 4. The mortality of bacteraemia during admission detected in those over 80 years of age was 35/147 (23.8%), and by place of acquisition was as follows: Community-acquired 16/85 (18.8%), Health-Care Related 5/17 (29.4%) and HOB 14/45 (31.1%). After examination of the HOB episodes, 33/45 (73%) were, in the authors' opinion, potentially avoidable.

Conclusions: HOB surveillance in the elderly, could be an easy to obtain, easy to follow, metric of infection control in these population. Episodes of HOB in the elderly must be considered failures of proper care and reviewed accordingly.

66. LONGITUDINAL STUDY OF CD4+ T CELLS POLARIZATION IN INDIVIDUALS WITH LONG-COVID SHOWS A PERSISTENT INCREASE IN PRO-INFLAMMATORY POPULATIONS AND A DECREASE IN ANTIVIRAL RESPONSE

Olivia de la Calle-Jiménez^{1,2}, Clara Sánchez-Menéndez^{1,3}, María Aránzazu Murciano-Antón⁴, Alicia Simón Rueda^{1,5}, Guiomar Casado¹, Elena Mateos^{1,6}, Susana Domínguez-Mateos⁴, Esther San José², **Montserrat Torres**^{1,6}, Maria Teresa Coiras^{1,6}

¹AIDS Immunopathology Unit, National Center of Microbiology, Instituto de Salud Carlos III, Madrid, Spain. ²Faculty of Sciences, Universidad Europea de Madrid, Madrid, Spain. ³Hematology and Hemotherapy Service, Instituto Ramón y Cajal de Investigación Sanitaria (IRYCIS), Hospital Universitario Ramón y Cajal, Madrid, Spain. ⁴Family Medicine, Centro de Salud Doctor Pedro Laín Entralgo, Madrid, Spain. ⁵Faculty of Sciences, Universidad Complutense de Madrid, Madrid, Spain. ⁶Centro de Investigación Biomédica en Red de Enfermedades Infecciosas (CIBERINFEC), Madrid, Spain.

Introduction: Persistent COVID-19 syndrome or Long-COVID is characterized by immunological alterations that seem to be related to chronic inflammatory responses. Affected individuals show high levels of cytotoxic cell populations which do not develop effective antiviral activity.

Objectives: In this study, we have analyzed the polarizing ability of CD4+ T lymphocytes in people diagnosed with Long-COVID, compared to individuals who fully recovered from COVID-19.

Methods: Longitudinal study with 28 individuals diagnosed with Long-COVID-19 49 weeks after SARS-CoV-2 infection and 13 individuals fully recovered from COVID-19 in the first 12 weeks after infection. Peripheral blood samples were collected at baseline and after 6 months. Polarization of CD4+ T lymphocytes was analyzed by flow cytometry, evaluating the surface expression of markers of different Th subpopulations: Th1, Th2, Th9, Th17, and Th22. Intracytoplasmic analysis of the production of specific cytokines by each Th subpopulation against SARS-CoV-2 peptides was performed.

Results: 1) Median age of individuals fully recovered from COVID-19 was 45 years (IQR 36-59) of which most were women (54%). Participants diagnosed with Long-COVID had a median age of 44 years (IQR 39.25-48.75) and 93% were women. 2) CD4+ Th1 lymphocytes levels were significantly reduced in participants with Long-COVID

(-1.3-fold; $p = 0.0217$), compared to recovered participants. This decrease remained after 6 months (-1.3-fold; $p = 0.0301$). No changes in the ability of Th1 cells to produce IFN γ in response to SARS-CoV-2 were observed. 3) Levels of CD4+ Th9 and Th17 lymphocytes, highly pro-inflammatory, were significantly increased in Long-COVID participants (1.9-fold; $p = 0.0005$ and 2.2-fold; $p < 0.0001$, respectively). These levels were still increased after 6 months. IL-9 production by Th9 was significantly decreased in people with Long-COVID (-2.2-fold; $p = 0.0357$), even after 6 months. 4) No significant changes were observed in CD4+ Th2 and Th22 levels between both groups. However, there were increased numbers of IL-4 production by Th2 cells in Long-COVID patients (1.7-fold; $p = 0.0107$) which continued to increase after 6 months, while IL-13 production by Th22 was decreased 4.0-fold ($p = 0.0002$) and maintained after 6 months. No changes in IL-22 production by Th22 were observed in response to SARS-CoV-2.

Conclusions: CD4+ T lymphocytes from people with Long-COVID show significant changes in Th subpopulations, with a reduction in Th1 cells capable of polarizing the immune response towards an effective antiviral response, as well as an increase in pro-inflammatory Th9 and Th17 subpopulations. These changes in the levels of Th subpopulations were maintained after 6 months, which supports the persistence of immunopathological aspects in people with Long-COVID.

Funding: This work was supported by project PI22CIII/00059, funded by the Strategic Action in Health of the Instituto de Salud Carlos III (ISCIII) and co-funded by European Regional Development Fund (ERDF), "A way to make Europe".

71. A NOVEL OPTIMIZED VACCINE CANDIDATE, MVA-COV2-S(3P), COMPLETELY PROTECT MICE AND HAMSTERS AGAINST SARS-COV-2 INFECTION WITH SEVERAL VARIANTS OF CONCERN

Patricia Pérez^{1,2}, David Astorgano¹, Guillermo Albericio¹, Rana Abdelnabi³, Kai Dallmeier³, Mariano Esteban¹, Juan Francisco García-Arriaza^{1,2}

¹Department of Molecular and Cellular Biology, Centro Nacional de Biotecnología, Consejo Superior de Investigaciones Científicas, Madrid, Spain. ²Centro de Investigación Biomédica en Red de Enfermedades Infecciosas (CIBERINFEC), Madrid, Spain. ³KU Leuven Department of Microbiology, Immunology and Transplantation, Rega Institute, Laboratory of Virology, Molecular Vaccinology and Vaccine Discovery, Leuven, Belgium.

Introduction: Development of optimized vaccines against COVID-19 capable of preventing the spread of SARS-CoV-2 and different variants of concern (VoCs) is necessary. Most COVID-19 vaccines are based on the SARS-CoV-2 spike (S) protein, the main target of neutralizing antibodies (NAb). The prefusion state of the S protein is the most suitable immunogen for the development of better vaccine candidates, as it preserves the conformation of the S trimer, facilitating the induction of NAb.

Objectives: We generated an optimized COVID-19 vaccine candidate based on the modified vaccinia virus Ankara (MVA) vector expressing a full-length prefusion-stabilized SARS-CoV-2 S protein, termed MVA-CoV2-S(3P), to enhance the S-specific immune responses and achieve protection against SARS-CoV-2 infection, through different immunization routes and against different VoCs.

Methods: We evaluated the immunogenicity and efficacy of MVA-CoV2-S(3P) in animal models. First, we assessed in mice (immunocompetent C57BL/6 and transgenic K18-hACE2 mice) the immunogenicity and efficacy against ancestral Wuhan-1 strain and against beta and omicron VoCs when MVA-CoV2-S(3P) was administered by intramuscular and intranasal routes. On the other hand, we studied the efficacy in hamsters, as an alternative animal model.

Results: One single intramuscular or intranasal dose of MVA-CoV2-S(3P) induced high titers of systemic IgGs and NABs against parental SARS-CoV-2 and several VoCs in C57BL/6 and K18-hACE2 mice. Moreover, one single intranasal dose of MVA-CoV2-S(3P) also induced in C57BL/6 mice mucosal S-specific IgA antibodies. Remarkably, one single intramuscular or intranasal administration of MVA-CoV2-S(3P) fully protected K18-hACE2 mice from SARS-CoV-2 (Wuhan strain) morbidity and mortality, reducing viral loads, histopathological lesions, and levels of pro-inflammatory cytokines in the lungs. Similar results were observed when MVA-CoV2-S(3P)-vaccinated K18-hACE2 mice were challenged with SARS-CoV-2 VoCs beta and omicron. Furthermore, one or two intramuscular doses of MVA-CoV2-S(3P) protected hamsters against SARS-CoV-2 infection, with induction of high titers of binding IgGs and NABs, and reduction in viral loads in lungs and nasal washes, lung histopathological lesions, and levels of pro-inflammatory cytokines in the lungs.

Conclusions: The potent immunogenicity and full efficacy against different VoCs triggered by the optimized MVA-CoV2-S(3P) vaccine candidate in different animal models support its use as a COVID-19 vaccine in clinical trials.

Funding: Fondo COVID-19 grant COV20/00151 (ISCIII), Fondo Supera COVID-19 grant (Crue Universidades-Banco Santander), CSIC grant 202120E079, and funds from CIBERINFEC co-financed with FEDER funds (to JG-A). CSIC grant 2020E84 (to ME). A MCIN/AEI/10.13039/501100011033 grant (PID2020-114481RB-I00) and EC-Next Generation EU through CSIC's PTI Salud Global (to JG-A and ME).

72. T-CELL IMMUNITY AGAINST SARS-COV-2 IS STRONGLY ASSOCIATED WITH PATIENT OUTCOMES IN VACCINATED PERSONS HOSPITALIZED WITH DELTA OROMICRON VARIANTS

Marta Fernández González^{1,2}, Vanesa Agulló^{1,2}, José Alberto García^{1,2}, Sergio Padilla^{1,2,3}, Javier García Abellán^{1,2,3}, Alba de la Rica^{1,4}, Paula Mascarell¹, Mar Masiá^{1,2,3}, Félix Gutiérrez^{1,2,3}

¹Infectious Diseases Unit, Hospital General Universitario de Elche, Elche, Spain. ²Centro de Investigación Biomédica en Red de Enfermedades Infecciosas (CIBERINFEC), Madrid, Spain. ³Clinical Medicine Department, Universidad Miguel Hernández, San Juan de Alicante, Spain. ⁴Microbiology Service, Hospital General Universitario de Elche, Elche, Spain.

Introduction: Understanding protective immunity against SARS-CoV-2 after COVID-19 vaccination may be important for predicting the risk of severe breakthrough infections. While neutralising antibodies have been associated with protection from reinfection and severe COVID-19, little is known about the protective role of pre-existing cellular immunity to SARS-CoV-2.

Objectives: We measured T-cell and antibody responses to SARS-CoV-2 in vaccinated patients hospitalized for COVID-19, and explored their potential value to predict outcomes.

Methods: Prospective, longitudinal study including fully vaccinated patients hospitalized for COVID-19 caused by Delta and Omicron variants between July 22, 2021, and April 23, 2022. We measured TrimericS-IgG antibodies (DiaSorin) and SARS-CoV-2 T-cell response using a specific quantitative interferon- γ release assay (IGRA, Euroimmun) at hospital admission. Primary outcome was all-cause 28-day mortality or need for intensive care unit (ICU) admission. Secondary outcomes were 28- 60- and 90-day mortality. Multivariable Cox-proportional hazards regression models were used to assess associations of immune responses with outcomes.

Results: 158 (87.3%) of 181 subjects meeting the eligibility criteria had detectable SARS-CoV-2 antibodies, 92 (50.8%) showed specific T-cell responses, and 87 (48.1%) had both antibodies and T-cell responses. Patients who died within 28 days or needed ICU admission were less likely to have unspicific interferon- γ release and SARS-

CoV-2 specific T-cell responses, and had quantitatively lower interferon- γ responses in IGRA. In the adjusted analyses, having both T-cell and antibody responses at admission (aHR, 0.17; 95%CI, 0.05-0.61) and Omicron variant (aHR, 0.38; 95%CI, 0.17-0.87) reduced the hazard of 28-day mortality or ICU, whereas higher Charlson comorbidity index (aHR, 1.27; 95%CI, 1.07-1.51) and lower SpO₂/FIO₂ (aHR, 2.33; 95%CI, 1.49-3.65) increased the risk (Figure). Similar trends were observed for secondary outcomes.

Variable	Hazard ratio	aHR (95% CI)	p-value
Age		0.99 (0.96, 1.03)	0.799
Sex	Male	Reference	
	Female	1.60 (0.68, 3.76)	0.283
Charlson.comorbidity.index		1.27 (1.07, 1.51)	0.006
SpO2/FIO2.ratio		2.33 (1.49, 3.65)	<0.001
SARS-CoV-2.variant	delta	Reference	
	omicron	0.38 (0.17, 0.87)	0.022
Immune.responses	TrimericS-IgG(-)	Reference	
	TrimericS-IgG(+) & IGRA(-)	0.40 (0.14, 1.16)	0.093
	TrimericS-IgG(+) & IGRA(+)	0.17 (0.05, 0.61)	0.006
Remdesivir	No	Reference	
	Yes	0.62 (0.25, 1.53)	0.302

Predictors for 28-day mortality or ICU admission in persons admitted to hospital with COVID-19. aHR, adjusted hazard ratio; ICU, intensive care unit; SpO₂/FIO₂ ratio, oxygen saturation to fraction of inspired oxygen ratio; TrimericS-IgG, immunoglobulin G antibody serum levels against the trimeric spike protein; IGRA, SARS-CoV-2 interferon gamma release assay.

Conclusions: Pre-existing immunity against SARS-CoV-2 is strongly associated with patient outcomes in vaccinated subjects requiring hospital admission for COVID-19. Persons showing both T-cell and antibody responses have the lowest risk of severe outcomes.

Funding: This research was supported by CIBER (CB21/13/00011), Instituto de Salud Carlos III, Ministerio de Ciencia e Innovación and Unión Europea-NextGenerationEU, and the Conselleria de Innovación, Universidades, Ciencia y Sociedad Digital of Generalitat Valenciana (AICO/2021/205).

75. POINT-OF-CARE (POC) BIOSENSOR DEVICE FOR THERAPEUTIC DRUG MONITORING (TDM) OF ANTIMICROBIALS

Alejandro Astua¹, Judith Poblet², Luisa Sorlí², Sònia Luque², M. Carmen Estevez¹, Milagro Montero², Santiago Grau², Juan-Pablo Horcajada², Laura M. Lechuga¹

¹Catalan Institute of Nanoscience and Nanotechnology (ICN²), Barcelona, Spain. ²Institut Hospital del Mar d'Investigacions Mèdiques (IMIM), Barcelona, Spain.

Introduction: New diagnostic tools for the efficient use of antibiotics to increase clinical success and reduce the occurrence of adverse events and antimicrobial resistance are needed. These diagnostic systems should be easy to use and offer rapid results in order to perform a POC instantaneous therapeutic drug monitoring.

Objectives: To develop a POC portable optical biosensor for the rapid quantification and monitoring of two narrow-range antibiotics of interest (amikacin and colistin) as innovative tool for therapeutic drug monitoring (TDM) in decentralized settings at the point-of-care.

Methods: The new diagnostic technology is based on a Superficial Plasmon Resonance (SPR) biosensor setup and implements a one-step indirect competitive immunoassay employing antibodies as bioreceptors. The biosensor is integrated in a compact and user-friendly platform for POC testing. The assay is fully optimized and allows the direct detection in serum samples with a time of analysis of less than 20 min. To assess the accuracy and feasibility of the biosensor test, quantification of antibiotic levels was made in 10 spiked serum samples (5 with amikacin and 5 with colistin) with known antibiotic concentrations.

Results: The accuracy of the immunosensor was higher than 90% for measuring the amikacin concentration in four of the five spiked samples, in which it was 74.4%. In the case of colistin in three samples the accuracy was about 90%, but in two it was less than 35%. For amikacin, the limit of detection (LOD) in the calibration curves was 0.14 ± 0.09 ng/ml (buffer) and 2.07 ± 0.13 ng/ml (serum 1/10), and for colistin, it was 9.4 ± 3.6 pg/ml (buffer) and 4.1 ± 0.9 pg/ml (serum 1/1,000).

Conclusions: Competitive immunoassays for direct, one-step detection and quantification of amikacin and colistin antibiotics have been developed employing a portable SPR biosensor. The optimized assay reaches excellent levels of sensitivity, enabling the detection of both antibiotics in serum samples with better results for amikacin in this series. On-going work is focused on finalizing the colistin assay (accuracy studies with spike samples) and a clinical validation study (prospective observational study) for amikacin and colistin quantification using real samples from hospitalized patients at Parc de Salut Mar, Barcelona, is about to start the patient's inclusions.

Funding: Alejandro Astúa acknowledges financial support from European Union's Horizon 2020 Research and Innovation Program under the Marie Skłodowska-Curie grant agreement No. 754397. Judith Poblet has a pre-doctoral contract from CIBERINFEC. Instituto de Salud Carlos III. We acknowledge the financial support from PHITBAC project (PLEC2021-007739) funded by the Ministry of Science and Innovation (MCIN/AEI/10.13039/501100011033) and European Union NextGenerationEU/PRTR.

77. NANOBODY BASED IMMUNOTHERAPY FOR THE TREATMENT OF INVASIVE FUNGAL INFECTIONS

Diego Sánchez-Martínez^{1,2}, Sergio Redrado³, Elena Dolader-Ballesteros⁴, Javier Macías⁵, María Pilar Domingo³, Patricia Esteban^{1,3}, Maykel Arias^{2,3}, Ariel Ramírez^{1,2}, Ramon Hurtado⁵, Julián Pardo^{1,2,4}, Eva María Gálvez^{2,3}

¹Fundación Instituto de Investigación Sanitaria Aragón (IIS Aragón), Centro de Investigación Biomédica de Aragón (CIBA), Zaragoza, Spain.

²Centro de Investigación Biomédica en Red de Enfermedades Infecciosas (CIBERINFEC), Instituto de Salud Carlos III (ISCIII), Zaragoza, Spain.

³Instituto de Carboquímica ICB-CSIC, Zaragoza, Spain. ⁴Departamento de Microbiología, Pediatría, Radiología y Salud Pública, Área de Inmunología, Facultad de Medicina, Universidad de Zaragoza, Zaragoza, Spain. ⁵Instituto de Biocomputación y Física de Sistemas Complejos (BIFI), Universidad de Zaragoza, Zaragoza, Spain.

Introduction: The invasive fungal infections ratios of mortality are between 25% and 70% depending on the type of microorganism and the population at risk, affecting mostly immunocompromised patients. *Aspergillus* spp. and *Cryptococcus* spp. are two of the main responsible for these infections. The late non-specific diagnosis and the increasing resistance of the strains highlight the importance of finding new therapeutic alternatives.

Objectives: Generate and validate a new nanobody (Nb3) targeting β -1,3-glucanotransferase, Gel, a key fungal enzyme involved in cell wall remodeling, that has been described as essential for fungal survival.

Methods: *A. fumigatus* and *C. neoformans* fungal growth was analysed by XTT reduction assay in RPMI 1640 medium with HEPES 20 mM. Cell wall sugar content of *C. neoformans* cultures treated and non-treated with Nb3 were analysed by HPLC. BALB/c mice were immunosuppressed with cyclophosphamide and/or hydrocortisone, infected and treated with Nb3. Survival, fungal load and Nb3 concentration were analysed.

Results: We have found that Nb3 exerts fungistatic activity *in vitro* against *Aspergillus fumigatus* and *Cryptococcus neoformans*, including antifungal resistant strains, which correlates with the localisation of Nb3 in the fungal cell wall where Gel enzyme is expressed.

Moreover, treatment of fungus with Nb3 alters cell wall polysaccharide composition confirming enzyme inactivation *in vitro*. Using *in vivo* mouse models of *Aspergillus* and *Cryptococcus* infections we show that therapeutic administration of Nb3 in infected animals is highly effective and significantly increases animal survival, correlating with a reduction of fungal burden in lung and brain. Importantly, *in vivo* biodistribution analysis shows that Nb3 is able to cross the blood-brain barrier reaching the brain, main tissue affected during cryptococcosis.

Conclusions: We have developed a new Nb targeting essential fungal enzymes as an efficient alternative to treat invasive fungal infections and overcome increasing antifungal drug resistance. This new antifungal immunotherapy could contribute to reduce morbidity and mortality of a high number of patients at risk of these infections including cancer, ICU and transplantation. In addition, we provide the basis to develop other immunotherapy treatments based on Nb3 (Nb3-based CAR cells, bispecific nanobodies) increasing the armoury to fight these lethal fungal infections.

Funding: Gobierno de Aragón, Group B29_20R LMP139_21, FEDER (Fondo Europeo de Desarrollo Regional) Ministerio de Ciencia, Innovación e Universidades (MCNU), Agencia Estatal de Investigación (PID2020-113963RB-I00) CIBERINFEC, Instituto de Salud Carlos III (ISCIII), Ministerio de Ciencia e Innovación and Unión Europea-Next-GenerationEU.

79. PLASMA BLASTS, PLASMACYTOID DCs AND CD56BRIGHT NK CELLS ARE IMMUNOLOGICAL HALLMARKS OF SARS-COV-2 SUSCEPTIBILITY

Laura Martín-Pedraza¹, Eulalia Rodríguez², Elena Moreno¹, Claudio Díaz-García¹, Jorge Díaz¹, Marta Rosas Cancio-Suárez¹, Laura Luna¹, Rubén Ballester González², Roberto Pariente Rodríguez², Mario Rodríguez³, Juan Carlos Galán³, Paulette Walo Delgado², Claudia Geraldine Rita², Santiago Moreno¹, M. Luisa Villar², Sergio Serrano-Villar¹

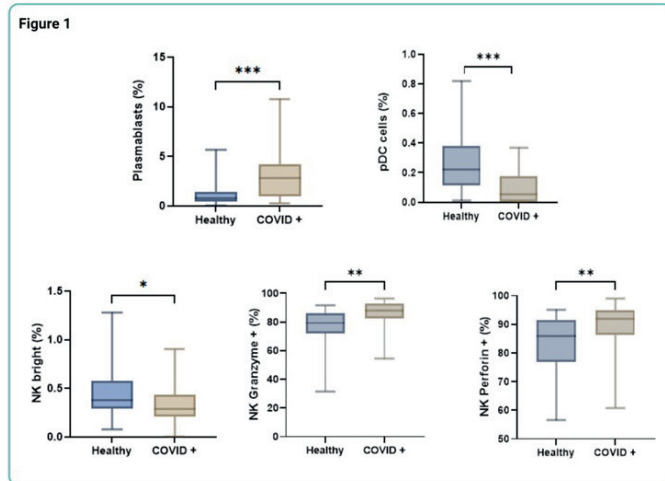
¹Servicio de Enfermedades Infecciosas, Hospital Ramón y Cajal, IRYCIS, Universidad de Alcalá y CIBER de Enfermedades Infecciosas (CIBERINFEC), Madrid, Spain. ²Servicio de Inmunología, Hospital Ramón y Cajal, IRYCIS, Universidad de Alcalá, Madrid, Spain. ³Servicio de Microbiología, Hospital Ramón y Cajal, IRYCIS, y CIBER de Epidemiología y Salud Pública (CIBERESP), Madrid, Spain.

Introduction: The mechanisms driving SARS-CoV-2 susceptibility remain poorly understood, especially the immunological hallmarks determining why a subset of unvaccinated individuals remained uninfected despite high-risk exposures during the first pandemic waves.

Objectives: We aimed to identify potential immunological markers that differentiate individuals susceptible to SARS-CoV-2 infection from healthcare workers exhibiting resistance to the disease.

Methods: We included 26 'susceptible' patients who provided blood samples within the first 7 days from the onset of symptoms and diagnosed SARS-CoV-2 infection by PCR from nasopharyngeal swabs, and 38 unvaccinated 'non-susceptible' healthcare workers on duty for at least three months in COVID-19 wards or intensive care units. Non-susceptible participants were asymptomatic and reported at least three high-risk exposures to SARS-CoV-2 without having experienced symptoms suggestive of SARS-CoV-2 infection. They were also persistently negative for SARS-CoV-2 PCR testing and did not have SARS-CoV-2 IgM and IgG in plasma. We extensively characterized phenotypically and functionally leukocyte subsets (including T and B cells, monocytes, NK and dendritic cells) by Flow Cytometry, acquired in a FACSCanto II flow cytometer (BD Biosciences). For data analysis, we used FACSDIVA software V.9.0 (BD Biosciences) and GraphPad Prism 8.0 software.

Results: Susceptible patients exhibited a marked expansion of plasmablasts – a B cell subset responsible of the production of neutralizing antibodies, which can also contribute to dysregulated immune responses in some viral infections–, which directly correlated with the disease severity. In contrast, non-susceptible individuals consistently showed low proportions of plasmablasts and greater proportions of plasmacytoid dendritic cells (pDCs) –which can produce high concentrations of interferons when activated by viral antigens–. In addition, in susceptible patients, the percentage of CD56bright NK cells –a subset particularly relevant for the innate response against viral infections– was lower than in non-susceptible individuals. In contrast, NK cells expressing perforin and granzyme –driving responses able to eliminate virus-infected cells by inducing apoptosis– were increased in susceptible patients (Figure).



Summary of main results of the project. Non-susceptible patients are named as “Healthy” and susceptible patients are named as “COVID+”.

Conclusions: We found several immunological hallmarks of SARS-CoV-2 infection. The plasmablast expansion during the early phase of SARS-CoV-2 compared to the lower levels in healthcare workers repeatedly exposed may indicate a dysregulated immune response. Strong pDCs and CD56brightNK responses, two relevant actors of the antiviral immune response, could explain protection against SARS-CoV-2 infection.

Funding: This work was supported by the public grants COV20/00349 Instituto de Salud Carlos III (ISCIII) and private funding IISP 60257 (Merck, Sharp & Dohme).

80. IMMUNOGENICITY AND EFFICACY OF A NOVEL MULTI-PATCH SARS-COV-2/COVID-19 VACCINE CANDIDATE

Laura Sin¹, Beatriz Perdiguero², Laura Marcos², Maria López-Bravo³, Pedro J. Sanchez-Cordón⁴, Carmen Zamora², Jose Ramon Valverde⁵, Carlos Oscar S. Sorzano⁶, Enrique Álvarez¹, Mariano Esteban², Carmen Elena Gómez²

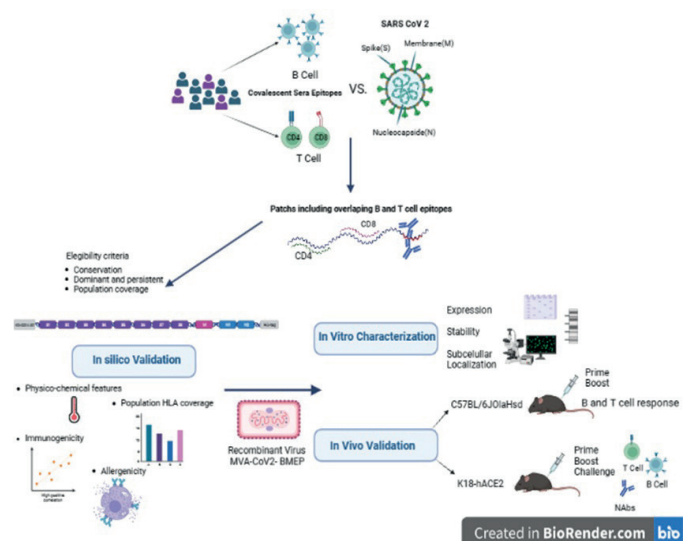
¹Centro de Investigación Biomédica en Red de Enfermedades Infecciosas (CIBERINFEC), Madrid, Spain. ²Department of Molecular and Cellular Biology, Centro Nacional de Biotecnología, Consejo Superior de Investigaciones Científicas, Madrid, Spain, Madrid, Spain. ³Department of Microbial Biotechnology, Centro Nacional de Biotecnología, Consejo Superior de Investigaciones Científicas, Madrid, Spain, Madrid, Spain. ⁴Instituto Nacional de Investigación y Tecnología Agraria y Alimentaria, Madrid, Spain. ⁵Scientific Computing, Centro Nacional de Biotecnología, Consejo Superior de Investigaciones Científicas, Madrid, Spain, Madrid, Spain. ⁶Biocomputing Unit and Computational Genomics, Centro Nacional de Biotecnología, Consejo Superior de Investigaciones Científicas, Madrid, Spain, Madrid, Spain.

Introduction: The coronavirus disease 2019 (COVID-19) pandemic caused by the severe acute respiratory syndrome coronavirus 2 (SARS-CoV-2) has led to major health, economic and social problems worldwide. The COVID-19 morbidity and mortality have been significantly reduced during these years thanks to the rapid approval and massive administration of effective vaccines against SARS-CoV-2, mainly targeting the surface-exposed spike glycoprotein (S). However, the emergence of new SARS-CoV-2 variants with enhanced transmissibility has impaired their efficacy. Therefore, it is desirable to design new vaccine candidates targeting other viral antigens to induce broad and long-lasting immunity with potential to counteract viral evolution and future outbreaks.

Objectives: The aim of this study is to design and validate *in vitro* and *in vivo* a novel polyvalent multi-patch immunogen containing functional and conserved regions from the SARS-CoV-2 S, M and N structural proteins that cluster B cell as well as overlapping CD4 and CD8 T cell epitopes when expressed by a highly attenuated poxvirus vector, MVA.

Methods: Viral patches included in the CoV2-BMEP synthetic protein were selected by manual sequence inspection of major dominant and persistent antigenic domains containing B and T cell epitopes recurrently recognized by SARS-CoV and SARS-CoV-2 survivors during natural infection and conserved across human endemic coronaviruses (HCoVs). The synthetic gene was inserted by homologous recombination into the MVA genome to generate MVA-CoV2-BMEP recombinant virus that was characterized in cultured cells and evaluated in mice for immunogenicity and efficacy.

Results: The multi-patch CoV2-BMEP protein was successfully expressed at high levels and in stable manner in MVA-CoV2-BMEP infected cells and was recognized by PBMCs from COVID-19 convalescent patients *in vitro*. In C57BL/6 mice, homologous prime/boost MVA/MVA immunization regimen induced broad SARS-CoV-2-specific T cells in lung and spleen as well as binding (bAbs) and neutralizing (NAb) antibodies against S and N proteins, while in susceptible K18-hACE2-Tg model this protocol partially protected vaccinated mice from SARS-CoV-2 infection. The protection correlates with the levels of NAb detected before the virus challenge.



Conclusions: In conclusion, the multi-patch CoV2-BMEP protein represents a novel immunogen with the capacity to control SARS-CoV-2 infection by inducing broad and cross-reactive B and T cell responses, and opens the field for improvements on this type of platform with potential for universal pan-coronavirus vaccine development.

Funding: This research was supported by CIBERINFEC (CB21/13/00108) and the MCIN (PID2020-117425RB-C22).

81. ASSOCIATION BETWEEN TELOMERE LENGTH IN COVID-19 PATIENTS AND RESPIRATORY PROGRESSION

Ana Virseda Berdices^{1,2}, Óscar Martínez González³, Celia Crespo Bermejo¹, Óscar Brochado Kith^{1,2}, Blanca López Matamala³, Carmen Martín Parra³, María Ángeles Alonso Fernández³, Miriam Chana García³, Sandra Sánchez López³, Madian Manso Álvarez³, Salvador Resino^{1,2}, Rafael Blancas Gómez Casero³, María Ángeles Jimenez Sousa^{1,2}, Amanda Fernández Rodríguez^{1,2}

¹Centro Nacional de Microbiología, Majadahonda, Spain. ²Centro de Investigación Biomédica en Red de Enfermedades Infecciosas (CIBERINFEC), Madrid, Spain. ³Hospital Universitario del Tajo, Aranjuez, Spain.

Introduction: Telomere shortening is associated with an impairment of the immune system, which is explained by the progressive decline in physiological homeostasis associated with aging. The severity of acute respiratory distress syndrome (ARDS) depends on the amount of etiologic substances with corresponding immune reactions, the duration of the appearance of specific immune cells, or the repertoire of specific immune cells that control the substances.

Objectives: To study the impact of telomere length in whole blood from COVID-19 patients at disease onset on the need for invasive and non-invasive mechanical ventilation, the need for pronation, days of pronation and the worst PaO₂/FiO₂ in patients admitted to the ICU.

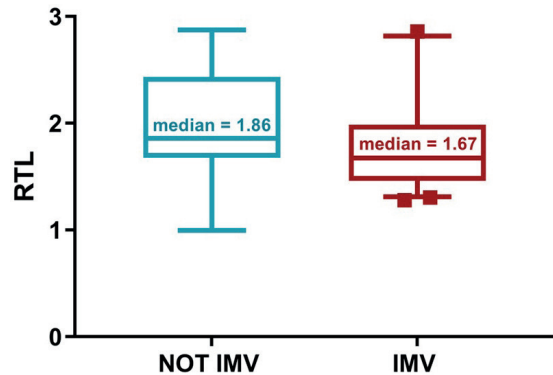
Methods: A cross-sectional prospective study enrolling critical non-vaccinated patients with COVID-19 recruited at Tajo University Hospital was carried out from March 2020 to April 2021. Blood samples were obtained upon admission to the ICU, prior to connection to any kind of mechanical ventilation. Relative telomere length (RTL) quantification was carried out using monochromatic multiplex real-time quantitative PCR (MMqPCR). The association analysis between RTL and several clinical variables was performed by generalized linear models (GLM), with binomial and gamma distribution, and adjusting for age, gender and BMI.

Clinical and epidemiological characteristics of COVID-19 patients according to need for invasive mechanical ventilation (IMV)

	All	Not IMV	IMV	p-value
No.	71	15	56	
Age (years)	63.00 [54.00-70.50]	57.00 [52.00-64.50]	64.00 [54.75-71.00]	0.161
Gender (male)	52/72 (73.2%)	12/15 (80.0%)	40/56 (71.4%)	0.736
BMI (kg/m ²) (n=47)	31.00 [26.22-34.83]	29.09 [24.24-31.46]	32.49 [26.57-35.16]	0.169
ARDS	70/71 (98.6%)	14/15 (93.3%)	56/56 (100.0%)	0.476
SAPS 3 (n=18)	49.00 [45.25-55.00]	45.50 [41.75-50.25]	51.50 [46.00-55.00]	0.425
APACHE II (n=18)	10.00 [7.25-13.75]	7.50 [6.00-11.75]	11.00 [9.00-13.75]	0.364
Hospital stay (days)	27.00 [19.00-38.00]	19.00 [15.00-23.50]	28.00 [20.75-41.50]	0.007
Days from symptom onset to ICU admission	9.00 [6.00-12.00]	10.00 [8.00-11.50]	8.00 [5.00-12.00]	0.385
ICU days	11.00 [7.50-21.50]	5.00 [3.50-7.00]	15.00 [9.00-26.25]	< 0.001
High-flow nasal cannula	52/71 (73.2%)	15/15 (100.0%)	37/56 (66.1%)	0.021
Prone positioning during first 7 days	20/71 (28.2%)	1/15 (6.7%)	19/56 (33.9%)	0.078
Days prone positioning (n=20)	2.00 [1.00-3.00]	3.00 [3.00-3.00]	2.00 [1.00-4.00]	0.529
Worst PaO ₂ /FiO ₂ (n=70)	130.00 [109.38-160.93]	117.67 [85.62-131.96]	136.00 [111.19-167.40]	0.056
Death	6/71 (8.5%)	1/15 (6.7%)	5/56 (8.9%)	0.999

The values are expressed as the absolute number (percentage) and median (interquartile range).

Results: Seventy-one unvaccinated COVID-19 patients were included in the study. The Table presents descriptive information of demographic and clinical characteristics. Initially, no association was found between RTL and the need for invasive mechanical ventilation (IMV) (OR 2.64; p-value = 0.155). However, after adjusting for age, gender and BMI, association becomes significant. Thus, patients who required invasive mechanical ventilation had a shorter RTL at disease onset than those who did not (Figure), with an OR = 13.70 (p-value = 0.019). No significant associations were found with the need for non-invasive mechanical ventilation, pronation, days of pronation and the worst PaO₂/FiO₂.



Representation of relative telomere length (RTL) in COVID-19 patients stratifying by need invasive mechanical ventilation (IMV).

Conclusions: The presence of a shortened RTL at ICU admission in patients with COVID-19 disease is associated with a greater need for invasive mechanical ventilation.

Funding: This study was supported by grants from Instituto de Salud Carlos III (ISCIII; grant number COV20/1144 [MPY224/20] to AFR/MAJS) and Fundación Universidad Alfonso X el Sabio (FUAX) – Santander (1.013.005). The study was also supported by the Centro de Investigación Biomédica en Red (CIBER) de Enfermedades Infecciosas (CB21/13/00044).

82. SHIFTS IN SYSTEMIC INFLAMMATION AFTER FECAL MICROBIOTA TRANSPLANT IN PEOPLE WITH HIV

Claudio Díaz-García^{1,2,3}, Elena Moreno^{1,3}, Alba Talavera^{1,3}, Laura Martín-Pedraza^{1,3}, Laura Luna^{1,3}, José A. Pérez-Molina¹, Fernando Dronza^{1,3}, María José Gosalbes¹, Jorge Díaz^{1,3}, Javier Martínez-Sanz^{1,3}, Raquel Ron^{1,2,3}, María Jesús Vivancos^{1,3}, Santiago Moreno^{1,2,3}, Sergio Serrano-Villar^{1,3}

¹Department of Infectious Diseases, Hospital Universitario Ramón y Cajal, IRYCIS, Madrid, Spain. ²Universidad de Alcalá, Department of Medicine, Madrid, Spain. ³Centro de Investigación Biomédica en Red de Enfermedades Infecciosas (CIBERINFEC), Madrid, Spain.

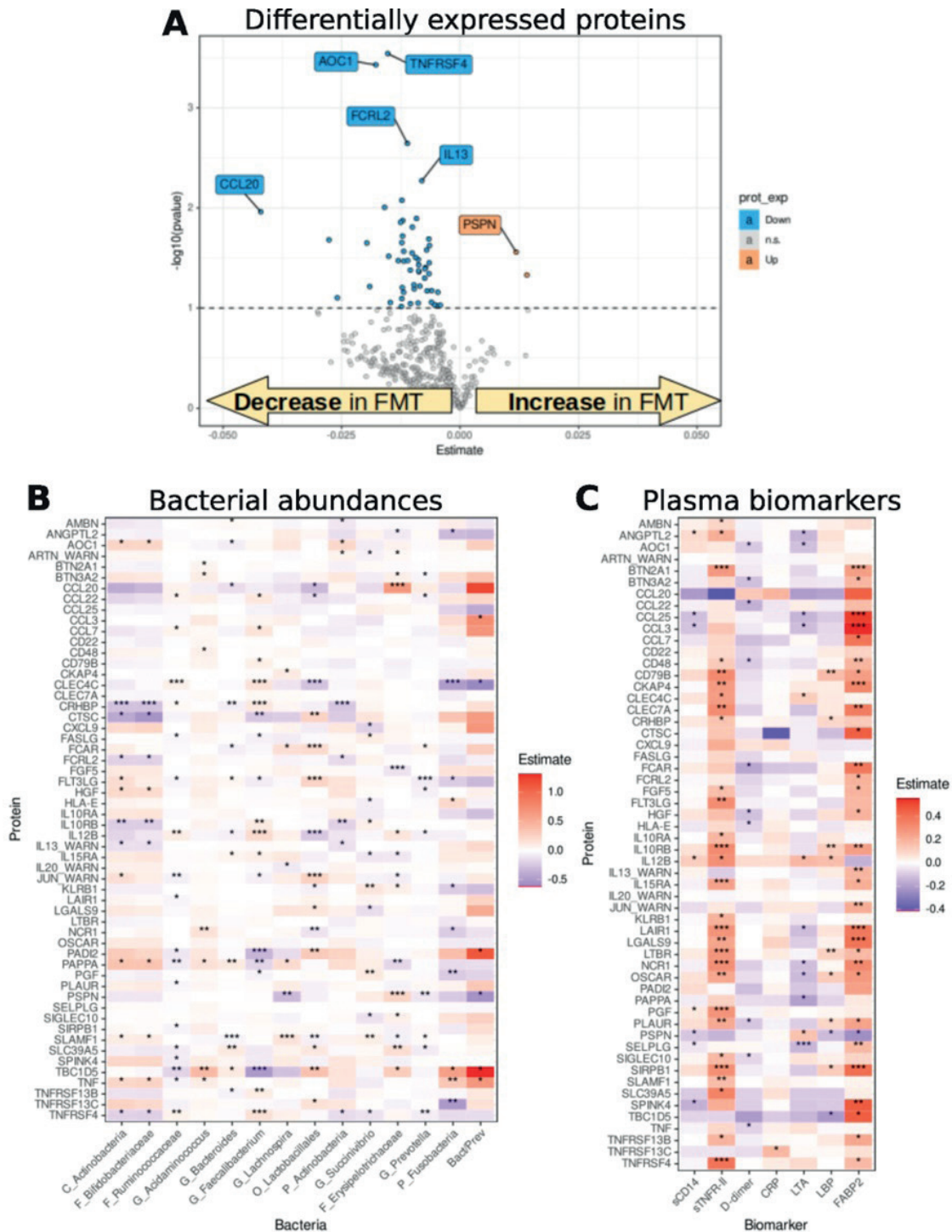
Introduction: HIV can be considered a chronic inflammatory disease, driven mainly by the microbiome, that increases the risk of mortality. That long-lasting inflammation, that is present even when antiretroviral therapy (ART) is effective, contributes to increased risk of non-AIDS events. It is unclear if targeting the microbiome therapeutically can restore the original immune functionality in people with HIV (PWH) and, as a result, improve clinical outcomes. In a fecal microbiota transplant (FMT) trial in PWH, we proved that FMT elicits changes in gut microbiota structure and we found that Lachnospiraceae and Ruminococcaceae families were the taxa more robustly engrafted across time points.

Objectives: Here, we aimed to evaluate the proteomic changes in inflammatory pathways following repeated FMT at low doses relative to placebo in PWH on effective ART with evidence of incomplete immune recovery and their relationship with other biomarkers (bacteria and plasma molecules).

Methods: We randomized 30 PWH on ART to either weekly fecal microbiota capsules or placebo for eight weeks. Stool donors were selected based on anti-inflammatory microbiota profiles (high Faecalibacterium and butyrate). We measured the plasma expression of 368

inflammatory proteins at weeks 0, 1, 8, and 24 using the Proximity Extension Assay by Olink. We fitted mixed models to compare the protein trajectories and selected the most significant to explore their correlations with 14 bacterial taxa and 7 biomarkers of inflammation. We performed a functional analysis using Gene Set Enrichment Analysis.

Results: FMT resulted in a significant decrease of 54 proteins related to cytokines and leukocyte activation and increase of 2 proteins with anti-inflammatory activity compared to placebo. CCL22, CD22, FGF5, and JUN showed the most consistent pattern of decline after each



A. Observed changes in the expression of 368 inflammatory proteins measured by Proximity Extension Assay (Olink Proteomics) between FMT and placebo. B. Correlations between differentially expressed proteins and the abundance of 14 relevant bacterial taxa. C. Correlations between differentially expressed proteins and plasma biomarkers of inflammation (4 inflammation proteins and 3 bacterial translocation molecules).

FMT; CCL22, IL20, and JUN were those for which the effect lasted until week 24; and TNFRSF4 and AOC1 showed the most significant differences between groups ($p = 0.0003$ and $p = 0.0004$) (Figure A). Increases in Erysipelotrichaceae and the Bacteroides/Prevotella ratio correlated with increased CCL20 ($p = 1^{-7}$) (Figure B). Also, the biomarkers of inflammation sTNFR-II and IFABP have positive strong correlations with most differentially expressed plasma proteins analysed (Figure C).

Conclusions: FMT from selected donors resulted in a shift towards lower inflammation through effect in proteins related to cytokines and leukocyte activation. CCL20 is a promising target to further explore its relationship with the microbiome and the inflammation processes. Our results support that the microbiome is a viable target to modulate systemic inflammation during treated HIV.

Funding: This work was supported by the Instituto de Salud Carlos III (PI18/00154, FI22/00111), Gilead (GLD16-00030), the SPANISH AIDS Research Network (RD16/0025/0001project), and co-financed by the European Regional Development Fund 'A way to achieve Europe' (ERDF).

87. IGG ANTIBODIES LEVELS AGAINST THE SARS-COV-2 SPIKE PROTEIN IN MOTHER-CHILD DYADS AFTER COVID-19 VACCINATION

María José Muñoz-Gómez^{1,2}, María Martín-Vicente¹, Sara Vigil-Vázquez³, Itziar Carrasco³, Alicia Hernanz-Lobo^{2,4,5}, Vicente Mas⁶, Mónica Vázquez⁶, Angela Manzaneres⁵, Olga Cano⁶, Clara Zamora⁷, Roberto Alonso⁸, Daniel Sepulveda-Crespo^{9,2}, Laura Tarancon-Diez¹⁰, María Ángeles Muñoz-Fernández^{10,11,12}, Mar Muñoz-Chapuli⁷, Salvador Resino^{9,2}, Maria Luisa Navarro^{2,4,5,13}, Isidoro Martínez^{9,2}

¹Centro Nacional de Microbiología, Instituto de Salud Carlos III, Majadahonda, Spain. ²Centro de Investigación Biomédica en Red de Enfermedades Infecciosas (CIBERINFEC), Instituto de Salud Carlos III, Madrid, Spain. ³Servicio de Neonatología, Hospital General Universitario Gregorio Marañón, Madrid, Spain. ⁴Grupo de Investigación en Infectología Pediátrica, Instituto de Investigación Sanitaria Gregorio Marañón, Madrid, Spain. ⁵Servicio de Pediatría, Hospital General Universitario Gregorio Marañón, Madrid, Spain. ⁶Unidad de Biología Viral, Centro Nacional de Microbiología, Instituto de Salud Carlos III, Madrid, Spain. ⁷Servicio de Obstetricia y Ginecología, Hospital General Universitario Gregorio Marañón, Madrid, Spain. ⁸Departamento de Microbiología Clínica y Enfermedades Infecciosas, Hospital General Universitario Gregorio Marañón, Madrid, Spain. ⁹Unidad de Infección Viral e Inmunidad, Centro Nacional de Microbiología, Instituto de Salud Carlos III, Majadahonda, Spain. ¹⁰Laboratorio de Inmunobiología Molecular, Sección de Inmunología, Hospital General Universitario Gregorio Marañón, Madrid, Spain. ¹¹Spanish HIV-HGM BioBank, Madrid, Spain. ¹²Centro de Investigación Biomédica en Red de Bioingeniería, Biomateriales y Nanomedicina (CIBER-BBN), Instituto de Salud Carlos III, Madrid, Spain. ¹³Universidad Complutense de Madrid, Madrid, Spain.

Introduction: Pregnant women are at increased risk of COVID-19-related intensive care admission, mortality, preterm delivery, pregnancy loss, and stillbirth. Although COVID-19 is usually mild in infants, severe illness and hospitalization can happen in this population. Therefore, protecting the mother-infant dyad against COVID-19 is crucial. Current data show that COVID-19 vaccination of pregnant women with mRNA vaccines is safe and prevents severe COVID-19. Vaccine-induced antibodies in mothers may also protect their infants through transplacental antibody transfer. However, additional studies are needed to confirm the magnitude, duration, and protective capacity of the vaccine-induced humoral immune response.

Objectives: We aimed to assess IgG antibodies against the SARS-CoV-2 spike protein in vaccinated mothers and their infants at delivery and 2-3 months later.

Methods: We conducted a prospective study on mothers who received at least one dose of the monovalent COVID-19 vaccine during pregnancy and on their infants. The baseline was at delivery ($n = 93$), and the end of follow-up was 2 to 3 months post-partum ($n = 53$). Serum anti-SARS-CoV-2 S IgG titers and ACE2 binding inhibition levels were quantified by immunoassays.

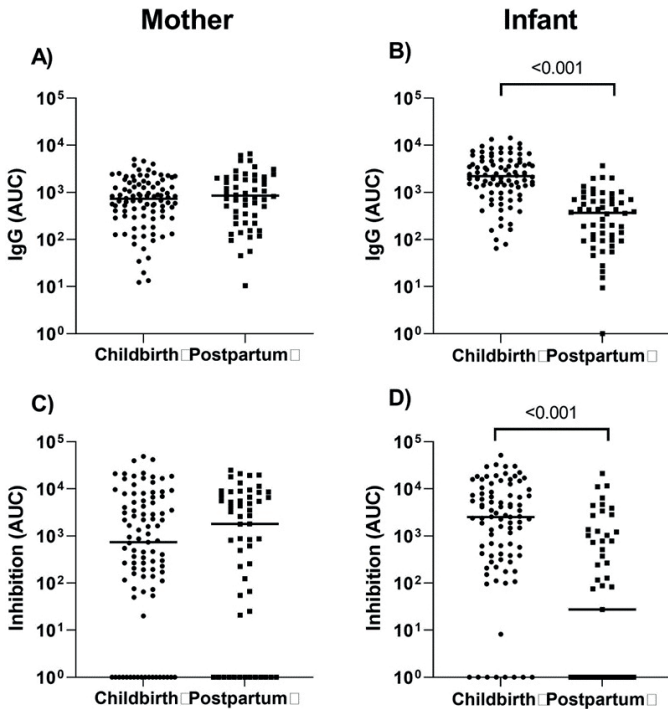
Characteristics of mothers and infants

Parameters	Values
A) Mothers	
No.	93
Age (years)	34.8 (32.2; 39.1)
Country of birth	
Spain	74 (79.6%)
Latin American Countries	15 (16.1%)
Other	4 (4.3%)
Comorbidities	
Hypertension	5 (5.4%)
Diabetes	8 (8.6%)
Hypothyroidism	8 (8.6%)
Preeclampsia	6 (6.5%)
Other	3 (3.2%)
SARS-CoV-2 Infection (+)	
Pre-perinatal (pre-pregnancy and pregnancy)	11 (11.8%)
Postnatal	21/53 (39.6%)
SARS-CoV-2 Vaccine	
First dose	
Pfizer-BioNTech (BNT162b2)	66 (71.0%)
Moderna (mRNA-1273)	26 (27.9%)
Oxford-AstraZeneca (ChAdOx1-S)	1 (1.1%)
Second dose (n =79)	
Pfizer-BioNTech (BNT162b2)	57 (72.2%)
Moderna (mRNA-1273)	22 (27.8%)
Third dose (n=6)	
Pfizer-BioNTech (BNT162b2)	4 (66.7%)
Moderna (mRNA-1273)	2 (33.3%)
Before pregnancy (n=6)	
First dose	3 (50%)
Second dose	3 (50%)
Before childbirth	
First dose	14 (15.1%)
Second dose	79 (84.9%)
After childbirth (n=53)	
First dose	7 (13.2%)
Second dose	40 (75.5%)
Third dose	6 (11.3%)
B) Newborns	
No.	93
Gestational age (weeks)	39.7 (38.3; 40.4)
Mode of delivery	
Vaginal	81 (87.1%)
Cesarean	12 (12.9%)
Sex (male)	53 (57.0%)
Breastfeeding	88 (94.6%)
Condition at birth	
APGAR1	9 (9; 9)
APGAR5	10 (10; 10)
Weight (gr.)	3.300 (3.000; 3.500)
Height (cm)	50 (49; 51)
Head circumference (cm)	34 (33; 35)
SARS-CoV-2 Infection (+)	
Postnatal	11/53 (20.7%)

Values are expressed as the median (Q1; Q3) and absolute count (percentage).

SARS-CoV-2, severe acute respiratory syndrome coronavirus 2; APGAR, Appearance, Pulse, Grimace, Activity, and Respiration; APGAR1, 1-minute APGAR; APGAR5, 5-minute APGAR.

Results: Mothers and children had high anti-SARS-CoV-2 S IgG titers against the B.1 lineage at childbirth. However, while the antibody titers were maintained at 2-3 months post-partum in mothers, they decreased significantly in children ($p < 0.001$). Positive and significant correlations were found between anti-SARS-CoV-2 S IgG titers and the ACE2 binding inhibition levels in mothers and infants at childbirth and 2-3 months post-partum ($r > 0.8$, $p < 0.001$). Anti-S antibodies were also quantified for the Omicron variant at 2-3 months post-partum. In mothers and infants, antibody titers against Omicron were significantly lower than those against B.1 ($p < 0.001$). Again, a positive correlation was observed for Omicron between IgG titers and ACE2 binding inhibition both in mothers ($r = 0.818$, $p < 0.001$) and infants ($r = 0.386$, $p < 0.005$). Previous SARS-CoV-2 infection and COVID-19 vaccination near delivery positively impacted anti-SARS-CoV-2 S IgG levels.



(A-B), IgG antibody levels against SARS-CoV-2 S protein (B.1 lineage) at childbirth and 2-3 months post-partum in maternal serum (A) and infant serum (B). (C-D), Inhibition of ACE2 interaction titers (B.1 lineage) at childbirth and 2-3 months post-partum in maternal serum (C) and infant serum (D). Statistics: Differences were calculated by the Wilcoxon test, and only p -values < 0.05 are shown. Medians are represented by a horizontal bar. Abbreviations: AUC, Area under the curve; IgG, anti-SARS-CoV-2 S IgG.

Conclusions: COVID-19 mRNA vaccines induce high titers of anti-SARS-CoV-2 S in pregnant women, which can inhibit the binding of ACE2 to protein S and are efficiently transferred to the fetus. However, there was a rapid decrease in antibody levels at 2 to 3 months post-partum, particularly in children.

Funding: This study was supported by a grant from Instituto de Salud Carlos III (grant numbers COV20/00808), and by Centro de Investigación Biomédica en Red (CIBER) de Enfermedades Infecciosas (CB21/13/00044 and CB21/13/00077) and Bioingeniería, Biomateriales y Nanomedicina (CIBER-BBN) (CB22/01/00041).

88. CORTICOSTEROIDS PROMOTE BIOFILM FORMATION IN PSEUDOMONAS AERUGINOSA

María Escobar Salom^{1,2}, Elena Jordana Lluich^{1,2}, Amanda Iglesias^{3,4}, Isabel M^a Barceló^{1,2}, Borja G. Cosío^{3,4}, Antonio Oliver^{1,2}, Carlos Juan^{1,2}

¹Servicio de Microbiología, Hospital Universitario Son Espases-Instituto de Investigación Sanitaria de las Islas Baleares (IdISBa), Palma de Mallorca, Spain. ²Centro de Investigación Biomédica en Red de

Enfermedades Infecciosas (CIBERINFEC), Madrid, Spain. ³Servicio de Neumología, Hospital Universitario Son Espases-Instituto de Investigación Sanitaria de las Islas Baleares (IdISBa) - Palma (España), Palma de Mallorca, Spain. ⁴Centro de Investigación Biomédica en Red de Enfermedades Respiratorias (CIBERES), Madrid, Spain.

Introduction: Chronic Obstructive Pulmonary Disease (COPD) is characterized by inflammation of the small airway, often with infectious exacerbations. *Pseudomonas aeruginosa* (PA) is one of the most prevalent pathogens colonizing the lungs of these patients, causing chronic bacterial infections (IBCs). IBCs are related to the presence of bronchiectasis and worse prognosis. In patients with bronchiectasis, a long-term persistence of AP seems to prevail, showing characteristic features of chronic infection such as biofilm formation (grouped cells, protected by an extracellular matrix). Inhaled corticosteroids fluticasone or budesonide are commonly used to reduce airway inflammation in COPD patients, but are associated with an increased risk of PA infection.

Objectives: Our objective was to determine if corticosteroids affect PA biology through a direct interaction, generating membrane stress (linked to increased production of outer membrane vesicles (OMVs) and extracellular DNA (eDNA) by PA), promoting the biofilm formation and contributing to the persistence of these infections.

Methods: Biofilms of PA01 and PA14 type strains were generated in 96-well chambers (8 wells, OD_{600nm} = 0.1, RPMI-1640), treated with fluticasone, budesonide or v/v DMSO (solvent), observing them under a confocal microscope at 24h (1 μ M, therapeutic dose) or 48h (0.1, 1 and 5 μ M). The eDNA was stained with Di-YO-1 (0.5-2.5 μ M, 15') prior to confocal observation. Biomass (cells and eDNA) was quantified with COMSTAT. The c-di-GMP (metabolite that promotes and regulates biofilm formation in PA) was quantified using a transcriptional reporter (PA01W_PcdrA::gfp), inoculating it in a plate (96 wells, OD_{600nm} = 0.01, RPMI-1640), and reading the fluorescence every 30' from 24 to 48h. OMVs were quantified by discarding cells from a culture (18h, 400 ml), ultracentrifuging the supernatant (44,100 rpm, 90') and using NanoSight technology.

Results: Although no biomass increase was observed after 24h, this parameter significantly increased after 48h of continuous treatment in a dose-dependent manner, as summarised in the Table, as well as the biomass of eDNA, the release of OMVs and the production of the secondary messenger c-di-GMP.

		Biomass 24h (μ m ³ / μ m ²)	Biomass 48h (μ m ³ / μ m ²)	eDNA 48h (μ m ³ / μ m ²)	c-di-GMP (AUC)	OMVs (particles/ml)
PA01	DMSO_control	7,5	8,4	8,8	78149	3,6 ¹⁰
	Fluticasone_0.1 μ M	-	10,1*	9,9	79150	-
	Fluticasone_1 μ M	7,3	12,0*	10,3*	86321*	4,5 ¹⁰
	Fluticasone_5 μ M	-	14,0*	14,7*	92159*	6,2 ^{10*}
	Budesonide_0.1 μ M	-	9,5*	9,2	79949	-
	Budesonide_1 μ M	6,9	12,2*	10,2*	94646*	8,3 ^{10*}
PA14	DMSO_control	5,4	8,4	9,0	-	4,5 ¹⁰
	Fluticasone_0.1 μ M	-	10,4*	11,1*	-	-
	Fluticasone_1 μ M	5,4	11,5*	12,8*	-	5,8E ^{10*}
	Fluticasone_5 μ M	-	13,1*	14,6*	-	8,7 ^{10*}
	Budesonide_0.1 μ M	-	10,0*	10,4*	-	-
	Budesonide_1 μ M	5,8	13,0*	11,4*	-	5,1 ¹⁰
	Budesonide_5 μ M	-	15,2*	13,9*	-	1,00 ^{11*}

Conclusions: According to our results, corticosteroids promote biofilm formation in PA, increasing its biomass in response to the membrane stress generated by said drugs and with an apparent cumulative effect. Therefore, corticosteroids could participate in the pathophysiology of IBCs due to PA linked to COPD by promoting this characteristic of strains adapted to chronic lung infection, contributing to the persistence of PA infections in these patients.

Funding: By the grants FPI/2206/2019 (Balearic Islands Government), IJC2019038836-I (Ministerio de Ciencia e Innovación, Spain), PILOT/JORDANA2019 (Hospital Son Espases), Research Grant 2022 (ESCMID); "Ayuda a la Movilidad (SEIMC); the Spanish Network for Research in Infectious Diseases (REIPI, RD16/0016/0004); PI18/00681, PI21/00753, PI21/00017, and FI19/00004 from the Instituto de Salud Carlos III (Spain), cofinanced by the European Regional Development Fund "A way to achieve Europe".

92. DRIED BLOOD SPOT USE IN VACCINE RESPONSE MONITORING IN CHILDREN (DRIVE STUDY)

Paula Rodríguez Molino^{1,2,3}, Ana Rodríguez Galet^{4,5}, **Jara Hurtado Gallego**^{1,2,3}, Sonia Alcolea Ruiz^{1,2,3}, Jorge Atucha^{1,2,3}, Ana Méndez Echevarría^{1,2,3}, Iker Falces Romero⁶, Carmen Cámara⁷, Teresa del Rosal^{1,3,8}, Milagros García López-Hortelano^{1,2,3}, Cristina Calvo^{1,2,3}, Juan Carlos Galan^{5,9}, África Holguín^{5,4,9}, Talía Sainz^{1,2,3}

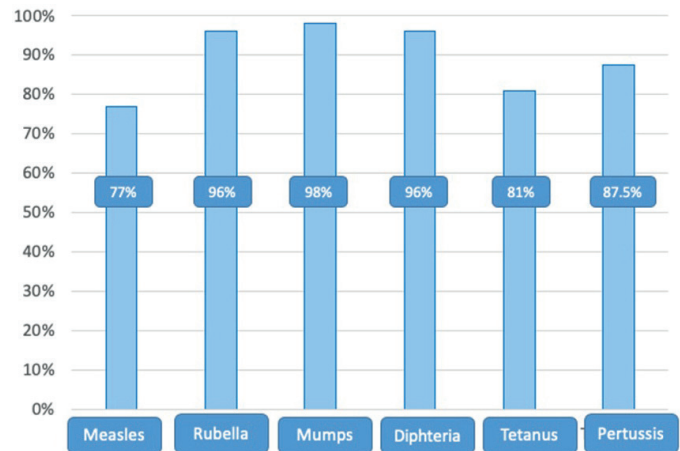
¹General Pediatrics, Infectious and Tropical Diseases Department, Hospital La Paz, Madrid, Spain, Madrid, Spain. ²Centro de Investigación Biomédica en Red de Enfermedades Infecciosas (CIBERINFEC), Madrid, Spain. ³La Paz Research Institute (IdiPAZ) Madrid, Spain, Madrid, Spain. ⁴Ramón y Cajal Research Institute (IRYCIS), Madrid, Spain. ⁵Department of Microbiology, Ramón y Cajal Hospital, Madrid, Spain. ⁶Department of Microbiology and Parasitology, La Paz University Hospital, Madrid, Spain. ⁷Department of Immunology, La Paz University Hospital, Madrid, Spain. ⁸Centro de Investigación Biomédica en Red de Enfermedades Raras (CIBERER), Madrid, Spain. ⁹Centro de Investigación Biomédica en Red de Epidemiología y Salud Pública (CIBERESP), Madrid, Spain.

Introduction: Most children with incomplete vaccination reside in countries where vaccination coverage is often unknown. Compared to serum samples, dried blood spots (DBS) are an inexpensive, non-invasive and easy to obtain, conserve and transport alternative, without cold chain requirements. Data on group protection is key for designing strategies to prevent future outbreaks of preventable diseases.

Objectives: To present the first preliminary data of the correlation in paired serum/DBS samples of protective IgG levels against 6 pathogens causing vaccine-preventable diseases in an ongoing prospective project.

Methods: Patients < 18 years old from a tertiary hospital in Madrid (Spain), who were requested serologies for the detection of vaccine antibodies, were included. Dried blood (2-3 cards per patient) was taken simultaneously with samples collected for routine vaccine serology. The presence of G-immunoglobulins (IgG) against 6 vaccine-preventable diseases (diphtheria, tetanus, pertussis, measles, mumps and rubella) was quantified in paired DBS/serum samples using the VirClia-IgG (VIRCELL) technique. In each specific VirClia-IgG test we used 5 µl of serum or 100 µl of a DBS dot eluted in 1 mL of phosphate-buffered saline (PBS), equivalent to 5 µl serum per test. Clinical and epidemiological variables were collected from patients, and the results obtained in DBS were compared with those of conventional serology.

Results: Paired serum/DBS samples were collected from 48 patients < 18 years of age in this preliminary and ongoing study. Different percentage of subjects with protective IgG in serum varied across pathogens: Measles 58%, rubella 85%, mumps 79%, diphtheria 96%, tetanus 68.75% and pertussis 8%. When testing DBS positive results were: measles 56%, rubella 87.5%, mumps 83%, diphtheria 100%, tetanus 66% and pertussis 2%. The correlation between the technique in serum and in DBS for each pathogen is shown in the Figure, ranging from 77% for measles to 98% for mumps. Coincident results were found in all markers in 54.1% of the patients.



Serum-DBS correlation for each pathogen.

Conclusions: Children included in the study had no humoral response against some of the immunopreventable pathogens analyzed, especially against measles, tetanus and pertussis. DBS shows similar results to those obtained in serum with a correlation higher than 80% in all pathogens except for Measles. Our preliminary results, when confirmed with a larger set of paired DBS/serum, will support the DBS utility to monitor vaccination coverage in seroprevalence studies in resource-limited settings in the absence of serum specimens.

Funding: This study is funded by European Society for Pediatric Infectious Diseases (ESPID).

93. DISTINCTIVE ANTIBODY PROFILE IN PATIENTS WITH POST-COVID-19 CONDITION

Gemma Moncunill¹, Ruth Aguilar¹, Hugo Rozas¹, Daniela Modena², Marta Vidal¹, Alfons Jimenez¹, Brian Silva¹, Dídac Macià¹, Mar Canyelles¹, Lucía Carrasco², Concepció Violán², Diana Puente², Carlota Dobaño¹, Anna Berenguera¹

¹ISGlobal, Barcelona, Spain. ²IDIAPJGol, Barcelona, Spain.

Introduction: Post-COVID-19 condition (PCC) affects around 10% of people infected with SARS-CoV-2, who continue to present symptoms months after the infection, which range from mild to debilitating. The lack of specificity of the PCC definition and the overlap of symptoms with other diseases leads to a delay in the diagnosis.

Objectives: The objective of this project is to identify biomarkers and mechanisms underlying PCC, assessing reactivation of viral infections, autoimmunity, immune dysregulation and other alterations. Specific objectives for this presentation include: i) the identification of clusters of symptoms; ii) the identification of anti-SARS-CoV-2 antibody patterns associated with clusters and symptoms; iii) and the assessment of herpes viruses reactivation.

Methods: 426 PCC were recruited from November 2021 to May 2022. Blood samples were collected for serological determinations, and demographic and clinical information was collected in self-filled questionnaires. Cluster analysis of symptoms was performed using the Multiple Correspondence Analysis algorithm followed by a K-Means. IgG, IgM and IgA were measured by Luminex against 11 SARS-CoV-2 antigens: Spike (S), RBD, S1, S2, nucleocapsid (N) and RBD from variants of concern: delta and omicron (BA1.1, BA2, BA4/5, BQ1.1 and XBB); and 6 herpes antigens from CMV, EBV, HSV1 and VZV. Antibody levels between groups were compared using Kruskal-Wallis and Wilcoxon tests.

Results: Mean age of the participants was 47.65 years (SD 9), 80% were females and 11.7% had comorbidities. Mean time since onset of

symptoms was 544 days (SD 141.6). Participants had a mean of 9.11 symptoms (SD 4.48) and 85.7% received COVID-19 vaccines. Four clusters were identified: one with high number of symptoms and three with lower number of symptoms: one with higher prevalence of cardiovascular symptoms, one with higher prevalence of menstrual symptoms, and a third with no specific symptoms. There were few differences in antibody levels between clusters, with higher RBDs IgA and IgG and S1 IgG in the cardiovascular cluster and a tendency for lower levels in the cluster with high number of symptoms. Differential antibody profile was also detected for specific symptoms like fever, vomiting, dysgeusia/anosmia, sexual desire, and menstruation alterations. Menstrual alteration was associated with several differences with higher RBDs, N, CMV, EBV and VZV IgM levels and lower RBDs and S IgG and IgA levels.

Conclusions: Preliminary analyses of antibody responses show specific profiles associated to symptoms and clusters of symptoms, especially cardiovascular and menstrual, reflecting altered antibody responses to SARS-CoV-2 and herpes viruses in these phenotypes. Funding: Fundació Privada Daniel Bravo Andreu, CIBERINFEC.

96. IN VITRO RESISTANCE DEVELOPMENT TO IMIPENEM/RELEBACTAM IN KPC-PRODUCING *KLEBSIELLA PNEUMONIAE* INVOLVES MULTIPLE MUTATIONS INCLUDING OMPK36 DISRUPTION AND KPC MODIFICATION

Jorge Arca-Suárez^{1,2}, Eva Gato¹, Isaac Alonso-García¹, Juan Carlos Vázquez-Ucha^{1,3}, Marta Martínez-Guitián¹, Tania Blanco-Martín⁴, Rosa Pedraza-Merino⁴, Michelle Outeda¹, Romina Maceiras¹, Cristina Lasarte.monterrubio¹, Concepción González-Bello⁵, Luis Martínez-Martínez^{6,7}, Alejandro Beceiro^{1,8}, Germán Bou^{1,8}

¹Complejo Hospitalario Universitario A Coruña, A Coruña, Spain.

²Centro de Investigación Biomédica en Red de Enfermedades Infecciosas CB21/13/00055, Instituto de Salud Carlos III, Madrid, Spain. ³Centro de Investigación Biomédica en Red de Enfermedades Infecciosas CB21/13/00055-Instituto de Salud Carlos III, Madrid, Spain. ⁴Hospital Universitario Reina Sofía, Córdoba, Spain. ⁵Universidad de Santiago de Compostela, A Coruña, Spain. ⁶Hospital Reina Sofía, Córdoba, Spain.

⁷Centro de Investigación Biomédica en Red de Enfermedades Infecciosas CB21/13/00049, Instituto de Salud Carlos III, Madrid, Spain. ⁸Centro de Investigación Biomédica en Red de Enfermedades Infecciosas CB21/13/00055-Instituto de Salud Carlos III, Madrid, Spain.

Introduction: Imipenem/relebactam (IMR) and ceftazidime/avibactam (CZA) are two recently developed beta-lactam/beta-lactamase inhibitor with high activity against KPC-producing *Klebsiella pneumoniae*.

Objectives: To predict potential strategies aimed at combating KPC-producing *K. pneumoniae* infections, we comparatively analysed IMR and CZA resistance development dynamics and resistance mechanisms in high-risk clones of KPC-2 and KPC-3-producing *K. pneumoniae*.

Methods: Two high-risk clones of KPC-2 (AI3042, ST11; AI2713, ST273) and KPC-3 (AI2811, ST512; AI2644, ST307)-producing *K. pneumoniae* clinical strains were evaluated. Resistance dynamics were determined in triplicate experiments through incubating each strain during 7 days in 10-mL Mueller-Hinton (MH) tubes containing 2x incremental concentrations of each antibiotic combination up to their 64x baseline MICs. Selected mutants were characterized through WGS. MICs were determined by reference broth microdilution. Impact on β -lactam resistance of KPC-variants selected under IMR exposure were evaluated through cloning in an *Escherichia coli* HB4 background (OmpC and OmpF-deficient). KPC-2 and the IMR-selected KPC-2 N132S variant were purified and inhibition constants with relebactam were determined. The role of the N132S substitution on relebactam

resistance was explored via molecular modeling. Growth rates in MH of parental and antibiotic-selected strains were assessed by continuously monitoring the OD600 until late-log phase using an Epoch 2 microplate spectrophotometer.

Results: Results: In all cases clinical strains developed resistance to both combinations. Mutants selected with CZA showed changes in KPC associated with high-level CZA resistance (16 - > 512 mg/L) but carbapenem susceptibility. Mutants selected with IMR developed IMR resistance (range from 4-128 mg/L) but collateral changes in the MIC of the rest of β -lactams which differed throughout the different mutants. IMR-selected mutants tended to accumulate mutations in genes coding for OmpK36, PBP2, KPC (S106L and N132S in KPC-2 and L167R in KPC-3) and other proteins associated with cell-wall and membrane functions were found in several mutants. *E. coli* HB4 KPC transformants demonstrated that the IMR-selected variants KPC-2 N132S and KPC-3 L167R confer IMR resistance. Inhibition kinetics and structural analysis demonstrate that the N132S mutation dramatically reduced the potency of relebactam inhibition (in terms of IC50, K2/K, tn) through rearrangement of the KPC-2 active site. Compared to CZA, a higher proportion of mutants selected with IMR exhibited impaired growth.

Conclusions: Development of resistance to IMR in KPC-producing *K. pneumoniae* is associated with OmpK36 inactivation, KPC modification, strain-specific mutations and high fitness costs. Substitutions L167R and N132S confer resistance to imipenem/relebactam through modification of the KPC active site which results in a major increase on resistance to the inhibitor.

Funding: This work was supported by MSD through the Investigator Initiated Studies Program, which provided financial support (to G.B.) and relebactam. This work was also supported by the Fondo de Investigación Sanitaria (grant numbers PI17/01482 and PI20/01212 for A.B., and PI18/00501 and PI21/00704 for G.B.), integrated in the Plan Nacional de I+D and funded by the Instituto de Salud Carlos III, ISCIII). CIBER-INFEC (CIBER de Enfermedades Infecciosas). The research was also funded by the Spanish Network of Research in Infectious Diseases (REIPI), N° RD16/0016/0004 and N° RD16/0016/0006, integrated in the National Plan for Scientific Research, Development and Technological Innovation 2013–2016 and funded by the ISCIII–General Subdirection of Assessment and Promotion of the Research–European Regional Development Fund (FEDER) “A way of making Europe.” The study was also funded by GAIN (Agencia Gallega de Innovación, Consellería de Economía, Emprego e Industria; IN607D2021/12, A.B. and IN607A 2016/22, G.B.). PGS was financially supported by IN606A-2021/021. I.A.-G was financially supported by the Rio Hortega program (ISCIII, CM21/00076). J.C.V.-U. was financially supported by the ISCIII project FI18/00315. C.L.-M. was financially supported by IN606A-2019/029. J.A.-S. was financially supported by the Juan Rodés program (ISCIII, JR21/00026). Financial support from the Spanish Agency of Research (PID2019-105512RB-I00/AEI/10.13039/501100011033, CG-B), the Xunta de Galicia [ED431C 2021/29 and the Centro singular de investigación de Galicia accreditation 2019-2022 (ED431G 2019/03), CG-B], and the European Regional Development Fund (ERDF) is gratefully acknowledged. AC acknowledges to Banco Santander for his fellowship. We are also grateful to the Centro de Supercomputación de Galicia (CESGA) for use of the Finis Terrae computer.

98. DEVELOPMENT AND INTERNAL VALIDATION OF A PREDICTIVE MODEL SCORE FOR MORTALITY IN PATIENTS WITH BLOODSTREAM INFECTIONS. DATA FROM THE PROBAC PROSPECTIVE MULTICENTRE COHORT

Sandra de la Rosa Riestra¹, Pedro María Martínez Pérez Crespo², Fátima Galán³, Inmaculada López Hernández¹, Jesús Rodríguez Baño¹, Luis Eduardo López Cortés¹

¹Virgen Macarena University Hospital, Seville, Spain. ²Valme University Hospital, Seville, Spain. ³Puerta del Mar University Hospital, Cadiz, Spain.

Introduction: Bloodstream infections are an important mortality cause. Although some mortality predictive scores have been validated, most of them were developed years ago; recent changes in epidemiology and management would require updated prediction systems.

Objectives: Our purpose was to develop a mortality predictive model in bloodstream infections.

Methods: A prospective cohort including consecutive adults with bacteraemia collected between October 2016 and March 2017 in 26 hospitals in Spain was analysed. We excluded patients who died during the first 24 hours and we created a derivation cohort (DC) and a validation cohort (VC) with randomly chosen 2/3 and 1/3 of patients respectively. The primary outcome was all-cause 30-day mortality. A logistic regression model was developed in DC for mortality predictors, with punctuation assignments to the selected variables; the model was applied to VC. Then we excluded patients who died during the first 48 hours and applied the model in the resulting group to assess if the discriminative power was good even in this group of patients. We repeated the model combining our variables with some currently utilised scores: Charlson-age-adjusted ≥ 2 , Pitt ≥ 2 and SOFA ≥ 2 as dichotomised variables and compared the resulting models with our model through discriminative value.

Results: Overall, 6,111 patients were included. Mortality was 11.8%, 95%CI (10.7-12.9) and 12.3% (95%CI 10.6-13.9) (p: 0.53) in DC and VC, respectively. Epidemiological features, predisposing factors, appropriateness empirical and targeted therapy, microorganisms, severity and source of infection did not show statistically significant differences in DC and VC. The variables selected in multivariate model for DC with the points assigned are shown in the Table. The AUROC of the model was 0.82 95%CI (0.80-0.84). After applying the scoring system to the VC, we obtained a similar AUROC. Sensitivity, specificity, positive and negative predictive value, positive and negative likelihood ratio and mortality for the scoring system in VC was calculated (these values obtained in the scoring system in DC were similar). We assessed the AUROC obtaining after apply the model excluding patients who died during the first 48 hours: AUROC: 0.81 95%CI (0.79-0.83). The discriminative power obtained in the resulting models obtained combining our model with Charlson-age-adjusted ≥ 2 , Pitt ≥ 2 and SOFA ≥ 2 were worse than the one obtained in our original model.

Variable:	OR adjusted	95%CI	p-value
Age:			< 0.001
< 65	Reference		
65-80	1.45	1.09-1.94	0.01
> 80	2.30	1.70-3.11	< 0.001
McCabe fatal condition.	4.34	3.40-5.54	< 0.001
Cancer	1.41	1.29-2.57	0.006
Liver disease.	1.82	1.42-2.22	< 0.001
High risk aetiology (<i>S. aureus</i> , <i>P. aeruginosa</i> , <i>A. baumannii</i> , <i>E. faecium</i> , <i>E. faecalis</i> , <i>L. monocytogenes</i> y <i>S. marcescens</i>)	2.05	1.58-2.66	< 0.001
Consumption broad spectrum antibiotics during the previous month (third or fourth generation cephalosporins, piperacillin-tazobactam, carbapenems, aminoglycosides or glucopeptides)	1.49	1.17-1.90	< 0.001
High risk sources of infection (unknown, central nervous system, respiratory, abdominal except biliary tract)	1.72	1.36-2.18	< 0.001
Polymicrobial bloodstreaminfection	1.70	1.15-2.51	0.007
Stupor or coma.	2.81	2.10-3.76	< 0.001
MBP < 70 mmHg or requirement of vasoactive amines	1.62	1.26-2.08	< 0.001
Pa O ₂ /FiO ₂ \leq 300 or equivalent	2.33	1.74-3.13	< 0.001

Conclusions: We developed and internally validated a prognostic scoring system based in a large, multicentre cohort, which showed a good discrimination power.

Funding: ISCIII(PI16/01432).

100. ASSESSING THE IMPACT OF THE MOST RELEVANT CHROMOSOMALLY-ENCODED AND HORIZONTALLY-ACQUIRED PSEUDOMONAS AERUGINOSA RESISTANCE MECHANISMS ON RESISTANCE TO CEFIDEROCOL, IMPENEM/RELEBACTAM, CEFEPIME/TANIBORBACTAM, CEFEPIME/ZIDEACTAM AND AZTREONAM/AVIBACTAM

Juan Carlos Vázquez-Ucha¹, Isaac Alonso-García², Pablo Arturo Fraile-Ribot³, Cristina Lasarte-Monterrubio², Paula Guijarro-Sánchez², Soraya Rumbo-Feal², Michelle Outeda², Romina Maceiras², Marta Martínez-Gutián², Alejandro Beceiro¹, Carlos Juan³, German Bou¹, Antonio Oliver³, Jorge Arca-Suárez¹

¹Servicio de Microbiología and Instituto de Investigación Biomédica A Coruña (INIBIC), Complejo Hospitalario Universitario A Coruña, A Coruña, Spain. ²Centro de Investigación Biomédica en Red de Enfermedades Infecciosas (CIBERINFEC), Madrid, Spain. ³Servicio de Microbiología and Unidad de Investigación, Hospital Universitario Son Espases, Palma, Spain.

Introduction: Cefiderocol, imipenem/relebactam, cefepime/taniborbactam, cefepime/zidebactam and aztronam/avibactam are antimicrobial agents that demonstrate high activity against MDR *Pseudomonas aeruginosa* strains. However, the precise mechanisms that may compromise their effectiveness in this pathogen remain poorly understood.

Objectives: We sought to precisely determine the impact of the most relevant chromosomal and horizontally-acquired *P. aeruginosa* resistance mechanisms on the effectiveness of these new agents.

Methods: We constructed a collection of 42 PAO1 derivatives. Twenty-three of them were obtained via cloning assays using the pUCP-24 plasmid and included recombinant isolates expressing the most widespread class A (GES, PER, VEB and KPC variants), B (VIM, IMP and NDM variants), C (FOX-4) and D (OXA-14, OXA-15 and OXA-48) horizontally-acquired β -lactamases in *P. aeruginosa*. The other 19 isolates were obtained via the crelox system for gene deletion and included a collection of PAO1 knockout mutants expressing the most frequent chromosomally encoded resistance mechanisms found in this pathogen: overexpression of blaPDC, efflux pumps (mexAB-oprM, mexXY, and mexCD-oprJ) and oprD deficiency, including isolates simultaneously expressing multiple of these mechanisms. MICs were determined by reference broth microdilution.

Results: Cefiderocol demonstrated excellent *in vitro* activity (MICs \leq 0.5-2 mg/L) for most of isolates producing horizontally-acquired enzymes with the exception of isolates producing PER-1 (MIC = 32 mg/L) or NDM variants (MIC = 8 mg/L). Imipenem/relebactam was active against isolates producing class A and C β -lactamases, although it was found inactive against MBL and OXA-48-producing isolates and against 2 producers of imipenem/relebactam-selected KPC derivatives (KPC-2 N132S and KPC-3 L167R). The activity of cefepime/taniborbactam was only limited against isolates producing IMP and NDM-type enzymes, whereas cefepime/zidebactam and aztreonam/avibactam were active against all transformants (MICs 2-8 mg/L and 4-16 mg/L respectively). Besides, cefiderocol (MICs \leq 0.12-0.25 mg/L) and imipenem/relebactam (MICs 0.25-1 mg/L) retained activity against isolates showing chromosomal resistance, whereas efflux pumps significantly raised the MICs of aztreonam/avibactam (MexAB-OprM, MIC = 8 mg/L), cefepime/taniborbactam (MexAB-OprM, MexXY and MexCD-OprJ, MIC = 8 mg/L), cefepime/zidebactam and zidebactam alone (MexAB-OprM, MICs of 8 and 16-32 mg/L, respectively).

Conclusions: These agents show complementary *in vitro* activity against *P. aeruginosa* resistance mechanisms. Cefiderocol and imipenem/relebactam show higher stability against mutational resistance than aztreonam/avibactam and cefepime-based combinations, which are significantly affected by efflux.

Funding: ISCIII PI20/01212, PI18/00501, and CIBER CB21/13/00055 AB and GB. PI21/00017 and CB21/13/00099 AO and CJ. In addition, IN607A 2020/05, IN607D 2021/12 and REIPI RD16/0016/006.JA-S (ISCIII, JR21/00026), JCV-U (Xunta, IN606B-2022/009), CL-M (Xunta, IN606A-2019/029) and PI20/01212 (ISCIII), PG-S (Xunta, IN606A 2021/021), MO and RM (Xunta, IN607D 2021/12) IA-G (ISCIII, CM21/00076), MM-G (MU, RSU.UDC.M505), PAF-R (ISCIII, CM21/00007).

102. ROLE OF INTESTINAL MICROBIOTA COMPOSITION IN HAEMATOPOIETIC STEM CELL TRANSPLANT (HSCT)

Claudia González-Rico^{1,2}, Sara Fernández-Luis³, Jorge Rodríguez-Grande⁴, Marta Hernández Pérez⁵, Francisco Arnaiz de Las Revillas Almajano^{1,2}, Lucrecia Yañez San Segundo^{3,6}, Arancha Bermúdez Rodríguez^{3,6}, Alain Ocampo-Sosa^{4,2}, Jorge Calvo Montes^{4,2}, Marta Fernández-Martínez^{7,2}, M. Carmen Fariñas Álvarez^{1,6,2}

¹Infectious Diseases Service, Marqués de Valdecilla University Hospital-IDIVAL, Santander, Spain. ²Centro de Investigación Biomédica en Red de Enfermedades Infecciosas (CIBERINFEC), Madrid, Spain. ³Haematology Service, Marqués de Valdecilla University Hospital-IDIVAL, Santander, Spain. ⁴Microbiology Service, Marqués de Valdecilla University Hospital-IDIVAL, Santander, Spain. ⁵Agricultural Technology Institute of Castilla and León (ITACyL), Valladolid, Spain. ⁶University of Cantabria, Santander, Spain. ⁷HSC Processing and Cell Therapy Unit, Blood and Tissue Bank of Cantabria, Marqués de Valdecilla Foundation, Hospital de la Santa Cruz de Liencres, Liencres, Spain.

Introduction: The microbiota appears to play an important role in the success of HSCT and the development of graft-versus-host-disease (GVHD). The dysbiosis that occurs during HSCT may lead to increased colonization by pathogenic microorganisms, such as multidrug-resis-

Characteristics of the study population

	Patients (N = 19)
Male/Female, n (%)	14/5 (73.68/26.32)
HCT-CI score, median (IQR)	2 (1-3)
Risk factors, n (%)	
Conditioning regimen	
Myeloablative	13 (68.42)
Non-myeloablative	6 (31.58)
GVHD prophylaxis	
CsA + MMF	6 (31.58)
CsA + MTX	2 (10.53)
Tacrolimus + MMF	1 (5.26)
Cyclophosphamide	3 (15.79)
Cyclophosphamide + Tacrolimus+MMF	7 (36.84)
Infections (3 months prior)	9 (47.37)
Antibiotic treatment (3 months prior)	10 (52.63)
Colonization by MDRE, n (%)	
Before HSCT	2 (10.53)
After HSCT	11 (57.89)
Post-transplant factors, n (%)	
Episode of MDRE Infection	3 (15.79)
Acute GVHD episode	8 (42.11)
Chronic GVHD episode	9 (47.37)
Underlying disease remission	14 (73.68)
Underlying disease recurrence	2 (10.53)
Death (1 year after HSCT), n (%)	2 (10.53)

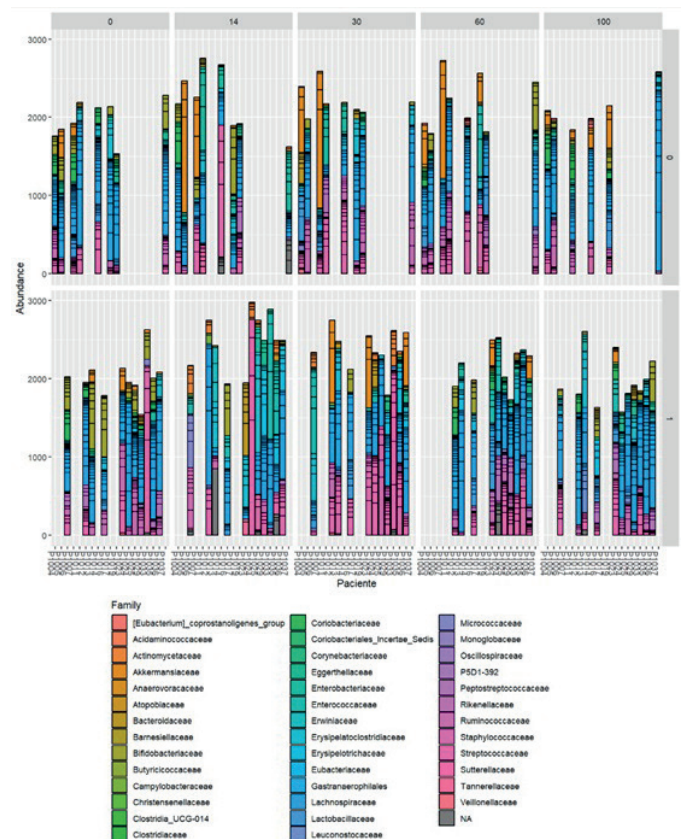
HCT-CI: Hematopoietic cell transplantation-specific comorbidity index; IQR: Interquartile Range; GVHD: Graft-Versus-Host-Disease; CsA: Cyclosporine; MMF: Mycophenolate mofetil; MTX: Methotrexate; MDRE: multidrug-resistant *Enterobacteriaceae*; HSCT: haematopoietic stem cell transplant.

tant *Enterobacteriaceae* (MDRE), and thus an increased risk of infection by these microorganisms.

Objectives: The aim of this study was to analyse the composition of the intestinal microbiome during HSCT, its relationship with the clinical outcome of patients and MDRE colonization.

Methods: A prospective cohort study was conducted between June 2017 and June 2021 in Marqués de Valdecilla University Hospital. Stool samples were collected before HSCT and on days 14, 30, 60 and 100 following transplantation. The V3-V4 region of the 16S rDNA was sequenced on Illumina MiSeq and the sequences were processed using the QIIME2 pipeline. All samples were down-sampled to 10k reads. Only taxa with a frequency of at least 0.2% in the analysed sample were selected. Patient outcomes were followed up to one year after HSCT.

Results: This is a preliminary analysis of 92 samples from 19 patients. The clinical characteristics of the patients are listed in the Table. Taxonomic profile of the intestinal microbiota by time and colonization status are represented in the Figure. The most abundant phylum are Firmicutes, followed by Actinobacteriota and Verrucomicrobiota. Several diversity metrics were performed to determine alpha and beta diversity. Non-metric multidimensional scaling (NMDS) analyses of Bray-Curtis, Jaccard and Shannon indices do not allow us to observe distinct groups when gathering the population according to some characteristics. Probably due to the small number of patients analysed.



0: Non-Colonized patients; 1: Colonized patients.

Conclusions: No significant differences were observed in the composition of the microbiota regarding to different characteristics of patients. Further analysis are needed to understand the relevance of the microbiome in these patients.

Funding: Supported by Plan Nacional de I+D+i 2013-2016 and Instituto de Salud Carlos III, Subdirección General de Redes y Centros de Investigación Cooperativa, Ministerio de Ciencia, Innovación y Universidades, Spanish Network for Research in Infectious Diseases-cofi-

nanced by European Development Regional Fund “A way to achieve Europe”, Operative Program Intelligent Growth 2014-2020 and grant PI16/01415. Emerging researchers support program “NEXT-VAL” 2021 - IDIVAL (NVAL 21/18).

104. EVALUATION OF NUCLEAR MAGNETIC RESONANCE-BASED URINE METABOLIC PROFILING TO MONITOR TREATMENT RESPONSE IN CHILDREN WITH TUBERCULOSIS

Andrea Lopez-Suárez^{1,2,3}, Paula Rodríguez-Molino^{2,4,5}, Yaiza Marín Oliver⁶, María del Pilar Alonso-Moreno⁶, Patricia Comella del Barrio^{3,7}, Antoni Noguera-Julian⁸, Daniel Blazquez-Gamero⁹, Ana Belen Jiménez¹⁰, Jara Hurtado Gallego^{2,4,5}, Sonia Alcolea Ruiz^{2,4,11}, Jorge Atucha^{2,4,5}, Talia Sainz Costa^{2,4,5}, Jose Luis Izquierdo-García^{2,6,12}, Begoña Santiago-García¹

¹Pediatric Infectious Diseases Unit, Department of Pediatrics, Gregorio Marañón University Hospital, Madrid, Spain. ²Centro de Investigación Biomédica en Red de Enfermedades Infecciosas (CIBERINFEC), Madrid, Spain. ³Gregorio Marañón Research Health Institute (IiSGM), Madrid, Spain. ⁴General Pediatrics, Infectious and Tropical Diseases Department, Hospital La Paz, Madrid, Spain. ⁵La Paz Research Institute (IdiPAZ), Madrid, Spain. ⁶NMR and Imaging in Biomedicine Group, Instituto Pluridisciplinar, Universidad Complutense de Madrid, Madrid, Spain. ⁷Pediatric Infectious Diseases Unit, Department of Pediatrics, Gregorio Marañón, Madrid, Spain. ⁸Pediatric Infectious Diseases Unit, Hospital Sant Joan de Déu, Universitat de Barcelona, Esplugues de Llobregat, Barcelona, Spain. ⁹Pediatric Infectious Diseases Unit, Hospital Universitario 12 de Octubre, Universidad Complutense, Instituto de Investigación Hospital 12 de Octubre (imas¹²), Madrid, Spain. ¹⁰Pediatric Department, Hospital Universitario Fundación Jiménez Díaz, Madrid, Spain. ¹¹La Paz Research Institute (IdiPAZ, Madrid, Spain. ¹²Department of Chemistry in Pharmaceutical Sciences, Pharmacy School, Universidad Complutense de Madrid, Madrid, Spain.

Introduction: In tuberculosis (TB) management, monitoring patients' progress during treatment is crucial to assess clinical response, and may be useful in deciding on the implementation of new short regimens. Recent research has shown the potential of urine metabolomics as a diagnostic and prognostic tool for TB. Nuclear Magnetic Resonance (NMR)-based metabolomics provides a unique fingerprint of the disease's metabolic status, making it a powerful tool for evaluating TB.

Objectives: This proof-of-concept study aims to follow the urinary metabolic profile of pediatric TB patients during anti-TB treatment. Urine is a promising sample for evaluating pediatric TB, as it is an easy and non-invasive sample to collect. The objectives of the study were to determine the urine metabolic fingerprint at different timepoints and analyze longitudinal changes in metabolomic profiles during treatment.

Methods: The study included 145 patients under 18 years of age from 10 hospitals belonging to the Spanish Pediatric TB Network (Table). Urine samples were collected at diagnosis, at 2 months, and at the end of treatment (4-6 months). The samples were analyzed using a 500 MHz Bruker NMR spectrometer at the Complutense University of Madrid (CIBERES). NMR spectra were processed using MNOVA software (Mestrelab Research, Santiago de Compostela). Multivariate Statistical Analysis were performed using Metaboanalyst web application. PLS-DA models were applied to investigate significant differences in the metabolic profile between samples collected at different time points. Variable Importance in Projection (VIP) was calculated to identify the metabolic signals that discriminate between groups.

Results: Preliminary results from 35 children with active TB show a metabolic reprogramming during anti-TB treatment. PLS-DA provided

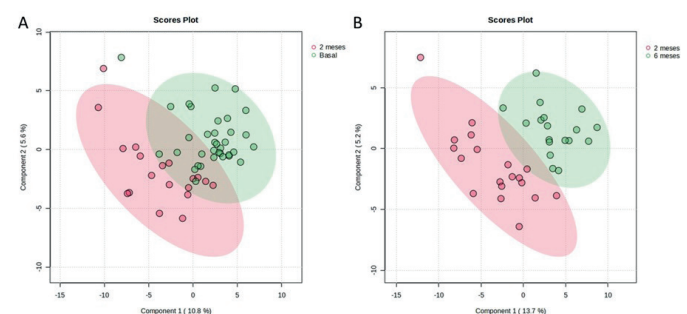
good discrimination between samples collected at diagnosis and at 2 months of the treatment, with an accuracy in the cross validation of 75% ($Q^2 = 0.18$). A second PLS-DA model discriminated between samples collected at 2 months and at the end of treatment, with an accuracy in the cross validation of 79% ($Q^2 = 0.30$). More than 80 NMR signals were identified as important in the classification.

Clinical and demographic features of the study population belonging to Spanish Pediatric TB Network

Variables	All (n = 145)	Active TB (n = 95)	Latent TB (n = 24)	TB contacts (Controls) (n = 26)
Gender				
Girls	59 (40,7%)	40 (42,1%)	6 (25,0%)	13 (50,0%)
Boys	86 (59,3%)	55 (57,9%)	18 (75,0%)	13 (50,0%)
Age				
< 1 year	12 (8,3%)	9 (9,5%)	0 (0,0%)	3 (11,5%)
1-5 years	48 (33,1%)	36 (37,9%)	4 (16,7%)	8 (30,8%)
5-12 years	46 (31,7%)	22 (23,1%)	16 (66,6%)	8 (30,8%)
> 12 years	39 (26,9%)	28 (29,5%)	4 (16,7%)	7 (26,9%)
BCG				
Yes	23 (15,9%)	15 (15,8%)	5 (20,8%)	3 (11,6%)
No	111 (76,5%)	74 (77,9%)	16 (66,7%)	21 (80,7%)
Unknown	11 (7,6%)	6 (6,3%)	3 (12,5%)	2 (7,7%)
TST				
Positive	94 (64,8%)	78 (82,1%)	15 (62,5%)	1 (3,9%)*
Negative	22 (15,2%)	8 (8,4%)	1 (4,2%)	13 (50,0%)
Not performed	29 (20,0%)	9 (9,5%)	8 (33,3%)	12 (46,1%)
QTF				
Positive	96 (66,2%)	74 (77,9%)	20 (83,3%)	1 (3,9%)*
Negative	34 (23,5%)	10 (10,5%)	1 (4,2%)	24 (92,3%)
Indeterminate	6 (4,1%)	3 (3,2%)	2 (8,3%)	1 (3,8%)
Not performed/UNK	9 (6,2%)	8 (8,4%)	1 (4,2%)	0 (0,0%)
Treatment length				
3 months	12 (8,3%)	3 (3,2%)	6 (25,0%)	3 (11,5%)
3-6 months	74 (51%)	61 (64,2%)	13 (54,2%)	1 (3,9%)
> 6 months	20 (13,8%)	16 (16,8%)	4 (16,7%)	0 (0,0%)
Observation	22 (15,2%)	0 (0,0%)	0 (0,0%)	22 (84,6%)
Unknown	17 (11,7%)	15 (15,8%)	1 (4,1%)	0 (0,0%)
Drug susceptibility				
Susceptible	-	35 (36,8%)	-	-
Monoresistant	-	3 (3,2%)	-	-
Poliresistant	-	1 (1,1%)	-	-
Unknown	-	56 (58,9%)	-	-

The cohort included 95 children with active TB, 24 cases of latent TB infection (LTBI), and 26 TB contacts as controls. The mean age of the cohort was 7.7 years old.*Positive TST result in a control patient with treated tuberculosis infection.

**Possible false positive.



Score plot of PLS-DA performed on the 1H NMR spectra of urine samples from pediatric tuberculosis patients collected A) at diagnosis (green) and at 2 months (red); B) at 2 months (red) and at the end of the treatment (green). Samples from three groups are clearly separated.

Conclusions: We have identified an NMR-based metabolic profile in urine that may be capable to monitor disease progression during

treatment and evaluate the outcome of treatment success. This urine metabolomic approach could be applied to monitor individualized treatment regimens of patients with longer treatment time and poor treatment outcomes as patients treated for drug-resistant TB.

Funding: This research was supported by grants: (i) PID2019-10656RJ-I00 from the Spanish Ministry of Science and Innovation and grant PI20/01607 from ISCIII AES 2020.

105. HYBRID IMMUNITY AGAINST VARIANTS OF CONCERN IN PEOPLE VACCINATED WITH TWO DOSES OF SPIKEVAX: EFFECT OF TIMING OF VACCINATION

Javier García-Pérez¹, Mercedes Bermejo¹, Almudena Ramírez García², Humberto Erick de la Torre Tarazona¹, Almudena Cascajero¹, María Castillo de la Osa¹, Paloma Jiménez¹, Marta Aparicio Gómez², Esther Calonge¹, Aránzazu Sancho-López², Concepción Payarés-Herrera², Rocío Layunta-Acero², Laura Vicente-Izquierdo², Cristina Avendaño-Solá², José Alcamí¹, Mayte Pérez-Olmeda¹, **Francisco Díez-Fuertes¹**

¹Instituto de Salud Carlos III, Majadahonda, Spain. ²Hospital Universitario Puerta de Hierro, Majadahonda, Spain.

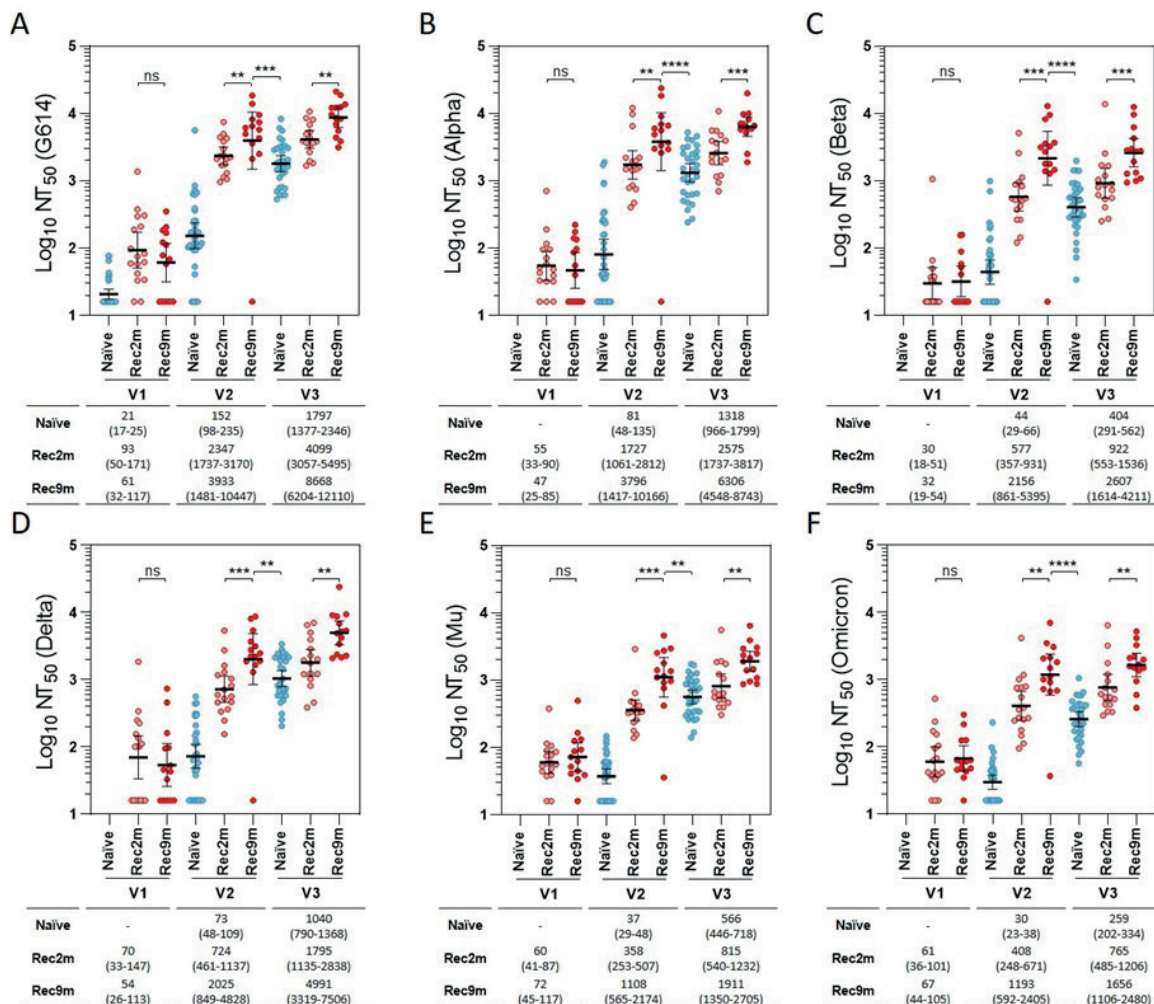
Introduction: The effectiveness of hybrid immunity against severe acute respiratory syndrome coronavirus 2 (SARS-CoV-2) re-infection is a matter of debate, especially after the appearance of the highly

diversified sublineages of omicron variant associated with a high transmissibility and immune evasion.

Objectives: This study aims to evaluate the humoral immune response elicited against SARS-CoV-2 variants of concern (VOCs) Alpha, Beta, Delta, and Omicron in recovered and naïve people vaccinated with two doses of SpikeVax (Moderna). To evaluate the effect of extending the vaccination schedule we compared the impact of immunization 1-3 months (Rec2m) versus 4-12 months (Rec9m) after the natural infection in recovered patients.

Methods: Sera from 66 health care workers were collected at days 0, 28 and 42 after the first dose of SpikeVax. A total of 31 out of the 66 participants had a documented prior history of SARS-CoV-2 infection, including 17 (53.1%) Rec2m within three months before vaccination and 14 (43.7%) Rec9m with a documented infection from 4 to 12-months before vaccination. Antibody-mediated immune responses were assessed by three commercial immunoassays and a SARS-CoV-2 lentiviral-based pseudovirus neutralization assay.

Results: Levels of immunoglobulins (Ig) to SARS-CoV-2 were lower in naïve participants at post-boost as compared with convalescents after a single dose of SpikeVax ($p < 0.05$). In recovered patients, after two vaccine doses total Ig to RBD were higher in Rec9m (21,618 BAU/ml; 95%CI: 18,092-25,831) as compared to Rec2m (10,219 BAU/ml; 95%CI: 7,572-13,792 BAU/ml) ($p < 0.001$). These differences were also observed for anti-trimeric spike IgG levels and anti-spike IgA. The SARS-CoV-2 neutralization titer 50 (NT50) observed in recovered participants after a single dose was consistently higher than in naïve



NT50 levels in pseudovirus neutralization assay in naïve, Rec2m and Rec9m vaccine recipients against SARS-CoV-2 variants D614G (A), Alpha (B), Beta (C), Delta (D), Mu (E), and Omicron (F). NT50 was summarized as geometric mean and 95% confidence interval.

	Naïve (n = 34)	Recovered (n = 32)
Age	32.6 (24.4-44.3)	32.1 (26.5-47.2)
Sex		
Female	23 (67.6%)	23 (71.9%)
Comorbidities		
Obesity	2 (5.9%)	1 (3.1%)
Arterial hypertension	2 (5.9%)	1 (3.1%)
Asthma	1 (2.9%)	0
Diabetes	1 (2.9%)	0
Immunosuppression	1 (2.9%)	1 (3.1%)
Severity of disease*		
No clinical or virological evidence of infection	34 (100%)	1 (3.1%)
Ambulatory, no limitation of activities	-	6 (18.7%)
Ambulatory, limitation of activities	-	20 (62.5%)
Hospitalized, mild disease, no oxygen therapy	-	4 (12.5%)
Hospitalized, mild disease, oxygen therapy	-	0
Hospitalized, non-invasive ventilation	-	0
Hospitalized, intubation and mechanical ventilation	-	1 (3.1%)
Hospitalized, ventilation + additional organ support	-	0
Death	-	0
Previous COVID-19		
< 3 months from vaccination (mean = 48 days)	-	17 (53.1%)
> 3 months from vaccination (mean = 266 days)	-	14 (43.7%)

*WHO Ordinal Scale for Clinical Improvement, COVID-19 Trial Design Synopsis (0-8 scale).

participants after two doses of SpikeVax against the ancestral variant G614 (1.7-fold), and VOCs Alpha (1.9-fold), Beta (2.7-fold), Delta (1.1-fold), and Omicron (2.7-fold). Fourteen days after the second dose of SpikeVax, the neutralizing potency observed in Rec9m was consistently higher than in Rec2m against VOCs Alpha, Beta, Delta, and BA.1 sublineage of Omicron with 2.2–2.8-fold increases.

Conclusions: Increasing more than 3 months the interval between SARS-CoV-2 infection and the immunization with mRNA-based vaccines generates a more efficient humoral immune response against VOCs. This improvement can be related with the time requested to mount a strong recall memory B cell response. Ongoing studies include the neutralization response against the new omicron variants circulating in Spain and the analysis of B and T cell responses in the participants.

Funding: Instituto de Salud Carlos III, CIBERINFEC.

106. RATES OF FAECAL/OROPHARYNGEAL COLONIZATION AND INFECTION BY MULTIRESTANT GRAM-NEGATIVE BACTERIA AMONG PATIENTS ADMITTED TO SEVEN ICUS IN SPAIN: MURAN-UCI PROJECT

Javier Cañada-García¹, Enrique Alemparte- Pardavila², Ester del Barrio Tofiño³, Mercedes Delgado⁴, Desiree Gijón Cordero⁵, Claudia González-Rico⁶, Cristina Riazzo⁷, Estrella Rojo-Moliner⁸, Francisco J Arroyo Muñoz⁹, Jorge Arca-Suárez¹⁰, Sergio García-Fernández⁵, Alba Mir-Cros¹¹, Carla López-Causapé¹², Jorge Rodríguez-Gómez⁷, Patricia Ruiz-Garbajosa¹³,
Eva Ramírez de Arellano¹

¹Centro Nacional de Microbiología, Instituto de Salud Carlos III, Madrid; CIBER Enfermedades Infecciosas (CIBERINFEC), Madrid, Spain.

²Complejo Hospitalario Universitario A Coruña, Servicio de Medicina Intensiva; A Coruña, Spain. ³Hospital Universitario Vall d'Hebron, Servicio de Microbiología; IBER Enfermedades Infecciosas (CIBERINFEC), Barcelona, Spain. ⁴Hospital Universitario Virgen Macarena, Sevilla, Servicio de Microbiología; ⁵CIBER Enfermedades Infecciosas (CIBERINFEC), Sevilla, Spain. ⁶Hospital Universitario Ramón y Cajal,

Madrid, Servicio de Microbiología, Madrid, Spain. ⁶Hospital Universitario Marqués de Valdecilla, Santander, Servicio de Enfermedades infecciosas; CIBER Enfermedades Infecciosas (CIBERINFEC), Santander, Spain. ⁷Hospital Universitario Reina Sofía de Córdoba, Servicio de Microbiología; CIBER Enfermedades Infecciosas (CIBERINFEC), Córdoba, Spain. ⁸Hospital Universitario Son Espases, Palma de Mallorca, Baleares, Servicio de Microbiología; CIBER Enfermedades Infecciosas (CIBERINFEC), Palma de Mallorca, Spain. ⁹Hospital Universitario Virgen Macarena, Sevilla, Unidad Clínica de Cuidados Intensivos, Sevilla, Spain. ¹⁰Complejo Hospitalario Universitario A Coruña, Servicio de Microbiología & Instituto de Investigación Biomédica A Coruña (INIBIC); CIBER Enfermedades Infecciosas (CIBERINFEC), A Coruña, Spain. ¹¹Hospital Universitario Vall d'Hebron, Servicio de Microbiología; CIBER Enfermedades Infecciosas (CIBERINFEC), Barcelona, Spain. ¹²Hospital Universitario Son Espases, Palma de Mallorca, Baleares, Servicio de Microbiología; CIBER Enfermedades Infecciosas (CIBERINFEC), Palma de Mallorca, Spain. ¹³Hospital Universitario Ramón y Cajal, Madrid, Servicio de Microbiología; CIBER Enfermedades Infecciosas (CIBERINFEC), Madrid, Spain.

Introduction: Although there are multiple bacteria that cause infections and outbreaks in ICUs, multidrug-resistant Gram-negative bacteria are the main challenge in ICUs around the world, mainly the carbapenemase-producing Enterobacterales (CPE), ESBL-producing Enterobacterales, and carbapenem-resistant (CR) *Pseudomonas aeruginosa* and *Acinetobacter* spp. The objective of this study is to know the impact of colonization/infection by these microorganisms in Spanish ICUs.

Objectives: To study the prevalence of colonization/infection on admission to ICUs of CPE, ESBL-producing Enterobacterales, and carbapenem-resistant (CR) *P. aeruginosa* and *Acinetobacter* spp., as well as their incidence acquired during the stay in ICUs.

Methods: All patients admitted to ICUs of seven Spanish hospitals during February 15th to March 30th, 2023, were included. Carrier status was studied by surveillance cultures of rectal and oropharyngeal exudates on admission, one week, and two weeks. The prevalence of colonization at admission and the incidence of colonization acquired during the stay in ICUs by CPE, ESBL-producing *Klebsiella pneumoniae*, and CR *P. aeruginosa* and *Acinetobacter* spp. were calculated. Information on infections caused by these bacteria was also recorded.

Results: 772 patients were included. The pooled prevalence of colonization by the bacteria under study upon ICUs admission was 3.10% (24/772) [interhospital range: 0.5%-10.3%]. On admission, five patients carried CPE (prevalence: 0.69%), 11 ESBL-K. *pneumoniae* (1.42%), seven CR *P. aeruginosa* (0.91%) and one CR *Acinetobacter* spp. (0.14%). The pooled incidence of ICU-acquired colonization during the first two weeks in six out of seven hospitals was 7.42% (19/256) [interhospital range: 0%-27.45%]. CPE colonization was observed in six patients (prevalence: 2.34%), ESBL-K. *pneumoniae* in one patient (0.39%) and CR *P. aeruginosa* in 12 (4.68%). Of all detected colonizations, 35 were identified in faecal samples, two in oropharyngeal samples and six in both samples. Finally, sixteen positive cases of infection by these bacteria were detected (pooled prevalence: 2%), nine of them previously colonized by the same microorganism; most of them were CR *P. aeruginosa* (11/16; 68.7%).

Conclusions: A relatively low prevalence and incidence of the targeted multidrug-resistant bacteria were observed in the majority of the participant hospitals, although individual hospital variations were detected. CR *P. aeruginosa* was the most frequent bacteria identified in both colonizations and infections. In this regard, it is strongly advisable to implement the guidelines for infection control measures to reduce transmission of multidrug-resistant Gram-negative bacteria. Funding: This research was funded by the Intramural Call for Research Projects CIBERINFEC 2022 (Consorcio Centro de Investigación Biomédica en Red, CIBER en Enfermedades Infecciosas).

107. GENOMIC CHARACTERIZATION OF *KLEBSIELLA PNEUMONIAE* ISOLATES BELONGING TO THE ST307 CLONE RECOVERED FROM 45 HOSPITALS IN ANDALUSIA (SPAIN) IN THE PERIOD 2014-2022

Manuel Alcalde-Rico¹, Mercedes Delgado-Valverde², Inés Portillo-Calderón², Patricia Pérez-Palacios², Ester Recacha², Inmaculada López-Hernández², Felipe Fernández-Cuenca², Marina R. Pulido³, Álvaro Pascual^{2,3}, Lorena López-Cerero^{2,3}

¹Centro de Investigación Biomedica en Red de Enfermedades Infecciosas (CIBERINFEC), Instituto de Salud Carlos III, Madrid, Spain.

²UGC Microbiología, Laboratorio de Referenci regional de tipado molecular de patógenos nosocomiales, Hospital Virgen Macarena, Sevilla, Spain. ³Departamento de Microbiología, Facultad de Medicina, Universidad de Sevilla, Sevilla, Spain.

Introduction: *Klebsiella pneumoniae* (KPN) is one of the most important opportunistic pathogens worldwide, easily acquires antibiotic resistance genes (ARGs) through horizontal gene transfer and some specific clones (STs) are predominant in specific regions and may cause nosocomial outbreaks. Tracing the emergence and spread of these predominant clones is important to monitor and control multiresistant pathogens.

Objectives: To describe the clonal evolution of KPN ST307 isolates collected from 45 hospitals in Andalusia among 2014-2022 and to analyse the genomic characteristics that could be influencing the expansion of ST307 in this region.

Methods: 2533 isolates were sent from 45 hospitals in Andalusia 2014-2022 to the PIRASOA reference laboratory (Hospital Universitario Virgen Macarena) for molecular typing. Initial characterisation was performed by PFGE and phenotypic tests following EUCAST recommendations. Whole genome sequencing (WGS) (Illumina Miseq 2x300 bp) of representative isolates of the different pulse types was carried out. Identification of relevant betalactamases was performed by lateral immunochromatography, inhibitors discs, WGS or PCR plus Sanger sequencing. Genomes sequences were de novo assembled with "SPAdes", annotated with "Bakta" and ARGs were identified with "RESFinder". The core and accessory genomes was performed with "Roary" and compared to Ridom scheme. The phylogenomic reconstruction was carried out with "RAXML" and "ClonalFrameML".

Results: In the recent years (2018-2022), a clonal shift was observed, in which ST307 emerged as predominant (23.9%) over ST512 and ST15, which were predominant in 2014-2017. ST307 was recovered from all sample type (clinical, colonization and hospital plumbing). The phylogenomic reconstruction showed a highly conserved core genome (4,360 genes present in 99% of the ST307 sequenced) and an

accessory genome with greater diversity among those cgMLSTs disseminated in different hospitals compared to those associated with specific hospitals or regions.

Conclusions: Both ST512 and ST15 clones had been progressively displaced by ST307. The ST307 genomes present a great similarity but with a diverse accessory genome that could explain their adaptation to different environments (infection, colonization and humid reservoirs) and, therefore, their expansion in hospital settings. Moreover, more analysis should be carried out to deep into this hypothesis.

Funding: This work has been financed by CIBERINFECT through a PhD researcher contract (M. Alcalde-Rico).

109. GENOMIC CHARACTERIZATION, ANTIMICROBIAL SUSCEPTIBILITY AND VACCINE REACTIVITY TO 4CMENB OF *NEISSERIA MENINGITIDIS* PRODUCING INVASIVE MENINGOCOCCAL DISEASE IN SPAIN

Josep Roca-Grande^{1,2}, Alba Mir-Cros^{1,2}, Carmen Ardanuy^{3,4}, Alba Bellés⁵, Jorge Calvo⁶, Jordi Càmaras^{3,4}, Emilio Cendejas-Bueno⁷, Emilia Cercenado^{4,8}, Pilar Egea⁹, Frederic Gómez-Bertomeu¹⁰, Luis Martínez-Martínez⁹, Carmen Muñoz-Almagro^{4,11}, Daniel Navarro de la Cruz¹², M. Ángeles Orellana¹³, Amaresh Pérez¹¹, Maria Dolores Quesada¹⁴, Carlos Rodrigo¹⁴, Ana Rodríguez-Fernández⁶, Enrique Ruiz de Gopegui^{2,15}, Carolina Sarvisé¹⁰, Juan José González-López¹²

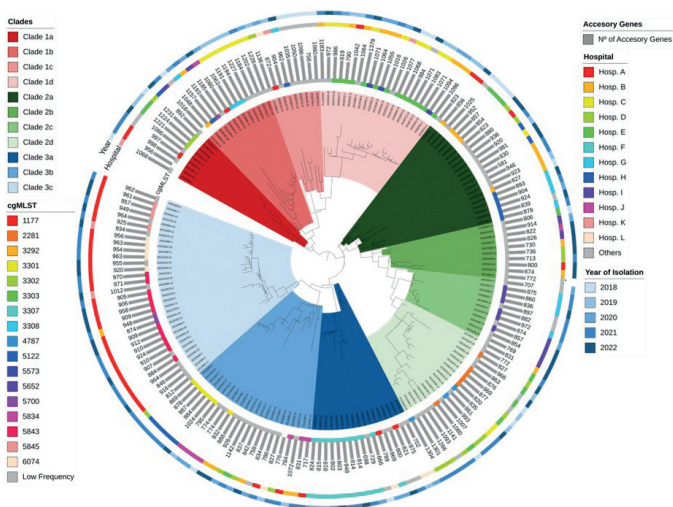
¹Hospital Universitari Vall d'Hebron, Barcelona, Spain. ²Centro de Investigación Biomédica en Red de Enfermedades Infecciosas (CIBERINFEC), Madrid, Spain. ³Hospital Universitari de Bellvitge, L'Hospitalet de Llobregat, Spain. ⁴Consorcio de Investigación Biomédica en Red de Epidemiología y Salud Pública (CIBERESP), Madrid, Spain. ⁵Hospital Universitari Arnau de Vilanova, Lleida, Spain. ⁶Hospital Universitario Marqués de Valdecilla, Santander, Spain. ⁷Hospital Universitario La Paz, Madrid, Spain. ⁸Hospital Universitario Gregorio Marañón, Madrid, Spain. ⁹Hospital Universitario Reina Sofía, Córdoba, Spain. ¹⁰Hospital Universitario Joan XXIII, Tarragona, Spain. ¹¹Hospital Sant Joan de Déu, Esplugues de Llobregat, Spain. ¹²Hospital Clínico Universitario de Santiago, Santiago de Compostela, Spain. ¹³Hospital Universitario 12 de Octubre, Madrid, Spain. ¹⁴Hospital Universitari Germans Trias i Pujol, Badalona, Spain. ¹⁵Hospital Universitari Son Espases, Palma, Spain.

Introduction: The four-component recombinant 4CMenB vaccine (Bexsero®) has demonstrated its effectiveness against invasive meningococcal disease (IMD) caused by serogroup B *Neisseria meningitidis* (Nm). Due to its composition, 4CMenB does not protect against all NmB variants and may cross-react with other serogroups.

Objectives: The objective of this study is to describe the genomic epidemiology, the antimicrobial susceptibility and the expected reactivity to 4CMenB of IMD-causing Nm in Spain.

Methods: A total of 282 Nm producing IMD were studied and collected from various clinical microbiology laboratories in Spain between 2011-2022. Molecular characterization was performed by whole genome sequencing. Serogroups were identified by analyzing the capsular genes and reactivity to 4CMenB was predicted by analysing the vaccine antigenic variants (MenDeVAR index). Antimicrobial susceptibility testing to macrolides, fluoroquinolones, beta-lactams, chloramphenicol, rifampicin and cotrimoxazole was performed by gradient diffusion test.

Results: An increase in IMD cases was observed from 2011 to 2019. However, an abrupt decrease was observed during the COVID-19 pandemic in 2020. Serogroup B was the most prevalent (57.4%), followed by W (23.0%), C (10.3%) and Y (7.1%). During the pandemic situation, serogroup B remains the predominant cause of IMD. Genomic epidemiology showed that the most prevalent lineage among NmB was CC-ST213 (35.8%), followed by CC-ST461 (13%), CC-ST269 (12.3%) and CC-ST32 (11.7%). For NmW and NmC, the most prevalent lineage was



Phylogenomic reconstruction based on the accessory genome of 186 isolates belonging to the ST307 clone collected in Andalusia.

CC-ST11 (89.2% and 82.8%, respectively). Prediction of antigenic reactivity revealed that 17.3% of NmB were expected to be covered by the 4CMenB vaccine, while 22.2% were not. The expected coverage of the 4CMenB vaccine was unknown for the remaining 60.5%. No isolates were resistant to cephalosporins, carbapenems nor chloramphenicol, and 7%, 10% and 41% of isolates were resistant to azithromycin, penicillin and cotrimoxazole, respectively. One isolate was resistant to ciprofloxacin (0,4%) and another one to rifampicin (0,4%).

Conclusions: NmB and W are currently the main causes of IMD in Spain. The genomic characterization reveals pandemic lineages as the main circulating strains, without changes observed during the COVID-19 pandemic. Although the reactivity of most NmB to 4CMenB is unknown, a significant number of cases of IMD are caused by NmB isolates that may escape 4CMenB protection (22.2%), particularly associated with isolates belonging to CC-ST213 lineage. Nm remains susceptible to all the antimicrobial agents used for treatment and prophylaxis. Monitoring the genomic epidemiology, antimicrobial susceptibility and vaccine reactivity of Nm is crucial to adapt vaccination schedules, to optimize antimicrobial therapies and to establish effective preventive measures.

Funding: This study has been funded by Instituto de Salud Carlos III (ISCIII) through the project "PI21/00132" and co-funded by the European Union.

112. IMPACT OF AN ENHANCED SCREENING PROGRAM ON THE DETECTION OF NON-AIDS NEOPLASIAS IN PATIENTS WITH HUMAN IMMUNODEFICIENCY VIRUS INFECTION

Leandro López Gutiérrez^{1,2}, Mar Masiá Canuto^{1,2}, Sergio Padilla Urrea^{1,2}, Javier García Abellán^{1,2}, Marta Fernández González^{1,2}, Antonio Rivero Román^{3,2}, Ángela Camacho Espejo^{3,2}, Ana González Cordon⁴, Ana Carina Silva Klug⁵, Daniel Podzamczar Palter⁵, Lucio García Fraile^{6,2}, Ignacio de los Santos^{6,2}, Onofre Juan Martínez⁷, Enrique Bernal Morell⁸, Carlos Galera Peñaranda⁹, Vicente Boix Martínez¹⁰, Gema García Rodríguez¹⁰, Juan Macías Sanchez^{11,2}, Marta Montero¹², Dácil García¹³, María Jesús Vivancos^{14,2}, Inmaculada González¹⁵, Miguel Torralba¹⁶, Jose Ramón Blanco¹⁷, Paula Dios¹⁸, Guillem Sirera¹⁹, Juan Flores²⁰, Jose Joaquín Portu²¹, Esteban Martínez Chamorro⁴, Félix Gutiérrez Rodero^{1,2}

¹Hospital General Universitario de Elche, Elche, Spain. ²Centro de Investigación Biomédica en Red de Enfermedades Infecciosas (CIBERINFEC), Madrid, Spain. ³Hospital Reina Sofía, Córdoba, Spain.

⁴Hospital Clínic de Barcelona, Barcelona, Spain. ⁵Hospital Universitari de Bellvitge, Barcelona, Spain. ⁶Hospital Universitario de La Princesa, Madrid, Spain. ⁷Hospital General Universitario Santa Lucía, Cartagena, Spain. ⁸Hospital General Universitario Reina Sofía, Murcia, Spain.

⁹Hospital Virgen de la Arrixaca, Murcia, Spain. ¹⁰Hospital Universitario de Alicante, Alicante, Spain. ¹¹Hospital Universitario Virgen de Valme, Sevilla, Spain. ¹²Hospital Universitari i Politècnic La Fe, Valencia, Spain. ¹³Hospital Universitario de Canarias, Canarias, Spain. ¹⁴Hospital Ramón y Cajal, Madrid, Spain. ¹⁵Hospital de la Vega Baja, Orihuela, Spain. ¹⁶Hospital Universitario de Guadalajara, Guadalajara, Spain. ¹⁷Hospital San Pedro, Logroño, Spain. ¹⁸Hospital Universitario de León, León, Spain. ¹⁹Hospital Universitario Germans Trias i Pujol, Badalona, Spain. ²⁰Hospital Arnau de Vilanova, Valencia, Spain. ²¹Hospital Universitario Araba, Vitoria-Gasteiz, Spain.

Introduction: The incidence of non-AIDS defining cancer is higher in people living with HIV (PLWH) than in the general population, and it is already one of the leading causes of death in the HIV-infected population. Early diagnosis through intensive cancer screening may improve the ability for therapeutic interventions and could be critical in reducing mortality, but it might also increase expenditure and harms associated with adverse events.

Objectives: The aim of this study is to evaluate the efficacy, safety, and efficiency of an enhanced screening program for early diagnosis of cancer in PLWH compared to standard practice.

Methods: A multicenter, non-blinded, randomized, controlled trial comparing two parallel arms: conventional vs enhanced screening. Conventional intervention group has followed the standard of care screening in the participating centers, according to the European-AIDS-Clinical-Society recommendations, and the enhanced intervention group an expanded screening aimed to early detection of lung, liver, anal, cervical, breast, prostate, colorectal, and skin cancer. The primary efficacy analysis will be the comparison of proportion of cancers diagnosed at early stage (1&2) in each group following the principle of intent to screen. A sample size of 1700 patients has been calculated with a follow-up of 6 years. Interim analyses for futility, safety, and efficacy are planned every 12 months.

Results: The recruitment began on 25 June 2019, but unfortunately, it was disrupted by the COVID-19 pandemic. Because of the overall delay in recruitment, the study duration has been extended. 1,164 patients have already been recruited with a follow-up of 22 (10-35) months. In the interim analysis, no safety concerns were raised and the trial is ongoing. So far, 10 carcinomas and 35 premalignant neoplastic lesions have been detected. Distribution of carcinomas is as follows: hepatocellular carcinoma, 2 cases (enhanced: 1, conventional: 1); colorectal adenocarcinoma 1 case (enhanced: 1), lung cancer 2 cases (enhanced: 1, conventional: 1), cervical cancer 1 case (enhanced: 1), and skin basal cell carcinoma, 3 cases, all of them in the enhanced screening-arm. Among premalignant lesions, most cases are anal and cervical high-grade squamous intraepithelial lesions (enhanced: 13; conventional-screening: 10 cases) and colorectal adenocarcinoma precursors lesions (enhanced: 5; conventional-screening: 8 cases). We will present the updated results in the meeting.

Conclusions: This multicenter pragmatic trial will help to determine whether the benefits of an enhanced cancer screening outweigh the harms in PLWH and if it is cost-effective for the Public Health Services. The information provided will be relevant since there are currently no studies on expanded cancer screening strategies in PLWH. **Funding:** This project has been financed by the ISCIII (PI18/01861) and supported by CIBER (CB21/13/00011), Instituto de Salud Carlos III, Ministerio de Ciencia e Innovación and Unión Europea – NextGenerationEU.

115. NATURAL EVOLUTION OF THE INTESTINAL LOAD OF KPC-PRODUCING *KLEBSIELLA PNEUMONIAE* AND RISK FACTORS ASSOCIATED WITH SUSTAINED ERADICATION OF COLONIZATION: A PROSPECTIVE OBSERVATIONAL COHORT (KLEBCOM STUDY)

Alejandra M. Natera^{1,2}, Juan Antonio Marín-Sanz¹, Manuel Recio-Rufián^{1,2,3}, Ángela Cano^{1,2,3}, Julia Guzmán-Puche^{1,2,4}, Juan José Castón^{1,2,3}, Isabel Machuca^{1,2,3}, Víctor Gálvez-Soto¹, Cristina Elías^{1,2,4}, Luis Martínez-Martínez^{1,2,4,5}, Julián Torre-Cisneros^{1,2,3,6}, Elena Pérez-Nadales^{1,2,5}

¹Maimonides Biomedical Research Institute of Cordoba, Reina Sofía University Hospital, University of Cordoba (IMIBIC/HURS/UCO), Córdoba, Spain. ²Centro de Investigación Biomédica en Red de Enfermedades Infecciosas (CIBERINFEC), Instituto de Salud Carlos III, Madrid, Spain. ³Unit of Infectious Diseases, Reina Sofía University Hospital, Córdoba, Spain. ⁴Unit of Microbiology, Reina Sofía University Hospital, Córdoba, Spain. ⁵Department of Agricultural Chemistry, Soil Science and Microbiology, University of Cordoba, Córdoba, Spain. ⁶Department of Medical and Surgical Sciences, University of Cordoba, Córdoba, Spain.

Introduction: The relative gastrointestinal load (RLKPC) of KPC-producing *Klebsiella pneumoniae* (KPC-KP) has been associated with increased risk of bacteremia and all-cause mortality in colonized patients.

Objectives: To examine if the RLKPC is associated with sustained eradication within 6 months.

Methods: KPC-KP colonized patients were recruited in a tertiary hospital with endemicity by a ST512/KPC-3 *K. pneumoniae* clone. Rectal swabs were collected at recruitment and monthly thereafter for one year. The RLKPC was estimated by qPCR and defined as the proportion of blaKPC relative to 16S rRNA gene copy number. Sustained eradication was defined as the absence of KPC-KP both by culture and qPCR and no subsequent positive swabs during follow-up. Factors associated with sustained eradication were evaluated by a Fine-Gray analysis, establishing death as competing risk. Whole-Genome Sequencing (WGS) (Illumina) was performed to study the clonality between KPC-KP colonizing and infection isolates.

Results: Among 80 patients recruited, 68 (85.0%) were hospitalized. Carriage of KPC-KP was confirmed in 89.6% (43/48), 71% (27/38), 41.4% (12/29) and 33.3% (7/21) patients with available follow-up samples at 1, 3, 6, and 12 months, respectively. The median RLKPC was 0.28% (range 0.001%-2.70%, minimum < 0.001%, maximum 59.39%) at baseline, 0.02% (range < 0.001%-0.41%, p-value relative to baseline = 0.055) at 1 month and remained below 0.001% (p < 0.001) thereafter. Twenty-four (27.5%) patients had at least one rectal swab sample negative for KPC-KP during follow-up, however only 15 (18.8%) showed sustained eradication, within a median time of 90 days (range 75-120). During follow-up, 43 (53.8%) patients died and 33 (41.3%) developed KPC-KP-related infections. In multivariable analysis, Charlson Comorbidity Index (SHR 0.473, 95%CI 0.23-0.97, p = 0.041) was independently associated with sustained eradication. WGS analysis showed high clonality between colonizing and clinical isolates, all belonging to the ST512/KPC-3 KP clone.

Conclusions: The RLKPC is not associated with sustained eradication of KPC-KP in colonized patients. A high Charlson comorbidity index is associated with lower probability of sustained eradication. This is important to implement adequate preventive measures.

Funding: This work was supported by (i) Plan Estatal de I+D+I 2013-2016, cofinanced by the ISCIII-Subdirección General de Evaluación y Fomento de la Investigación and FEDER (FIS PI16/01631 granted to E.P.N.); (ii) Plan Nacional de I+D+I 2013-2016 and ISCIII, Subdirección General de Redes y Centros de Investigación Cooperativa, and cofinanced by the European Development Regional Fund "A Way to Achieve Europe" Operative Program Smart Growth 2014-2020, (REIPI) (RD16/0016/0008); and (iii) Consejería de Salud y Familias, Junta de Andalucía (RH-0065-2020 granted to E.P.N.).

120. NOVEL CYCLIC PEPTIDES AS EFFLUX PUMP INHIBITORS: AN INTERESTING APPROACH AGAINST MULTIDRUG-RESISTANT *P. AERUGINOSA*

Natalia Rosón-Calero¹, Clara Ballesté-Delpierre¹, Jordi Vila Estapé^{1,2}

¹ISGlobal, Barcelona, Spain. ²Hospital Clínic Barcelona, Barcelona, Spain.

Introduction: The spread of multidrug resistant (MDR) Gram-negative pathogens is a global health threat. Among the mechanisms that

drive resistance in MDR pathogens, overexpression of multidrug efflux pumps is one of the most prevalent. The lack of development of new antimicrobials effective against MDR pathogens makes efflux pumps inhibitors (EPIs), like the well-studied Phenylalanine-arginine- β -naphthylamide (PA β N), a promising new strategy to restore antimicrobial susceptibility.

Objectives: The objective of this study was to analyse the antimicrobial susceptibility profile of two novel synthetic cyclic peptides (CPs): CP1 and CP3 against a collection of *Pseudomonas aeruginosa* presenting different genetic backgrounds.

Methods: After phenotypic characterization of the efflux pump overexpression and checking that CPs do not inhibit cell growth, Minimum Inhibitory Concentrations (MIC) of tetracycline (TET), minocycline (MINO), tigecycline (TIGE), aztreonam, cefepime, meropenem, imipenem, chloramphenicol and netilmicin were determined using broth microdilution assay. Ten *P. aeruginosa* strains presenting different RND-efflux pump expression profiles were selected for the study. The assays were performed in the presence of a constant concentration of 100 μ g/mL of PA β N and CPs to compare their activity.

Results: Among the antibiotics screened, tetracycline (TET) and minocycline (MINO) showed activity combined with CP1 and CP3, and tigecycline (TIGE) in combination with CP1 (CP3 currently being tested) as seen in the Table. Chloramphenicol showed synergistic activity only when combined with CP1 in strains 125A and 125B reducing the MIC by 3 and 4-folds, respectively (MIC = 8 μ g/mL in the presence of CP1). In the case of netilmicin, only CP3 showed a reduction in the MIC to up to 3-folds for most of the strains tested, except for three.

Conclusions: These preliminary results suggest that CP1 and CP3 have potential auxiliary activity *in vitro* when combined with different antibiotics, particularly for tetracycline-related antibiotics. Susceptibility to tetracycline and its derivatives minocycline and tigecycline, in the case of CP1, is higher in combination of the CPs tested. Further studies regarding the characterization of the compounds are being performed to disclose how the active compounds found in our study act as EPIs.

Funding: This study is part of the intramural CIBERInfec project IM22/INF/4.

121. FUNCTIONAL AND GENOMIC ANALYSIS OF *LEISHMANIA* CLINICAL ISOLATES: PROMOTING GENOMIC PERSONALIZED MEDICINE IN LEISHMANIASIS

Jose Carlos Solana^{1,2}, Lorena Bernardo^{1,2}, Sandra González-de-la-Fuente³, Carmen Chicharro^{1,4}, Emilia García¹, Eugenia Carrillo^{1,2}, Begoña Aguado³, Juan Víctor San Martín^{2,4}, Begoña Monge^{5,2}, Jose María Requena^{6,2}, Javier Moreno^{7,2}

¹WHO Collaborating Centre for Leishmaniasis, Centro Nacional de Microbiología, Instituto de Salud Carlos III, Majadahonda, Spain.

²Centro de Investigación Biomédica en Red de Enfermedades Infecciosas (CIBERINFEC), Instituto de Salud Carlos III, Madrid, Spain. ³Centro de Biología Molecular Severo Ochoa (CSIC-UAM), Genomic and NGS

120	TET	TET + CP1	Fold change	TET + CP3	Fold change	MINO	MINO + CP1	Fold change	MINO + CP3	Fold change	TIGE	TIGE + CP1	Fold change
41A	16	8	1	16	-	8	2	2	2	2	8	2	2
41B*	16	8	1	16	-	16	2	3	2	3	8	2	2
125A	8	2	2	8	-	8	1	3	1	3	8	1	3
125B*	8	2	2	8	-	8	1	3	1	3	8	1	3
PAO1 (wt)	8	2	2	4	1	8	2	2	2	2	8	2	2
PAOM*	1	0,5	1	0,06	4	2	0,5	2	0,5	2	1	1	0
PAOMxR*	16	4	2	8	1	8	1	3	1	3	8	1	3
PAOW (wt)	16	2	3	8	1	16	1	4	1	4	8	1	3
PAOW*	64	16	2	32	1	8	1	3	1	3	4	1	2
PAO Δ mexZ*	16	2	3	-	-	8	1	3	1	3	16	2	3

*41B: overexp. mexY, Δ oprD; 125B: Overexp. mexB; PAOM: Δ oprM; PAOMxR: def mexR; PAOW: Δ oprF; PAO1: Δ mexZ. Results are expressed in μ g/mL.

Facility (GENGS), Madrid, Spain. ⁴Servicio de Medicina Interna, Hospital Universitario de Fuenlabrada, Fuenlabrada, Spain. ⁵Unidad de Referencia Nacional para Enfermedades Tropicales, Servicio de Enfermedades Infecciosas, Hospital Universitario Ramón y Cajal, Madrid, Spain. ⁶Centro de Biología Molecular Severo Ochoa (CSIC-UAM), Departamento de Biología Molecular, Instituto Universitario de Biología Molecular (IUBM), Universidad Autónoma de Madrid, Madrid, Spain. ⁷WHO Collaborating Centre for Leishmaniasis, Centro Nacional de Microbiología, Instituto de Salud Carlos III, Majadahonda, Spain.

Introduction: Leishmaniasis is the second most important parasitic disease after malaria, and the ninth most significant infectious disease worldwide. Treatment consists on a very limited number of antiparasitic drugs. The extraordinary genomic plasticity of *Leishmania* parasite leads to the appearance of drug resistance, associated with treatment failure and selection of multiresistant strains, especially in immunosuppressed individuals.

Objectives: This work aims to achieve a genetic and phenotypic characterization of *Leishmania* clinical isolates to evaluate the pathogenic features of the strains and find individualized and appropriate treatments.

Methods: Cell viability was measured using resaruzin in *Leishmania* strains isolated from patients of Spanish hospitals and the collaborators of the WHO Collaborating Centre for Leishmaniasis when challenged with leishmanicidal drugs: amphotericin B, antimonials, miltefosin and paromomycin. On the other hand, DNA from clinical strains was isolated for its whole genome sequencing. The reads were aligned with the *Leishmania* reference genome and gene copy number

variation was examined, besides ploidy and some analyses. Moreover, maxicircle DNA of each strain was assembled for genotyping.

Results: The phylogenetic study of *Leishmania* strains has revealed the existence of at least two populations of the parasite circulating in Spain in different evolutionary stages, probably related with the inclusion of new reservoirs in the last leishmaniasis outbreak in Madrid, the most important in Europe. It has been also observed differences in resistance and susceptibility profiles to drug treatment, regarding EC50 values of each drug. The suitability of these analyses has been demonstrated in collaboration with Begoña Monge, from Jose Antonio Pérez Molina's CIBER group, in clinical isolates from patients suffering continuous relapses and receiving different treatments. A genetic profile of resistance to some of those has been found, including gene mutations related with the resistant phenotype.

Conclusions: The combination of genomic and phenotypic studies of *Leishmania* clinical isolates has been demonstrated to be useful for genotyping and determining the virulence and drug resistance profile, enabling to select an appropriate treatment, preventing therapeutic failures and emergence of resistances. In light of this research, future collaborations will be prompted with more CIBER groups specialized in leishmaniasis and bioinformatic analyses, in order to perform this kind of analysis in collaboration with Spanish hospitals in the framework of genomic and personalized medicine. This would undoubtedly result in a substantial improvement in the health and wellness of patients, reducing the cost of treatment and disease burden.

Funding: CB21/13/00018, LeishAccess (EDCTP-RIA2020S-3301), CB21/13/00085.